NACA

RESEARCH MEMORANDUM

for the

Air Materiel Command, Army Air Forces

WIND-TUNNEL DEVELOPMENT OF MEANS TO ALLEVIATE BUFFETING ON THE NORTH AMERICAN XP-82 AIRPLANE AT HIGH SPEEDS

By Joseph L. Anderson

Ames Aeronautical Laboratory
Moffett Field, Calif.

NATIONAL ADVISORY COMMITTEE FOR AERONAUTICS

WASHINGTON

JAN 9 1947

NACA RM No. A6L10

NATIONAL ADVISORY COMMITTEE FOR AERONAUTICS

RESEARCH MEMORANDUM

for the

Air Materiel Command, Army Air Forces

WIND-TUNNEL DEVELOPMENT OF MEANS TO ALLEVIATE BUFFETING ON THE NORTH AMERICAN XP-82 AIRPLANE AT HIGH SPEEDS

By Joseph L. Anderson

SUMMARY

This report presents the results of wind-tunnel tests of a 0.22-scale model of the North American XP-82 airplane with several modifications designed to reduce the buffeting of the airplane. The effects of various modifications on the air flow over the model are shown by means of photographs of tufts. The drag, lift, and pitching-moment coefficients of the model with several of the modifications are shown. The results indicate that, by reflexing the trailing edge of the center section of the wing and modifying the radiator air-scoop gutter and the inboard lower-surface wing fillets, the start of buffeting can be delayed from a Mach number of 0.70 to 0.775, and that the diving tendency of the airplane would be eliminated up to a Mach number of 0.80.

INTRODUCTION

During flight tests by North American Aviation, Inc., of the XP-82 airplane, buffeting started at a Mach number of about 0.70 and

increased in severity with further increase of Mach number so that the maximum Mach number attained was 0.75. North American found that there was a definite relationship between the action of the tufts on the airplane wing and the buffeting. Motion pictures of the tufts on the airplane were compared with photographs of tufts on a 0.22-scale model of the XP-82 airplane, and it was found that the flow as indicated by the tufts was similar on the airplane and the model.

The U. S. Army Air Forces, Air Materiel Command, requested that research be conducted in the Ames 16-foot high-speed wind tunnel using the 0.22-scale model of the airplane in order to find means of alleviating the buffeting of the airplane.

Representing North American Aviation, Inc. during the tests was Mr. Willis S. Bowman.

DESCRIPTION OF MODEL AND APPARATUS

The XP-82 airplane is a twin-engine, twin-fuselage, long-range fighter, and it is manned by a pilot and co-pilot, one in each fuselage. The model, similar to the airplane, consisted of the wing, two fuselages, empennage with the 32.8-percent-chord elevator, two carburetor air scoops, engine exhaust stacks, two radiator air scoops, and two pilot's enclosures. (See reference 1.) Figure 1 shows the important dimensions of the model. All the control surfaces were maintained in a neutral position.

Support for the model in the wind tunnel (fig. 2) was provided by two struts connected to the wing and by two pitch stings connected to two pitch booms which extended from the trailing edge of

the wing. Angle-of-attack control was obtained by vertical movement of the pitch stings.

The tufts were pieces of wool yarn fastened to the model by cellulose tape. The action of these tufts was photographed with a high-speed motion-picture camera.

Pertinent dimensions of the 0.22-scale model and the airplane are as follows:

	Model	Airplane
Wing		
Area, square feet	19.774	408.55
Span, feet	11.270	51.23
Mean aerodynamic chord, feet	1.809	8.221
Section profile		
root	NACA 66,2-215 (a=0.6)	
tip	NACA 66,1-212 (a=0.6)	
General		
Design gross weight, pounds		19,100
Design wing load, pounds per square foot		46.8
Design center-of-gravity position		
Horizontal, percent M.A.C.		24.74
Vertical, inches below fuselage reference plane		10.10

The chord of the horizontal stabilizer was parallel to the wing and fuselage reference planes.

REDUCTION OF DATA

Coefficients

The results are reduced to the following NACA standard coefficients:

C_L lift coefficient (lift/qS)

C_D drag coefficient (drag/qS)

$C_{m_{c.g.}}$ pitching-moment coefficient about the design center of gravity of the airplane ($M_{c.g.}$/qS M.A.C.)

Symbols

The symbols used in the report are defined as follows:

L lift, pounds

D drag, pounds

$M_{c.g.}$ pitching moment about the design center of gravity, pound-feet

M Mach number (V/a)

a speed of sound in the free air stream, feet per second

V velocity of the free air stream, feet per second

q dynamic pressure of the free air stream ($\frac{1}{2}\rho V^2$), pounds per square foot

ρ density of the free air stream, slugs per cubic foot

S wing area, square feet

M.A.C. mean aerodynamic chord, feet

α angle of attack of the model, degrees (The angle of attack is measured relative to the wing reference plane.)

α_u angle of attack of the model uncorrected for wind-tunnel-wall and mounting interference, degrees

Wind-Tunnel Calibration and Correction of Data

The Mach number and dynamic pressure calibration of the free air stream, as well as the correction due to the blocking of the air stream by the model and its wake, were evaluated by the methods outlined in reference 2. The corrections due to air stream inclination caused by the mounting system were evaluated by comparison of results obtained with the model mounted erect and inverted in the wind tunnel. No corrections were made for the interference between the mounting system and the model, but the data were corrected for the lift, drag, and pitching moment of the mounting system with the model not mounted on the struts.

As determined by the method outlined in reference 3, the corrections for the wind-tunnel-wall interference were made by adding the following:

$$\Delta\alpha \text{ (deg)} = 0.734\ C_L$$

$$\Delta C_D = 0.0128\ C_L^2$$

$$\Delta C_{m_{c.g.}} = 0.0092\ C_L \text{ (tail on)}$$

RESULTS

The test results are presented in this report in the following groups:

1. Profiles of several wing center sections and the calculated pressure distributions for them. (See figs. 3 through 5.) Modifications to the radiator air-scoop gutter and the lower-surface inboard

wing fillet. (See fig. 6.)

2. Photographs of tufts on the wing center section and radiator air scoops. (See figs. 7 through 26.)

3. Lift, drag, and pitching-moment characteristics of the model. (See figs. 27 through 44.)

4. Drag and pitching-moment data for comparison of various model arrangements. (See figs. 45 through 56.)

5. Predicted longitudinal control of the airplane. (See figs. 57 and 58.)

DISCUSSION

The pressure-recovery gradient over the original center section was rather steep. Figure 12 shows that at a Mach number of 0.7 there was some separation of air flow over the center section and further increase in Mach number increased the separation, thus indicating increased buffeting of the airplane. Modifications were made to the after portion of the center section of the wing. The long-chord extension consisted of extending the trailing edge back so as to reduce the relative thickness of the section. This change delayed separation to about 0.025 higher Mach number. The second modification consisted of reflexing the center-section trailing edge so as to reduce the steepness of the pressure-recovery gradient and to reduce the lift carried by that panel. Figure 15 shows that at a Mach number of 0.80 (fig. 16) the air flow was separated over this surface. A Mach number of 0.80 is the design limit for this airplane; so the reflexed trailing edge maintained satisfactory flow

to the design condition.

Investigation of the lower surface of the model with the reflexed-trailing-edge center section showed that the flow over the inboard surfaces of the radiator air scoops was separated. The air scoop was lowered, and the profile of the gutter modified so as to increase the gutter area and eliminate abrupt changes (fig. 6); these changes delayed separation to about 0.025 higher Mach number. With the louvers (fig. 6), there was some separation back of the gutter exit. The constant-radius fillet was changed so that the fillet radius increased with increase of distance from the wing leading edge (fig. 6). The expanding fillet alone produced better flow on the lower surface than had the louvers and almost made the flow on the lower surface equal to that on the upper surface. The air flow over the model being improved, correspondingly the drag of the model was reduced (figs. 46 and 52).

The airplane in the original condition had a diving tendency above a Mach number of 0.70. Figure 57 shows this diving tendency as a reversal in the variation with Mach number of elevator angle for trim at a Mach number of 0.70. The airplane with the reflexed-trailing-edge center section is indicated to have no reversal in the variation of elevator angle for trim up to 0.775 Mach number, and with the addition of the expanding fillets there is no reversal indicated.

CONCLUDING REMARKS

The results of tests of the 0.22-scale model indicate that the speed at which buffeting begins can be delayed from a Mach number of

0.70 to 0.775 if certain modifications are made to the airplane. These changes are the reflexed trailing-edge center section, the lowered air scoop, and the expanding wing air-scoop fillet. It is indicated that the modified airplane will have no diving tendency up to a Mach number of 0.80.

Ames Aeronautical Laboratory,
National Advisory Committee for Aeronautics,
Moffett Field, Calif.

Joseph L. Anderson

Joseph L. Anderson,
Aeronautical Engineer.

Approved:

Donald H. Wood

Donald H. Wood,
Aeronautical Engineer.

REFERENCES

1. Anderson, Joseph L., and Tkac, Victor B.: High-Speed Wind-Tunnel Tests of a Model of the North American XP-82 Airplane. NACA MR No. A6D03, 1946.

2. Nissen, James M., Gadeburg, Burnett L., and Hamilton, William T.: Correlation of the Drag Characteristics of a P-51B Airplane Obtained from High-Speed Wind-Tunnel and Flight Tests. NACA ACR No. 4K02, 1945.

3. Silverstein, Abe, and White, James A.: Wind-Tunnel Interference with Particular Reference to Off-Center Positions of the Wing and to the Downwash at the Tail. NACA Rep. No. 547, 1935.

FIGURE LEGENDS

Figure 1.– The 0.22-scale model of the North American XP-82 airplane.

Figure 2.– The 0.22-scale model of the North American XP-82 airplane mounted in the Ames 16-foot high-speed wind tunnel.

Figure 3.– Calculated pressure distribution for the original center section on the North American XP-82 airplane. α, 0°.

Figure 4.– Calculated pressure distribution for the original center section and the long-chord center section extension on the North American XP-82 airplane. α, 0°.

Figure 5.– Calculated pressure distribution for the original center section and the reflexed trailing-edge center section on the North American XP-82 airplane. α, 0°.

Figure 6.– Modifications to the radiator air scoop of the North American XP-82 airplane.

Figure 7.– Photographs of tufts on the model of the North American XP-82 airplane for several arrangements. α_u, −1°; M,0.70.

Figure 8.– Photographs of tufts on the model of the North American XP-82 airplane for several arrangements. M,0.725; α_u, −1°.

Figure 9.– Photographs of tufts on the model of the North American XP-82 airplane for several arrangements. M,0.75; α_u, −1°.

Figure 10.– Photographs of tufts on the model of the North American XP-82 airplane for several arrangements. M,0.775; α_u, −1°.

Figure 11.– Photographs of tufts on the model of the North American XP-82 airplane for several arrangements. M,0.8; α_u, −1°.

Figure 12.– Photographs of tufts on the model of the North American XP-82 airplane for several arrangements. α_u, 0°; M,0.70.

Figure 13.– Photographs of tufts on the model of the North American XP-82 airplane for several arrangements. M,0.725; α_u, 0°.

Figure 14.– Photographs of tufts on the model of the North American XP-82 airplane for several arrangements. M,0.75; α_u, 0°.

Figure 15.– Photographs of tufts on the model of the North American XP-82 airplane for several arrangements. M,0.775; α_u, 0°.

Figure 16.– Photographs of tufts on the model of the North American XP–82 airplane for several arrangements. M,0.8; α_u, 0°.

Figure 17.– Photographs of tufts on the model of the North American XP–82 airplane for several arrangements. M,0.70; α_u, 1°.

Figure 18.– Photographs of tufts on the model of the North American XP–82 airplane for several arrangements. M,0.725; α_u, 1°.

Figure 19.– Photographs of tufts on the model of the North American XP–82 airplane for several arrangements. M,0.75; α_u, 1°.

Figure 20.– Photographs of tufts on the model of the North American XP–82 airplane for several arrangements. M,0.775; α_u, 1°.

Figure 21.– Photographs of tufts on the model of the North American XP–82 airplane for several arrangements. M,0.8; α_u, 1°.

Figure 22.– Photographs of tufts on the model of the North American XP–82 airplane for several arrangements. M,0.70; α_u, 2°.

Figure 23.– Photographs of tufts on the model of the North American XP–82 airplane for several arrangements. M,0.725; α_u, 2°.

Figure 24.– Photographs of tufts on the model of the North American XP–82 airplane for several arrangements. M,0.75; α_u, 2°.

Figure 25.– Photographs of tufts on the model of the North American XP–82 airplane for several arrangements. M,0.775; α_u, 2°.

Figure 26.– Photographs of tufts on the model of the North American XP–82 airplane for several arrangements. M,0.8; α_u, 2°.

Figure 27.– Variation of the drag coefficient with the lift coefficient for the model of the North American XP–82 airplane. Original center section.

Figure 28.– Variation of the lift coefficient with the angle of attack for the model of the North American XP–82 airplane. Original center section.

Figure 29.– Variation of the pitching-moment coefficient with the lift coefficient for the model of the North American XP–82 airplane. Original center section.

Figure 30.– Variation of the drag coefficient with the lift coefficient for the model of the North American XP–82 airplane. Long-chord center section extension.

Figure 31.– Variation of lift coefficient with angle of attack for the model of the North American XP–82 airplane. Long–chord center section extension.

Figure 32.– Variation of pitching–moment coefficient with lift coefficient for the model of the North American XP–82 airplane. Long–chord center section extension.

Figure 33.– Variation of drag coefficient with lift coefficient for the model of the North American XP–82 airplane. Reflexed trailing–edge center section.

Figure 34.– Variation of lift coefficient with angle of attack for the model of the North American XP–82 airplane. Reflexed trailing–edge center section.

Figure 35.– Variation of pitching–moment coefficient with lift coefficient for the model of the North American XP–82 airplane. Reflexed trailing–edge center section.

Figure 36.– Variation of drag coefficient with lift coefficient for the model of the North American XP–82 airplane less the empennage. Reflexed trailing–edge center section.

Figure 37.– Variation of lift coefficient with angle of attack for the model of the North American XP–82 airplane less the empennage. Reflexed trailing–edge center section.

Figure 38.– Variation of the pitching–moment coefficient with the lift coefficient for the model of the North American XP–82 airplane less the empennage. Reflexed trailing–edge center section.

Figure 39.– Variation of the drag coefficient with the lift coefficient for the model of the North American XP–82 airplane. Reflexed trailing–edge center section; louvers over air–scoop by–pass exit.

Figure 40.– Variation of the lift coefficient with angle of attack for the model of the North American XP–82 airplane. Reflexed trailing–edge center section; louvers over air–scoop by–pass exit.

Figure 41.– Variation of pitching–moment coefficient with lift coefficient for the model of the North American XP–82 airplane. Reflexed trailing–edge center section; louvers over the air–scoop by–pass exit.

Figure 42.– Variation of drag coefficient with lift coefficient for the model of the North American XP–82 airplane. Reflexed trailing–edge center section; expanding wing–air scoop fillet.

Figure 43.— Variation of lift coefficient with angle of attack for the model of the North American XP-82 airplane. Reflexed trailing-edge center section; expanding wing-air scoop fillet.

Figure 44.— Variation of pitching-moment coefficient with lift coefficient for the model of the North American XP-82 airplane. Reflexed trailing-edge center section; expanding wing-air scoop fillet.

Figure 45.— Variation of the pitching-moment coefficient, drag coefficient, and angle of attack with Mach number for several center section trailing edges on the model of the North American XP-82 airplane. C_L, -0.1.

Figure 46.— Variation of pitching-moment coefficient, drag coefficient, and angle of attack with Mach number for several center section trailing edges on the model of the North American XP-82 airplane. C_L, 0.0.

Figure 47.— Variation of pitching-moment coefficient, drag coefficient, and angle of attack with Mach number for several center section trailing edges on the model of the North American XP-82 airplane. C_L, 0.1.

Figure 48.— Variation of pitching-moment coefficient, drag coefficient, and angle of attack with Mach number for several center section trailing edges on the model of the North American XP-82 airplane. C_L, 0.2.

Figure 49.— Variation of pitching-moment coefficient, drag coefficient, and angle of attack with Mach number for several center section trailing edges on the model of the North American XP-82 airplane. C_L, 0.3.

Figure 50.— Variation of pitching-moment coefficient, drag coefficient, and angle of attack with Mach number for several center section trailing edges on the model of the North American XP-82 airplane. C_L, 0.4.

Figure 51.— Variation of pitching-moment coefficient, drag coefficient, and angle of attack with Mach number for several air-scoop configurations on the model of the North American XP-82 airplane with the reflexed trailing edge center section. C_L, -0.1.

Figure 52.— Variation of pitching-moment coefficient, drag coefficient, and angle of attack with Mach number for several air-scoop configurations on the model of the North American XP-82 airplane with the reflexed trailing edge center section. C_L, 0.0.

Figure 53.– Variation of pitching-moment coefficient, drag coefficient, and angle of attack with Mach number for several air-scoop configurations on the model of the North American XP-82 airplane with the reflexed trailing edge center section. C_L, 0.1.

Figure 54.– Variation of pitching-moment coefficient, drag coefficient, and angle of attack with Mach number for several air-scoop configurations on the model of the North American XP-82 airplane with the reflexed trailing edge center section. C_L, 0.2.

Figure 55.– Variations in pitching-moment coefficient, drag coefficient, and angle of attack with Mach number for several air-scoop configurations on the model of the North American XP-82 airplane with the reflexed trailing edge center section. C_L, 0.3.

Figure 56.– Variation of pitching-moment coefficient, drag coefficient, and angle of attack with Mach number for several air-scoop configurations on the model of the North American XP-82 airplane with the reflexed trailing edge center section. C_L, 0.4.

Figure 57.– Predicted elevator angle to balance the North American XP-82 airplane in level flight at sea level and at 10,000 feet altitude. Wing loading 46.8 pounds per square foot; elevator tab 0°.

Figure 58.– Predicted elevator angle to balance the North American XP-82 airplane in level flight at 20,000 and 30,000 feet altitude. Wing loading 46.8 pounds per square foot; elevator tab, 0°.

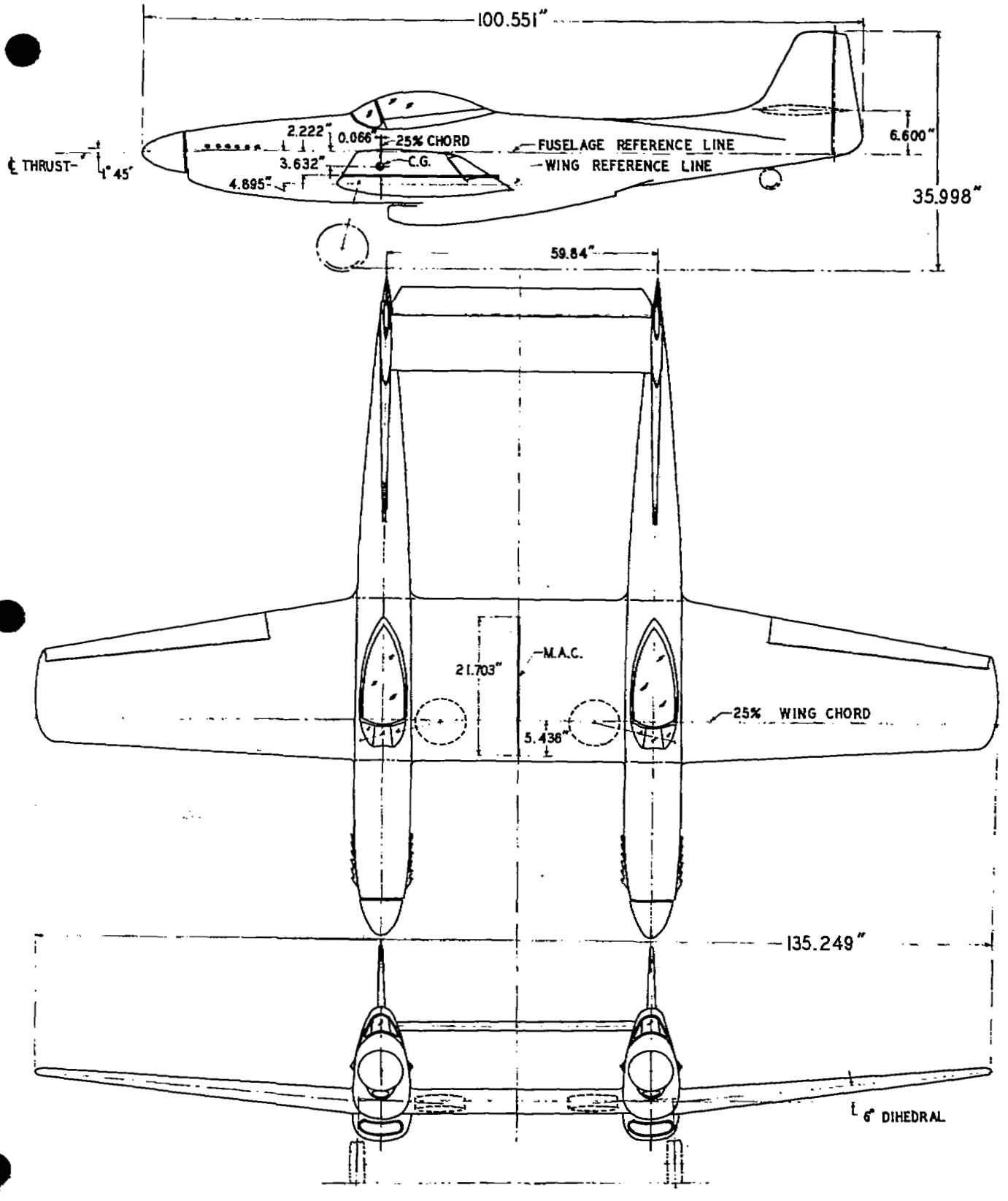

FIGURE 1:- THE 0.22-SCALE MODEL OF THE NORTH AMERICAN XP-82 AIRPLANE.

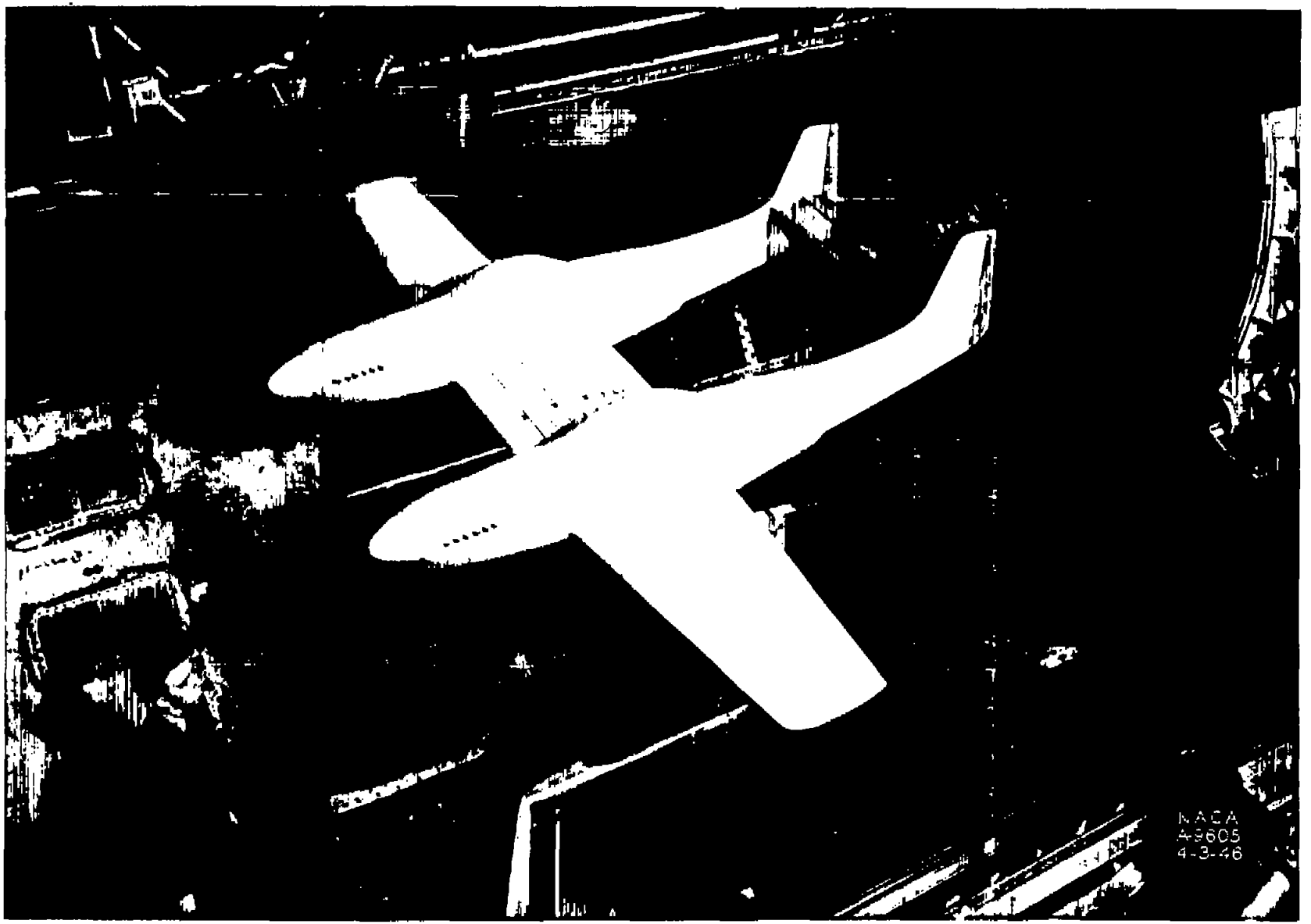

Figure 2.– The 0.22-scale model of the North American XP–82 airplane mounted in the Ames 16-foot high-speed wind tunnel.

NATIONAL ADVISORY COMMITTEE FOR AERONAUTICS
AMES AERONAUTICAL LABORATORY — MOFFETT FIELD, CALIF.

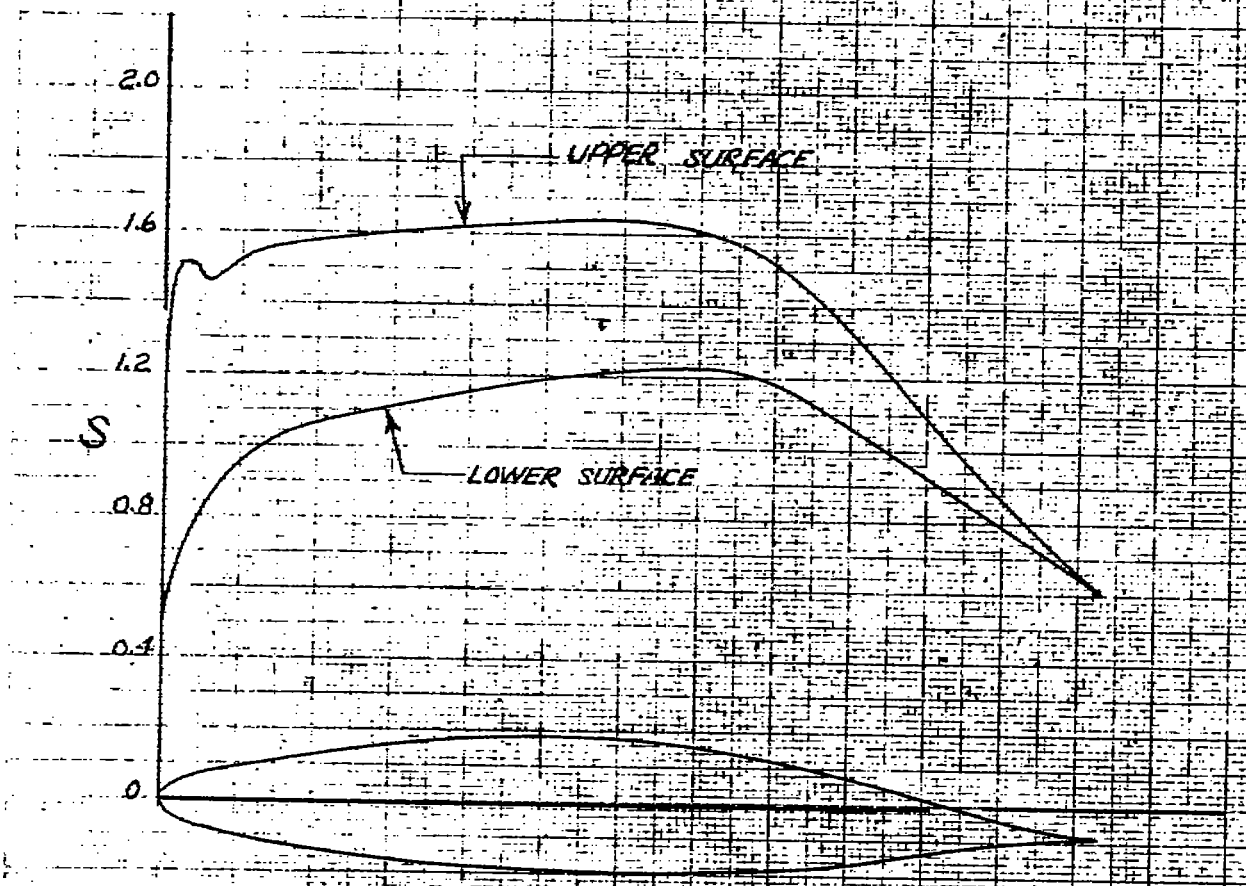

FIGURE 3 - CALCULATED PRESSURE DISTRIBUTION FOR THE ORIGINAL CENTER SECTION ON THE NORTH AMERICAN XP-82 AIRPLANE. α, 0°.

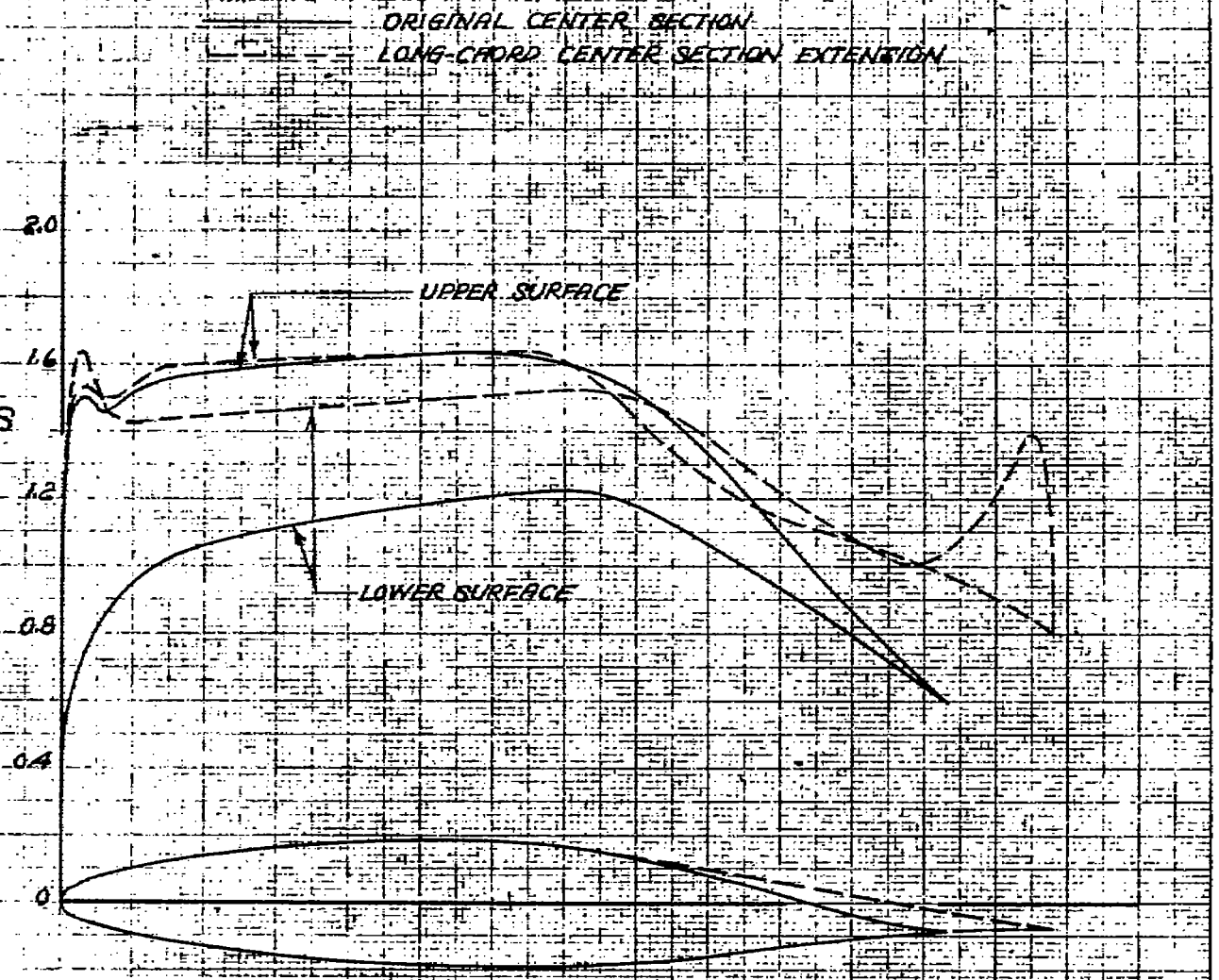

FIGURE 4. - CALCULATED PRESSURE DISTRIBUTION FOR THE ORIGINAL CENTER SECTION AND THE LONG-CHORD CENTER SECTION EXTENSION ON THE NORTH AMERICAN XP-82 AIRPLANE. α, 0°

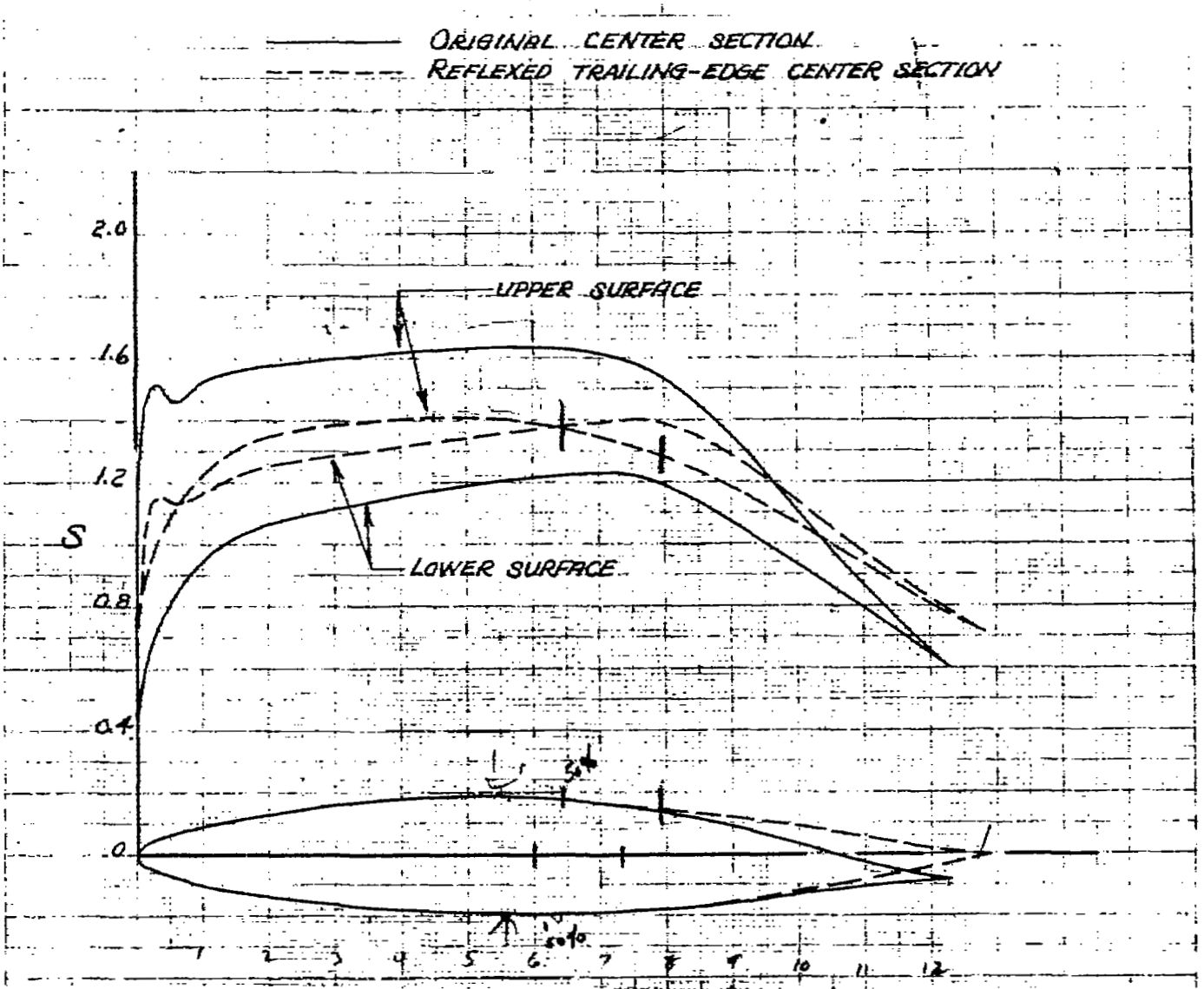

FIGURE 5.- CALCULATED PRESSURE DISTRIBUTION FOR THE ORIGINAL CENTER SECTION AND THE REFLEXED TRAILING-EDGE CENTER SECTION ON THE NORTH AMERICAN XP-82 AIRPLANE. α, 0°.

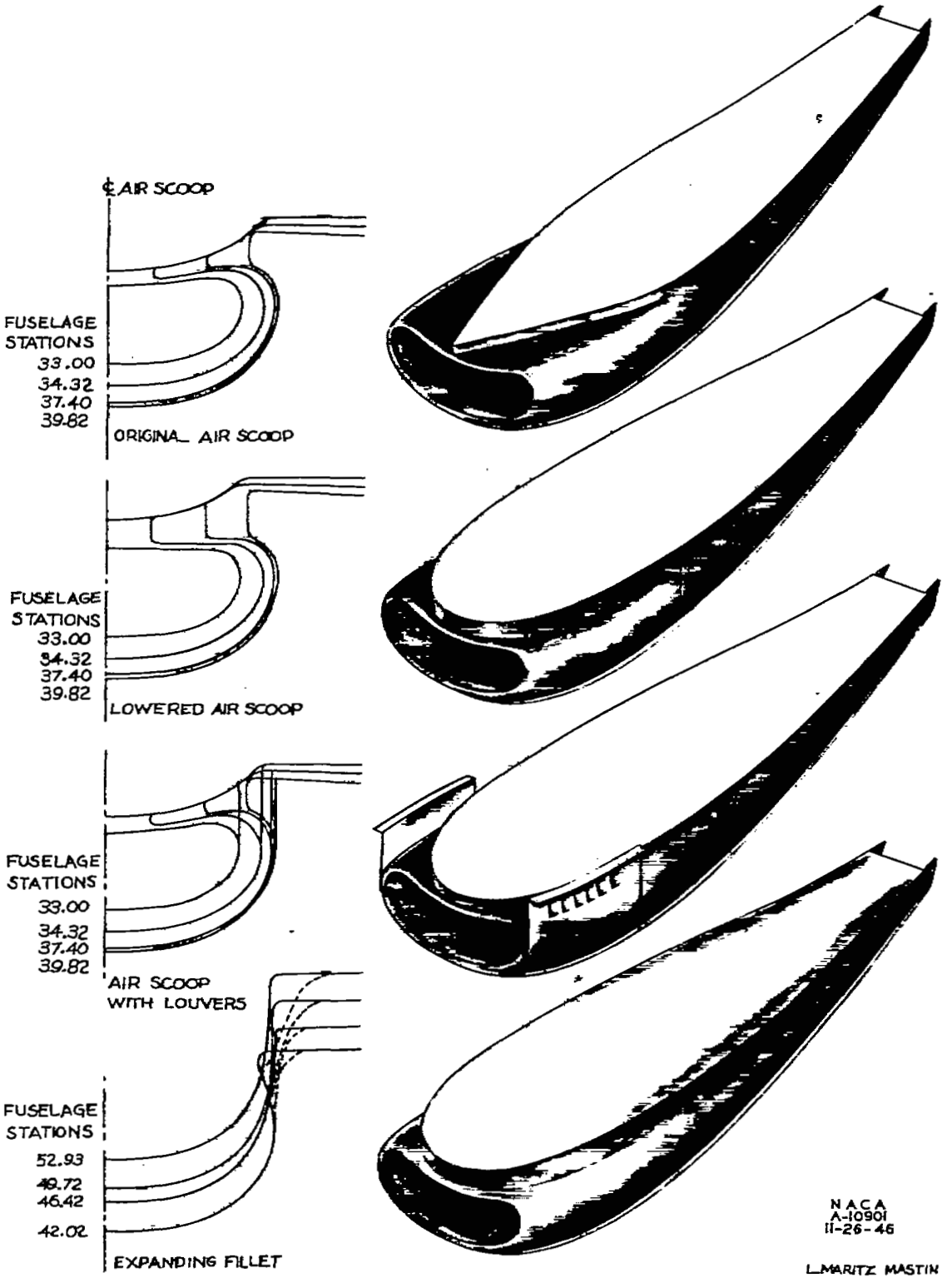

Figure 6.- Modifications to the radiator air scoop of the North American XP-82 airplane.

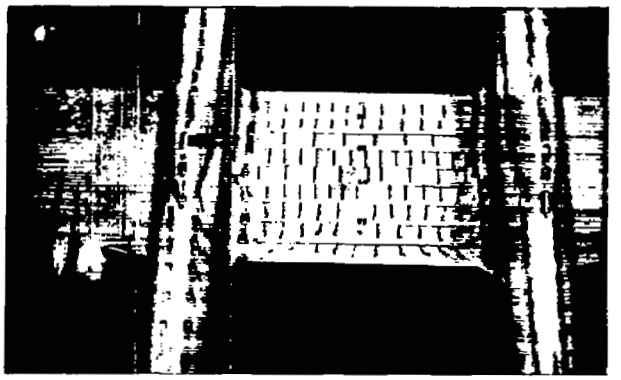

Original center section.

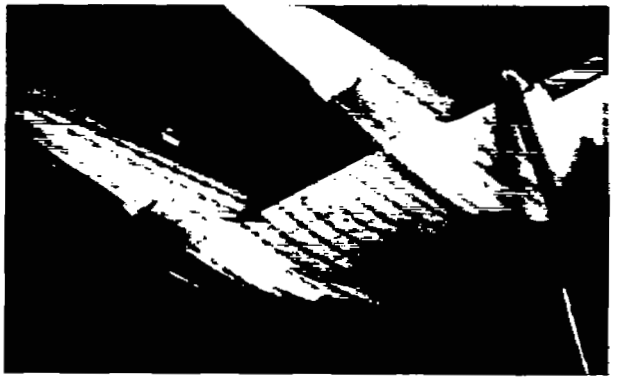

Lowered air scoop.

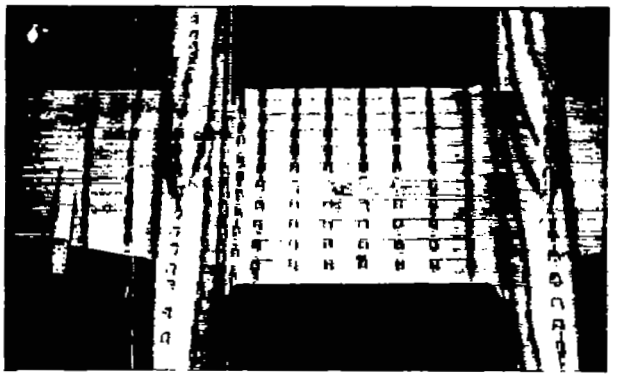

Long-chord center-section extension.

Louvers over air-scoop by-pass exit.

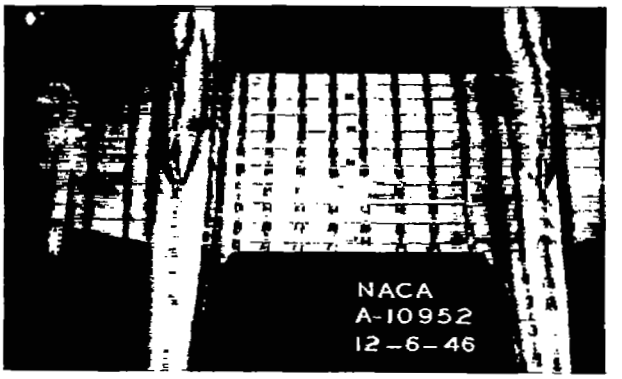

Reflexed trailing-edge center section.

Figure 7.- Photographs of tufts on the model of the North American XP-82 airplane for several arrangements. α_u, -1°; M,0.70.

NATIONAL ADVISORY COMMITTEE FOR AERONAUTICS
AMES AERONAUTICAL LABORATORY - MOFFETT FIELD, CALIF.

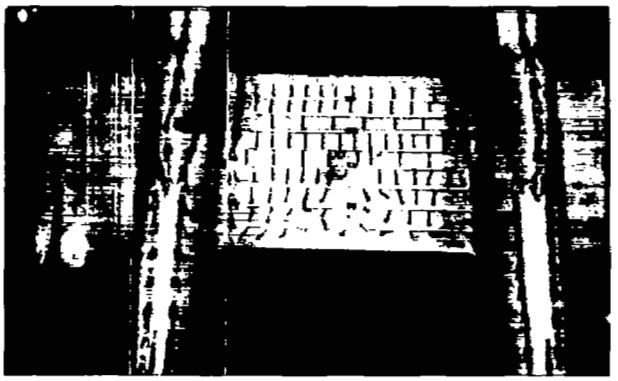

Original center section.

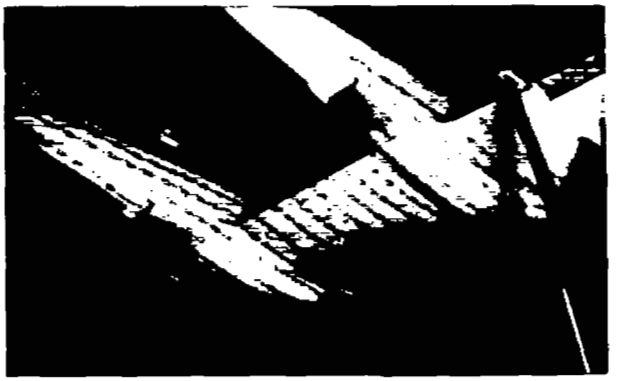

Lowered air scoop.

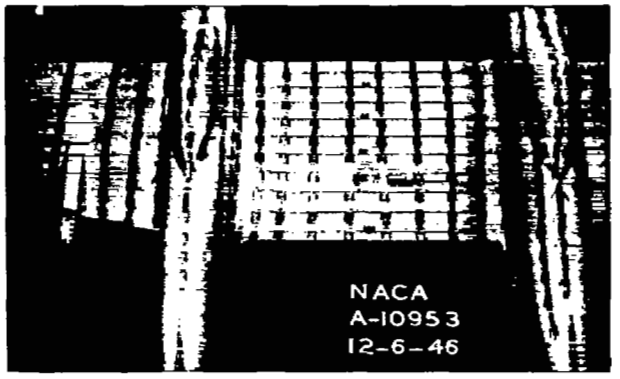

Reflexed trailing-edge
center section.

Figure 8.- Photographs of tufts on the model of the North American XP-82 airplane for several arrangements. M,0.725; α_u, -1°.

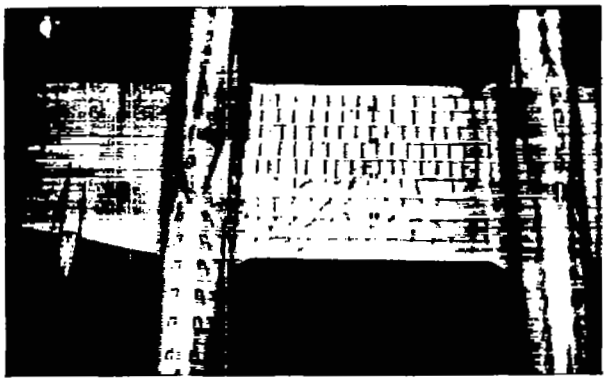

Original center section.

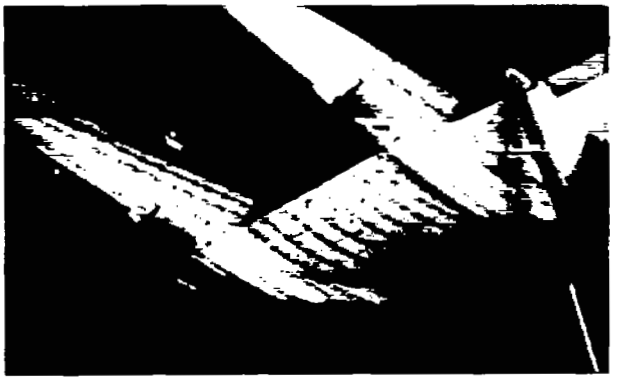

Lowered air scoop.

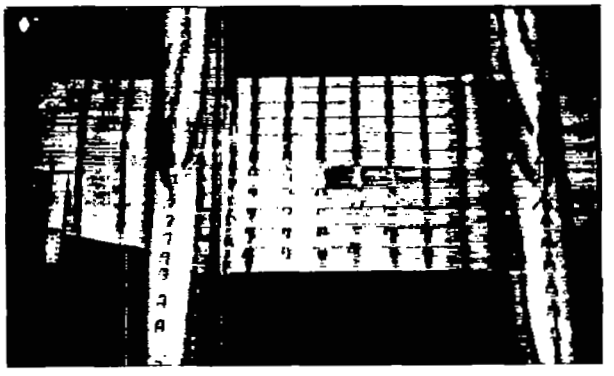

Long-chord center-section extension.

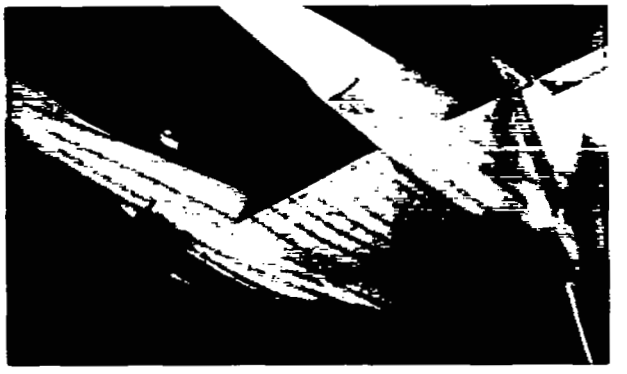

Louvers over air-scoop by-pass exit.

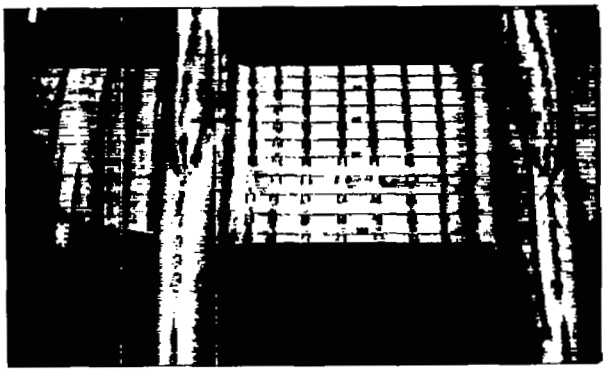

Expanding wing air-scoop juncture fillet.

Reflexed trailing-edge center section.

Figure 9.- Photographs of tufts on the model of the North American XP-82 airplane for several arrangements. M,0.75; α_u, -1°.

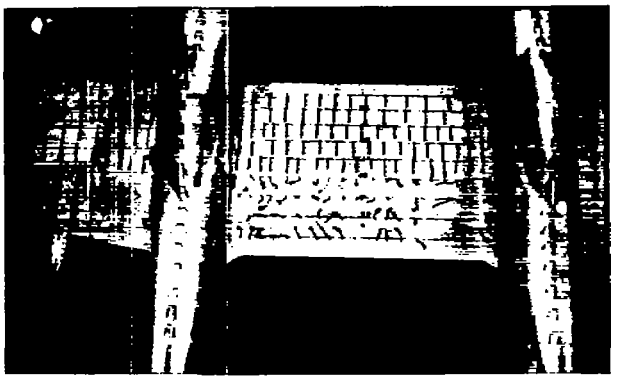

Original center section.

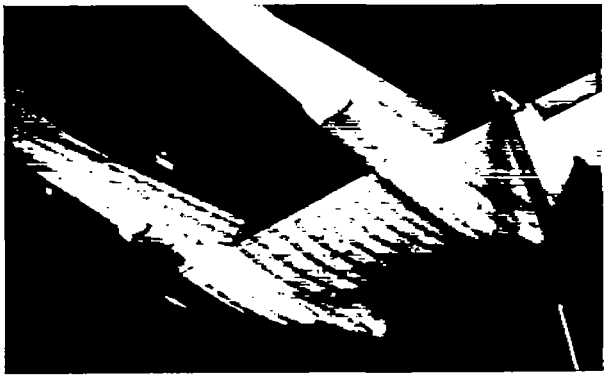

Lowered air scoop.

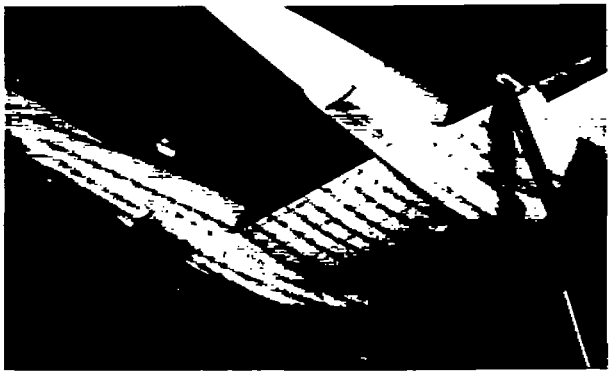

Louvers over air-scoop,
by-pass exit.

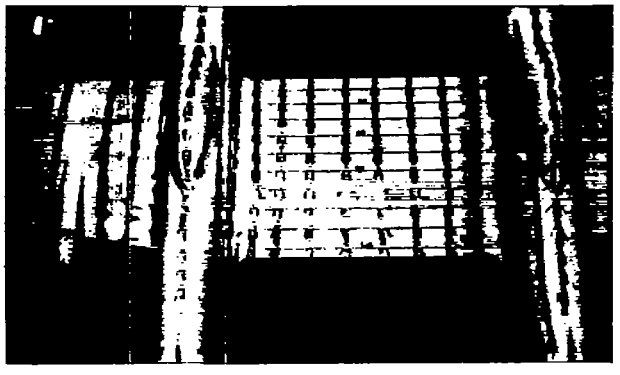

Reflexed trailing-edge
center section.

Expanding wing air-scoop
juncture fillet.

Figure 10.- Photographs of tufts on the model of the North American XP-82 airplane for several arrangements. M,0.775; α_u, -1°.

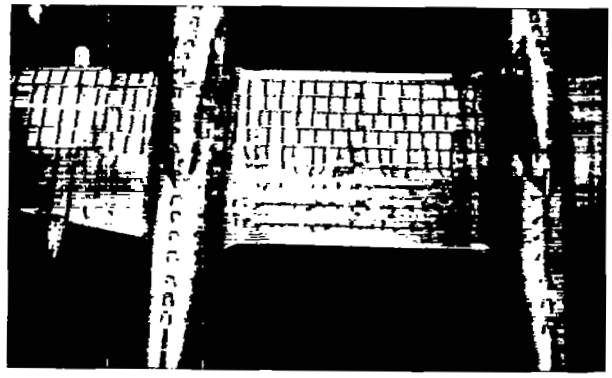

Original center section.

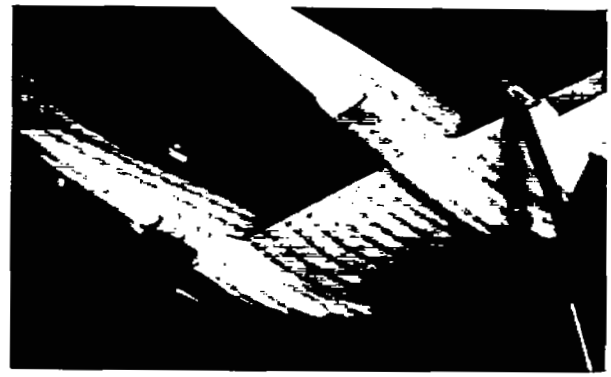

Lowered air scoop.

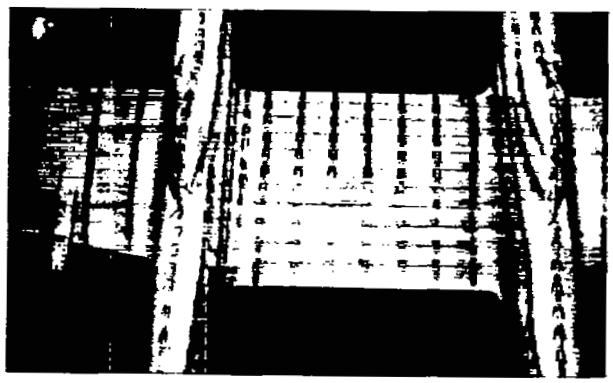

Long-chord center-section extension.

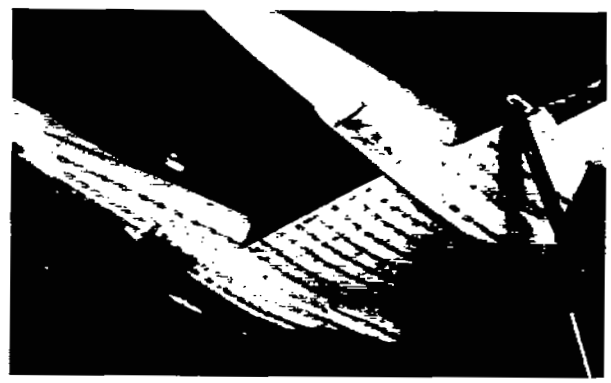

Louvers over air-scoop, by-pass exit.

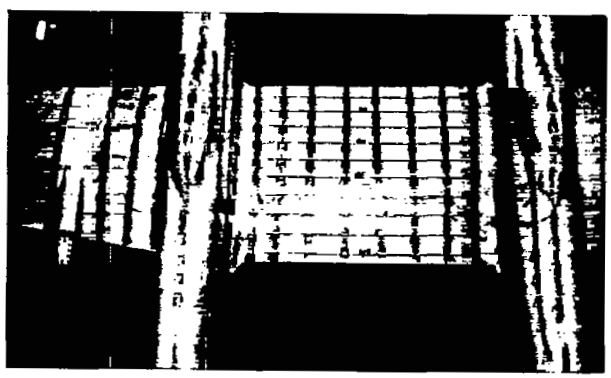

Reflexed trailing-edge center section.

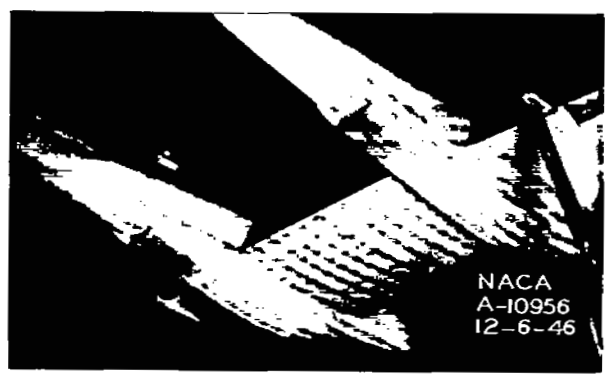

Expanding wing air-scoop juncture fillet.

Figure 11.- Photographs of tufts on the model of the North American XP-82 airplane for several arrangements. M,0.8; α_u, -1°.

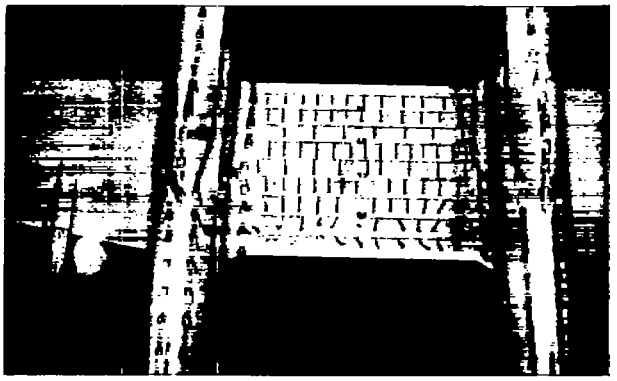

Original center section.

Lowered air scoop.

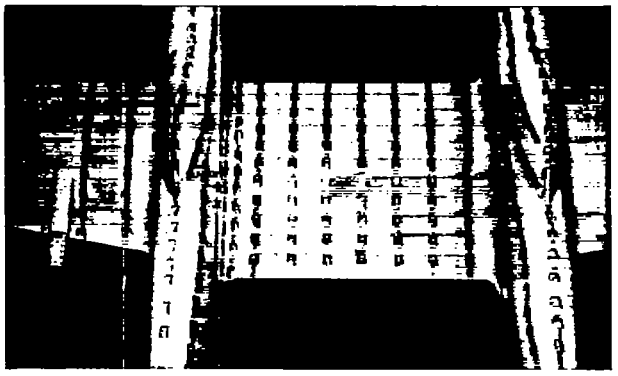

Long-chord center-section extension.

Louvers over air-scoop, by-pass exit.

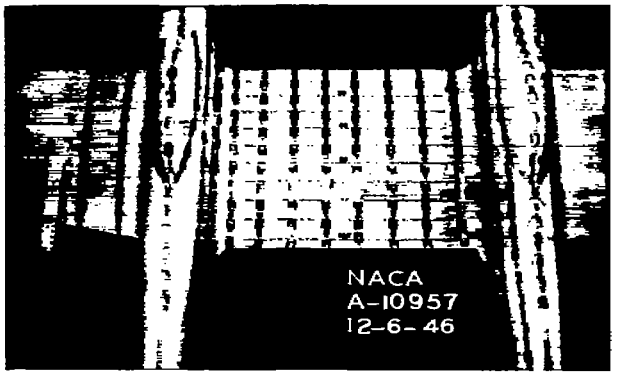

Reflexed trailing-edge center section.

Figure 12.- Photographs of tufts on the model of the North American XP-82 airplane for several arrangements. α_u, 0°; M,0.70.

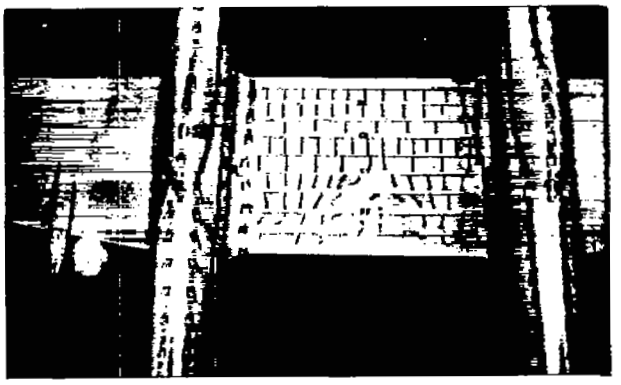

Original center section.

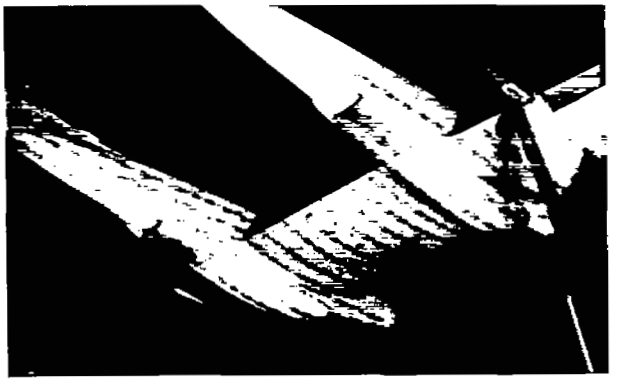

Lowered air scoop.

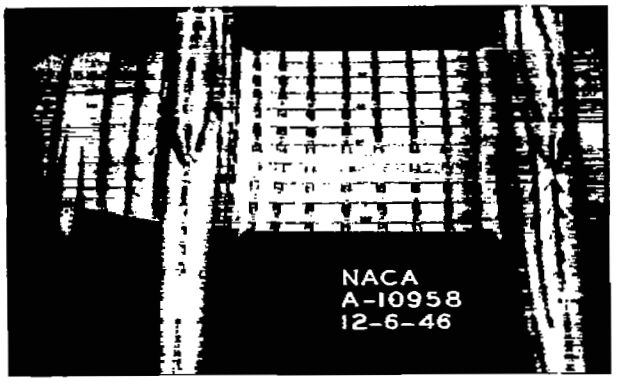

Reflexed trailing-edge
center section.

Figure 13.- Photographs of tufts on the model of the North American XP-82 airplane for several arrangements. M,0.725; α_u, 0°.

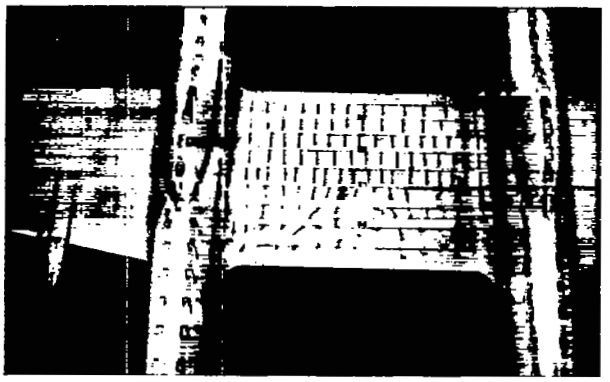

Original center section.

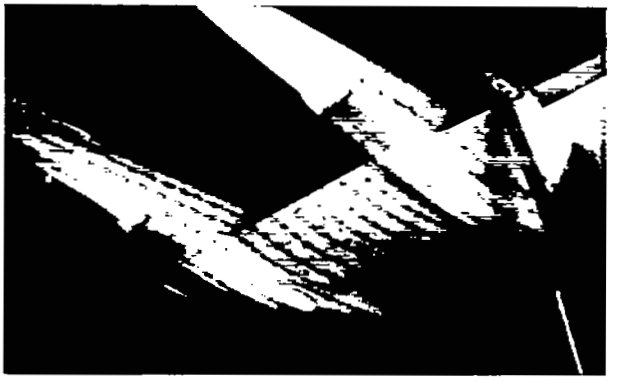

Lowered air scoop.

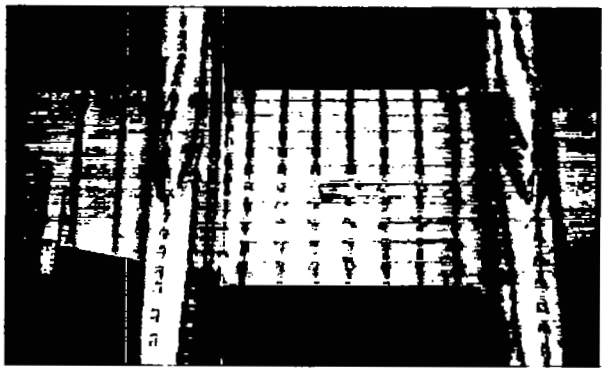

Long-chord center-section extension.

Louvers over air-scoop by-pass exit.

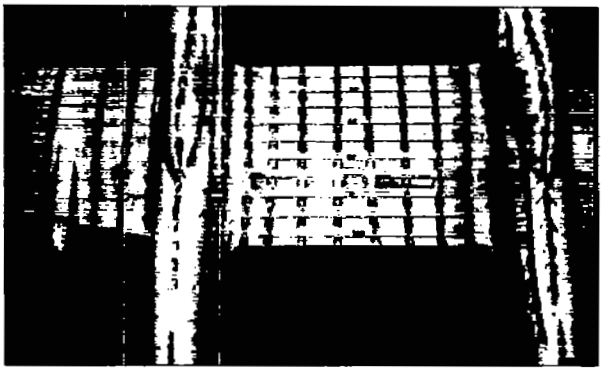

Expanding wing air-scoop juncture fillet.

Reflexed trailing-edge center section.

Figure 14.- Photographs of tufts on the model of the North American XP-82 airplane for several arrangements. M,0.75; α_u, 0°.

Original center section.

Lowered air scoop.

Louvers over air-scoop
by-pass exit.

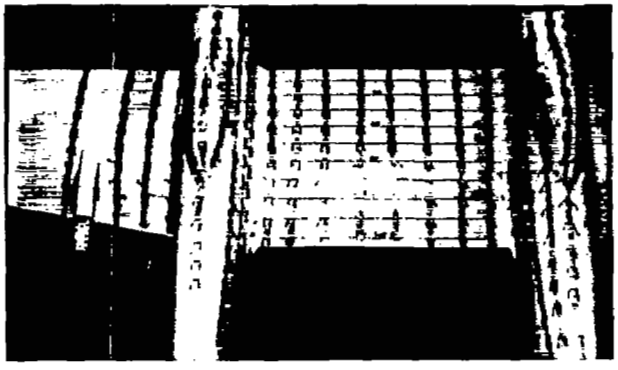

Reflexed trailing-edge
center section.

Expanding wing air-scoop
juncture fillet.

Figure 15.- Photographs of tufts on the model of the North American XP-82 airplane for several arrangements. M,0.775; α_u, 0°.

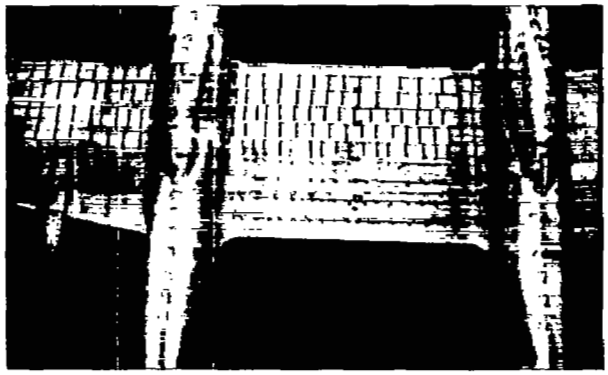

Original center section.

Lowered air scoop.

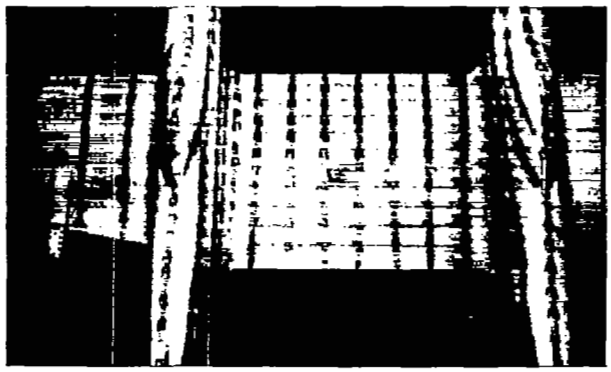

Long-chord center-section extension.

Louvers over air-scoop by-pass exit.

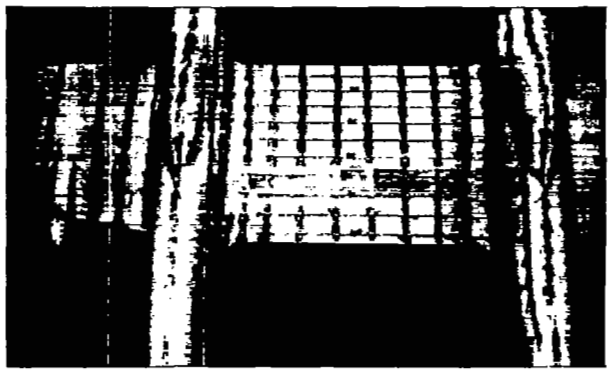

Reflexed trailing-edge center section.

Expanding wing air-scoop juncture fillet.

Figure 16.— Photographs of tufts on the model of the North American XP-82 airplane for several arrangements. M,0.8; α_u, 0°.

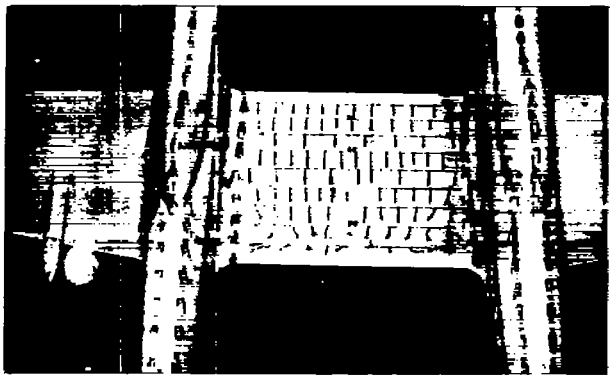

Original center section.

Lowered air scoop.

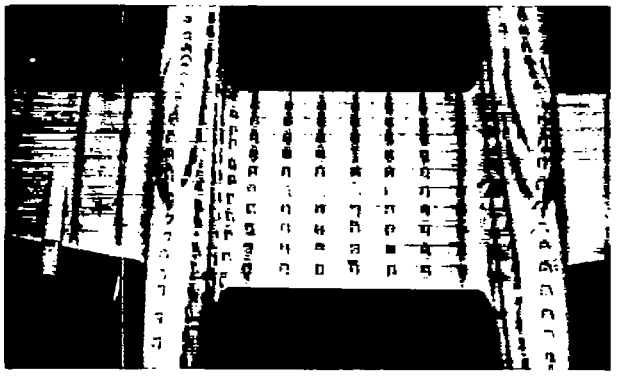

Long-chord center-section extension.

Louvers over air-scoop by-pass exit.

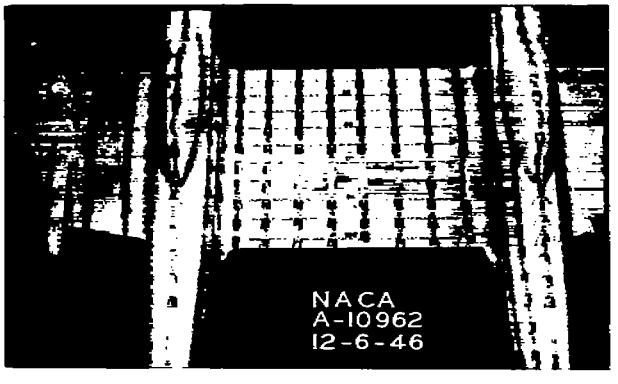

Reflexed trailing-edge center section.

Figure 17.- Photographs of tufts on the model of the North American XP-82 airplane for several arrangements. M,0.70; α_u, 1°.

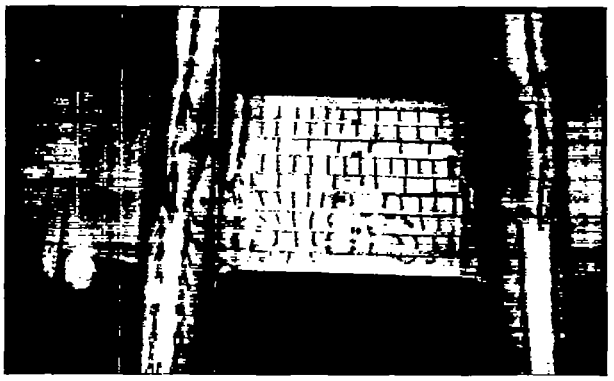

Original center section.

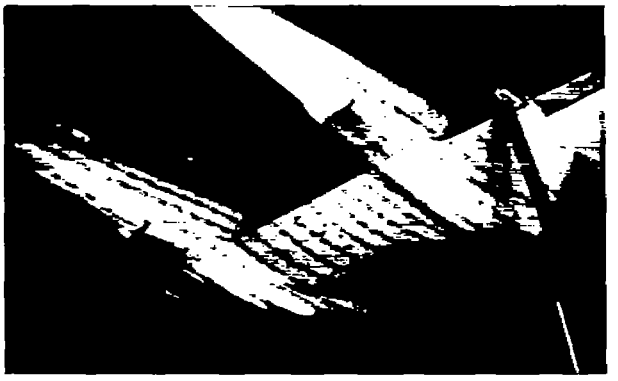

Lowered air scoop.

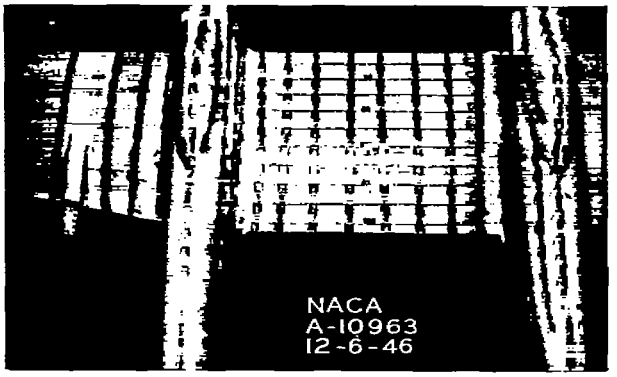

Reflexed trailing-edge
center section.

Figure 18.- Photographs of tufts on the model of the North American XP-82 airplane for several arrangements. M,0.725; α_u, 1°.

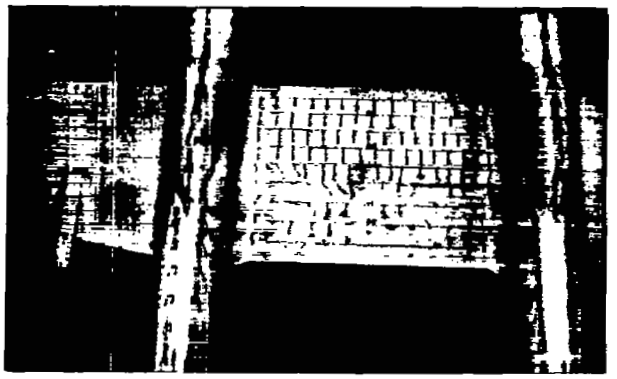

Original center section.

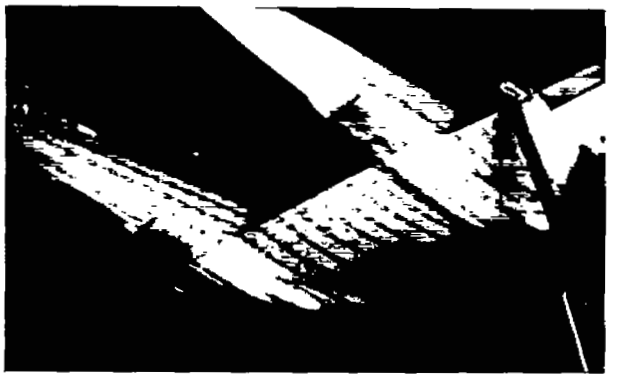

Lowered air scoop.

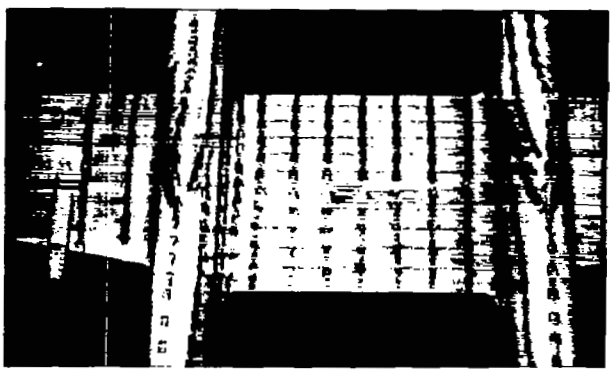

Long-chord center-section extension.

Louvers over air-scoop by-pass exit.

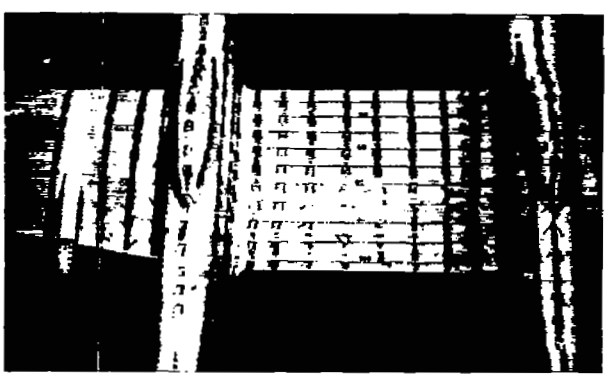

Reflexed trailing-edge center section.

Expanding wing air-scoop juncture fillet.

Figure 19.- Photographs of tufts on the model of the North American XP-82 airplane for several arrangements. M,0.75; α_u, 1°.

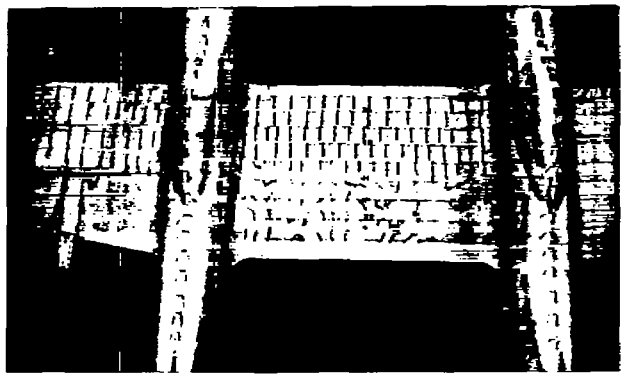

Original center section.

Lowered air scoop.

Louvers over air-scoop
by-pass exit.

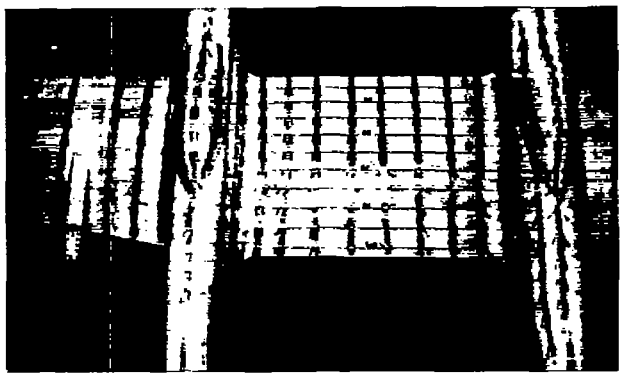

Reflexed trailing-edge
center section.

Expanding wing air-scoop
juncture fillet.

Figure 20.- Photographs of tufts on the model of the North American XP-82 airplane for several arrangements. M,0.775; α_u, 1°.

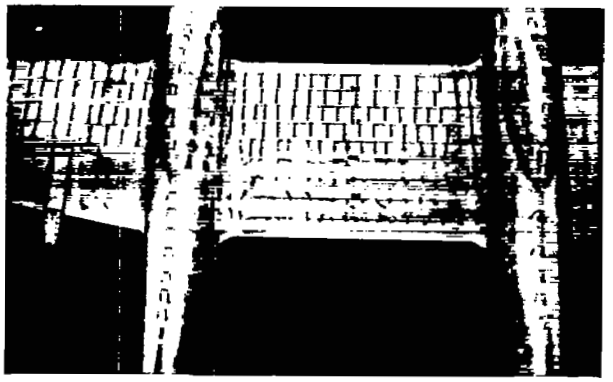

Original center section.

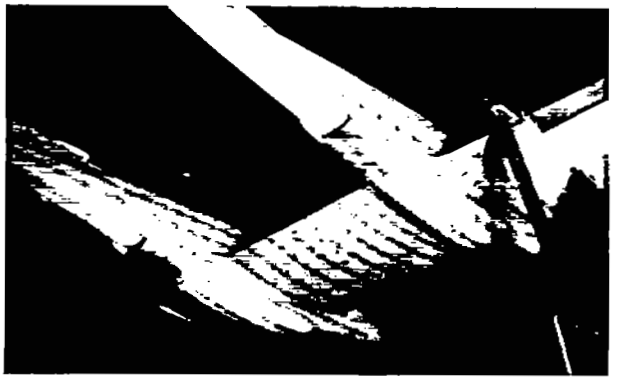

Lowered air scoop.

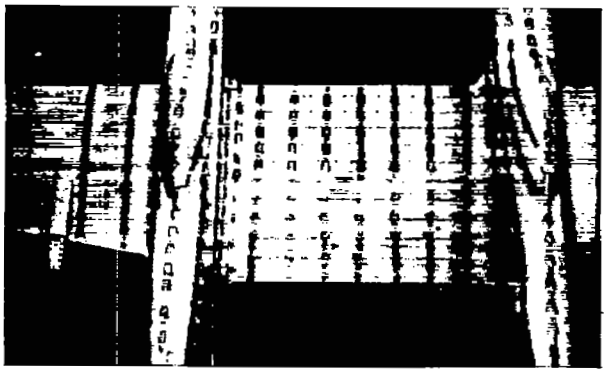

Long-chord center-section extension.

Louvers over air-scoop by-pass exit.

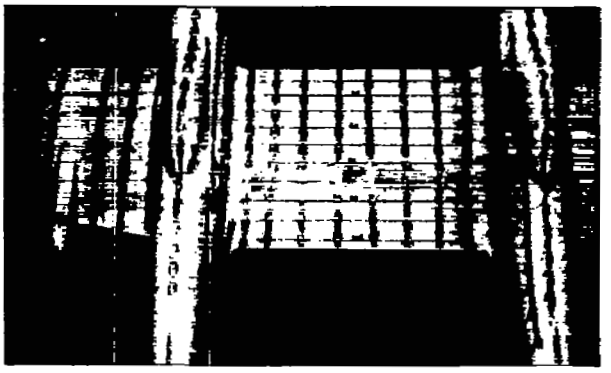

Reflexed trailing-edge center section.

Expanding wing air-scoop juncture fillet.

Figure 21.- Photographs of tufts on the model of the North American XP-82 airplane for several arrangements. M,0.8; α_{t_1}, 1°.

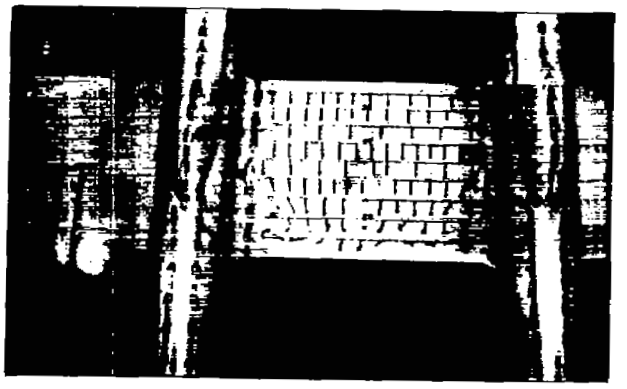

Original center section.

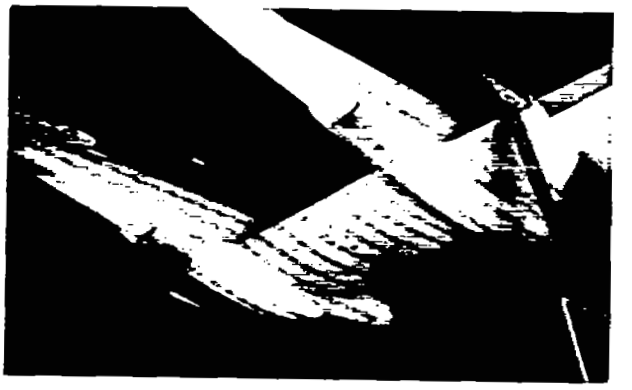

Lowered air scoop.

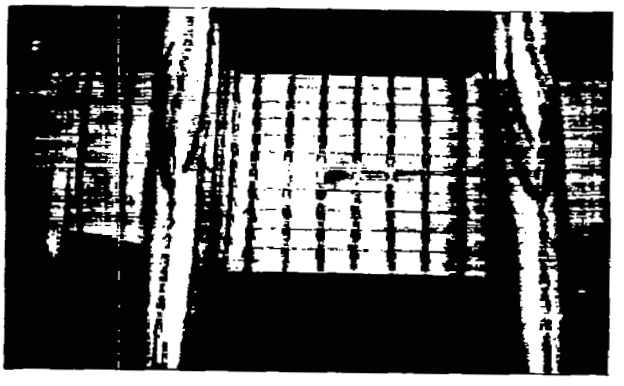

Long-chord center-section extension.

Louvers over air-scoop by-pass exit.

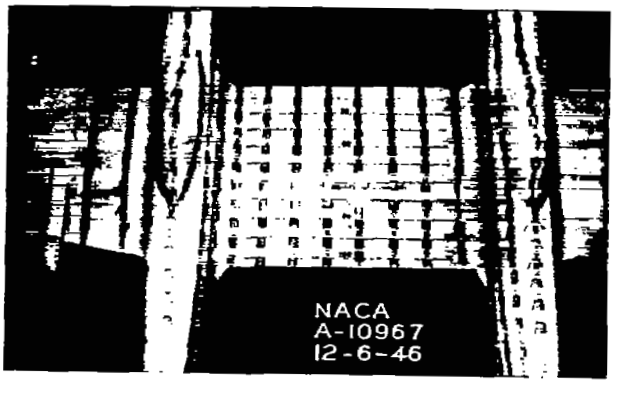

Reflexed trailing-edge center section.

Figure 22.- Photographs of tufts on the model of the North American XP-82 airplane for several arrangements. M,0.70; α_u, 2°.

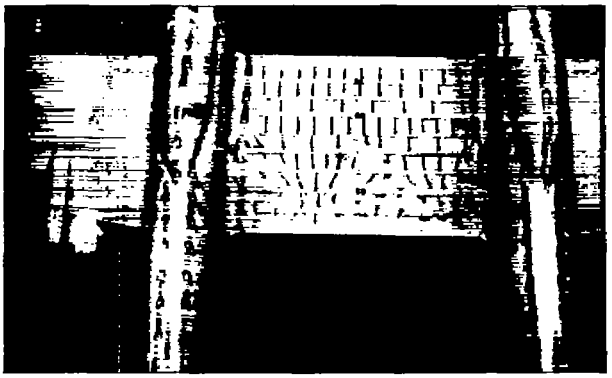

Original center section.

Lowered air scoop.

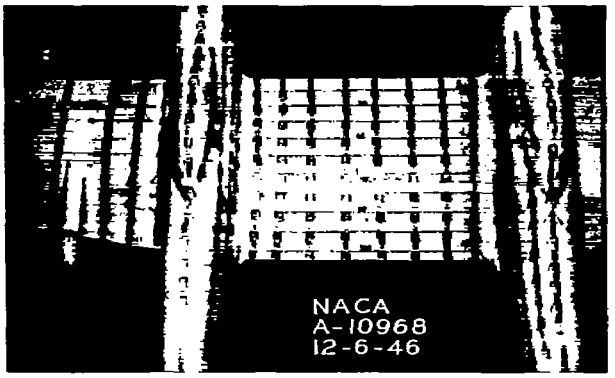

Reflexed trailing-edge
center section.

Figure 23.- Photographs of tufts on the model of the North American XP-82 airplane for several arrangements. M, 0.725; α_u, 2°.

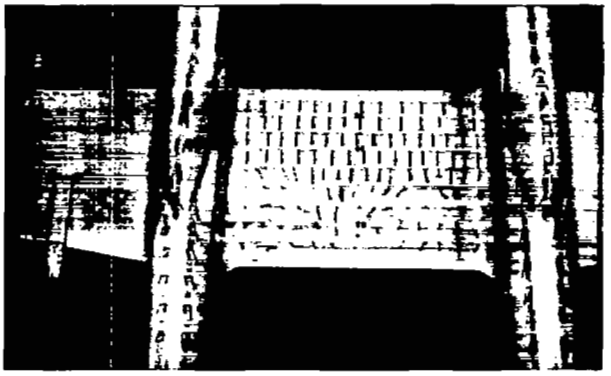

Original center section.

Lowered air scoop.

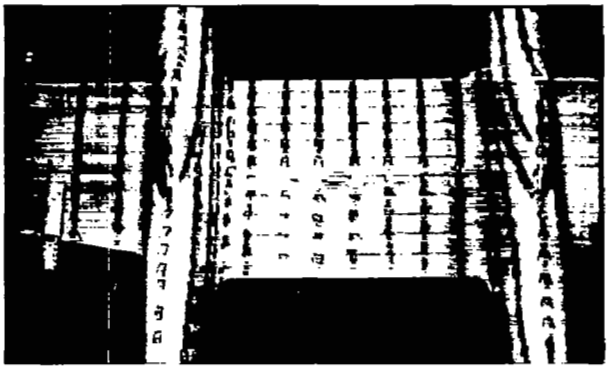

Long-chord center-section extension.

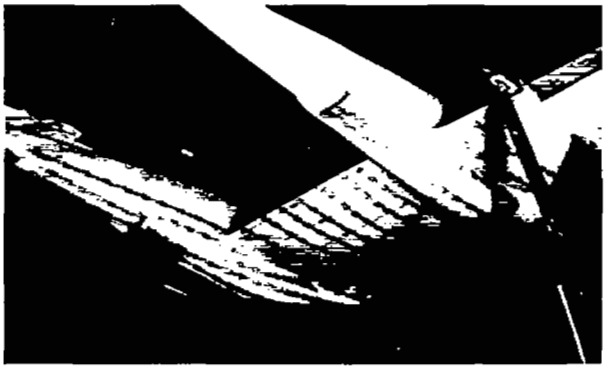

Louvers over air-scoop by-pass exit.

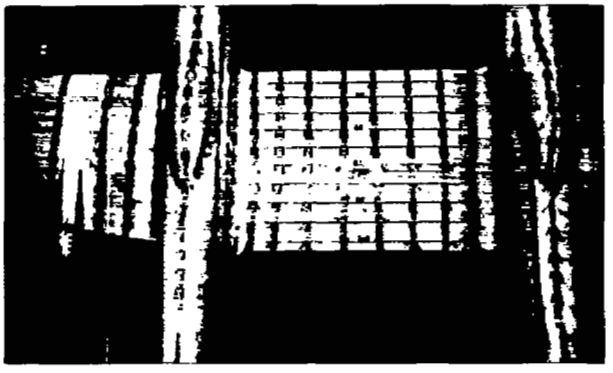

Reflexed trailing-edge center section.

Expanding wing air-scoop juncture fillet.

Figure 24.- Photographs of tufts on the model of the North American XP-82 airplane for several arrangements. M,0.75; a_u, 2°.

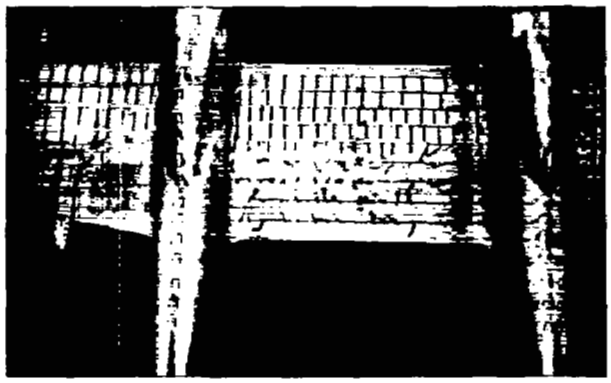

Original center section.

Lowered air scoop.

Louvers over air-scoop
by-pass exit.

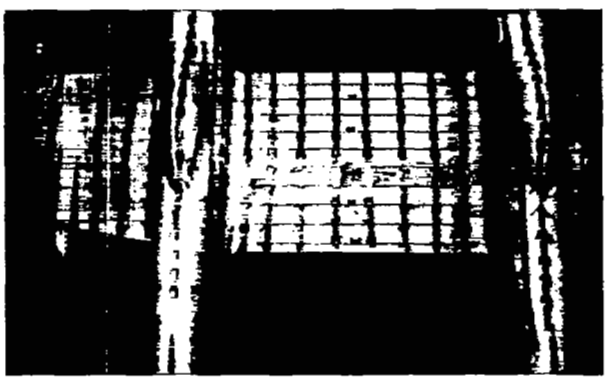

Reflexed trailing-edge
center section.

Expanding wing air-scoop
juncture fillet.

Figure 25.- Photographs of tufts on the model of the North American XP-82 airplane for several arrangements. M, 0.775; α_u, 2°.

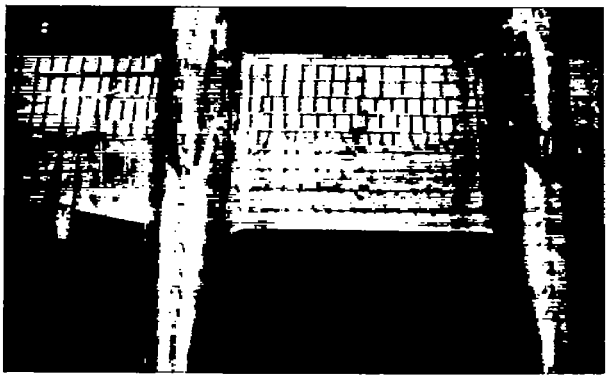

Original center section.

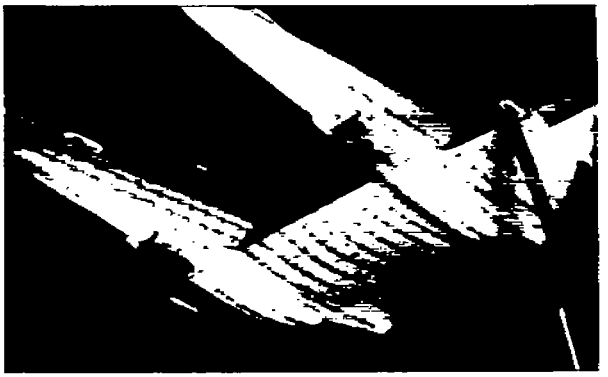

Lowered air scoop.

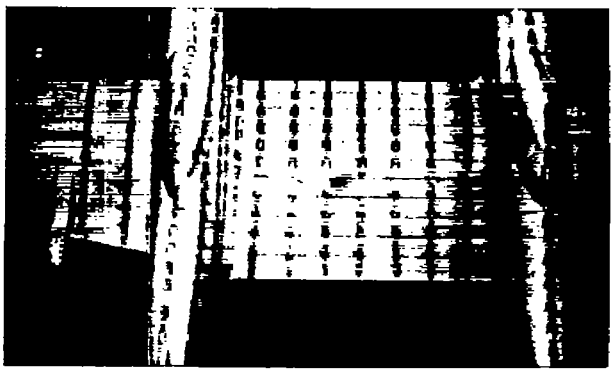

Long-chord center-section extension.

Louvers over air-scoop by-pass exit.

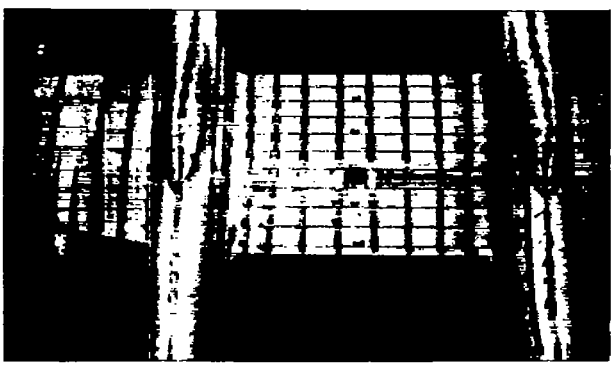

Reflexed trailing-edge center section

Expanding wing air-scoop juncture fillet.

Figure 26.- Photographs of tufts on the model of the North American XP-82 airplane for several arrangements. M,0.8; α_u, 2°.

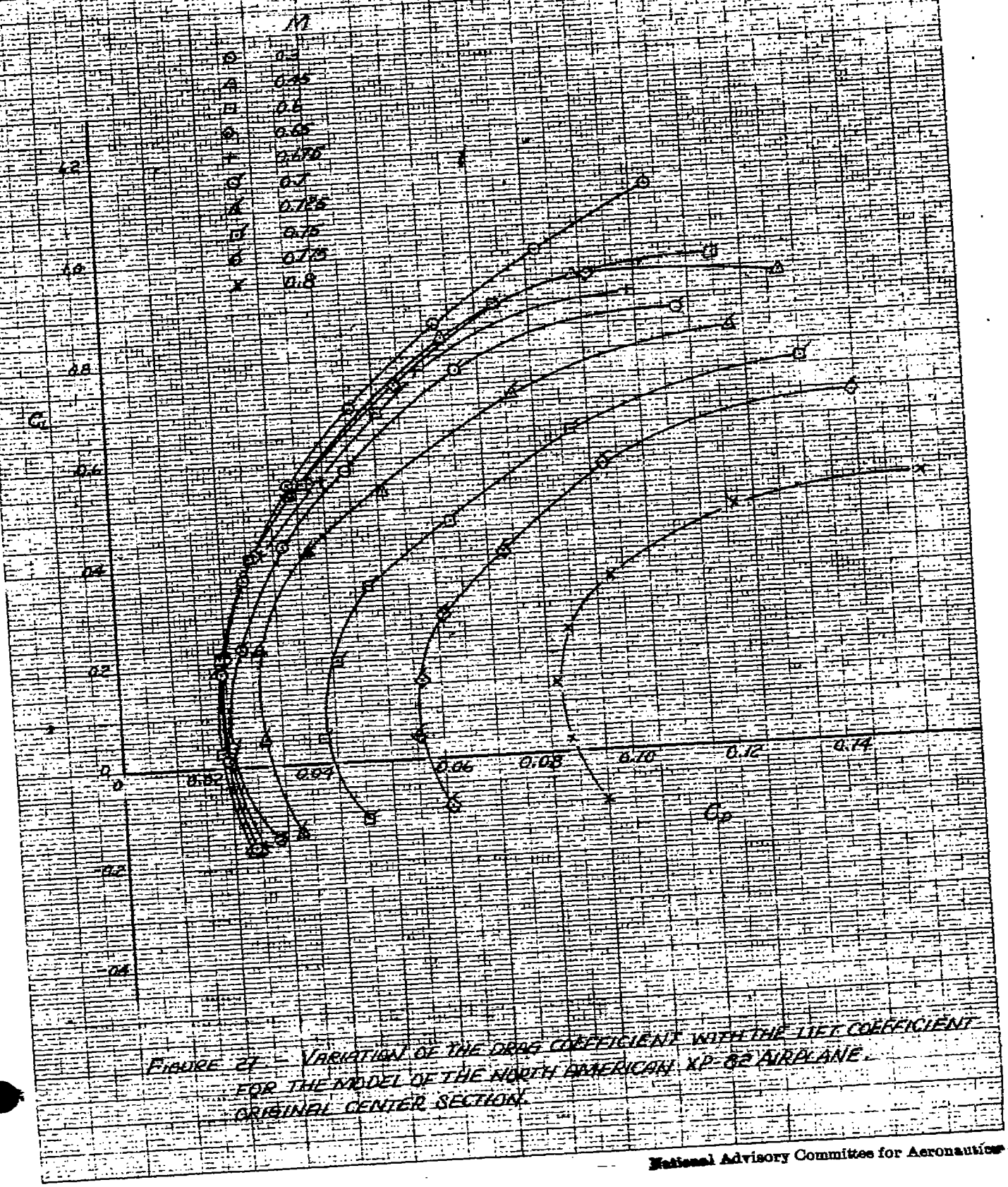

FIGURE 27 — VARIATION OF THE DRAG COEFFICIENT WITH THE LIFT COEFFICIENT FOR THE MODEL OF THE NORTH AMERICAN XP-82 AIRPLANE. ORIGINAL CENTER SECTION.

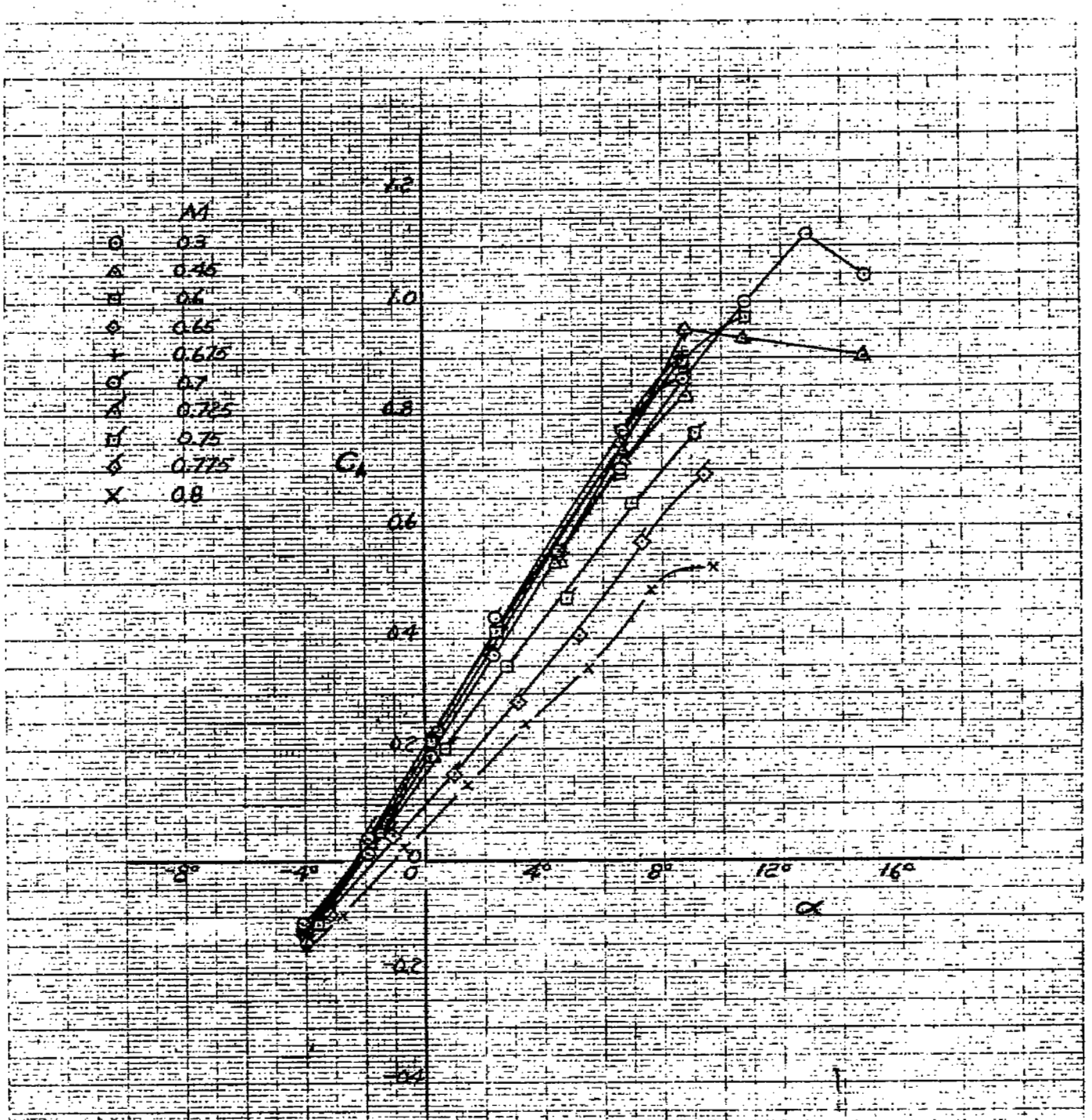

FIGURE 28. – VARIATION OF THE LIFT COEFFICIENT WITH THE ANGLE OF ATTACK FOR THE MODEL OF THE NORTH AMERICAN XP-82 AIRPLANE. ORIGINAL CENTER SECTION.

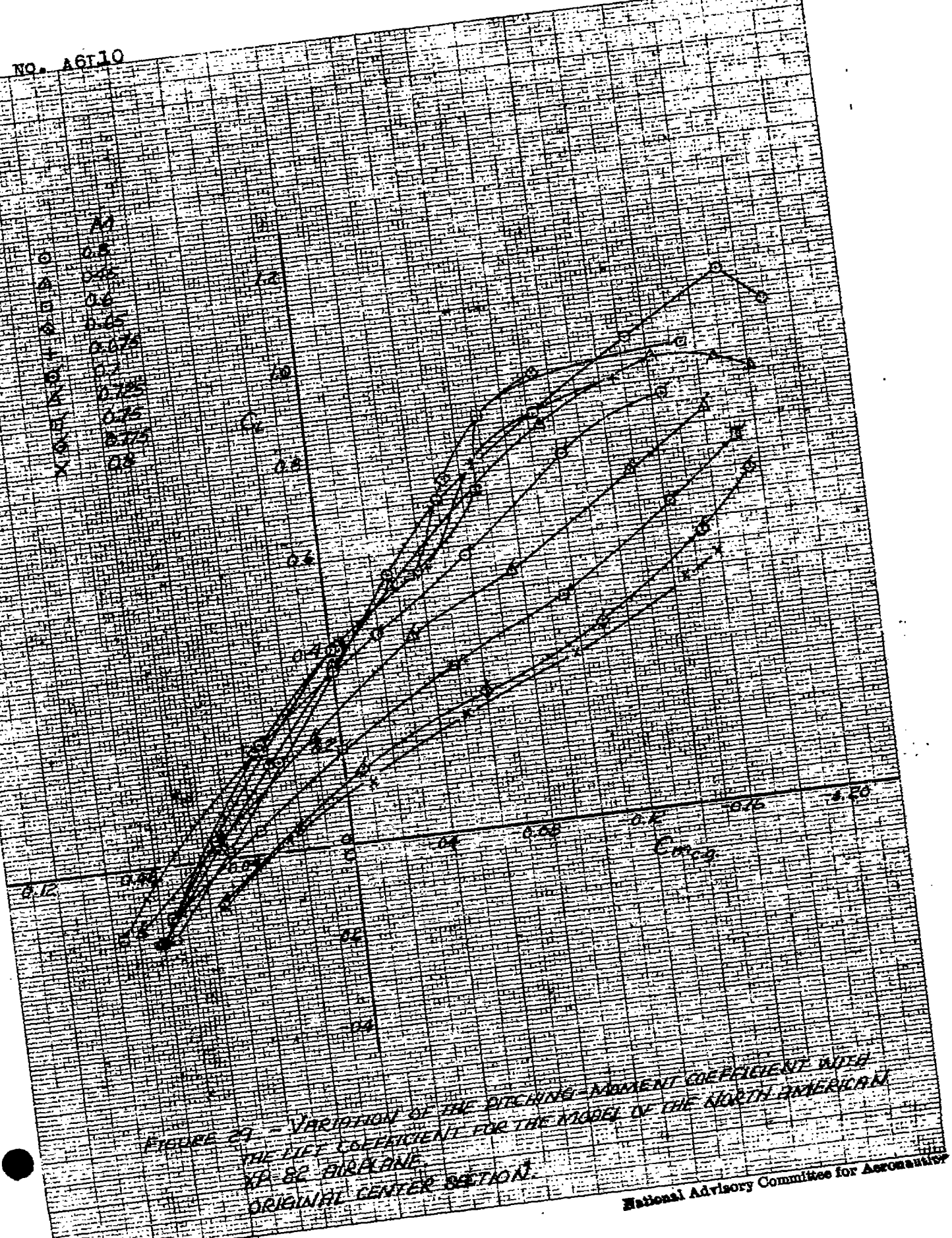

FIGURE 29 - VARIATION OF THE PITCHING-MOMENT COEFFICIENT WITH THE LIFT COEFFICIENT FOR THE MODEL OF THE NORTH AMERICAN XP-82 AIRPLANE. ORIGINAL CENTER SECTION.

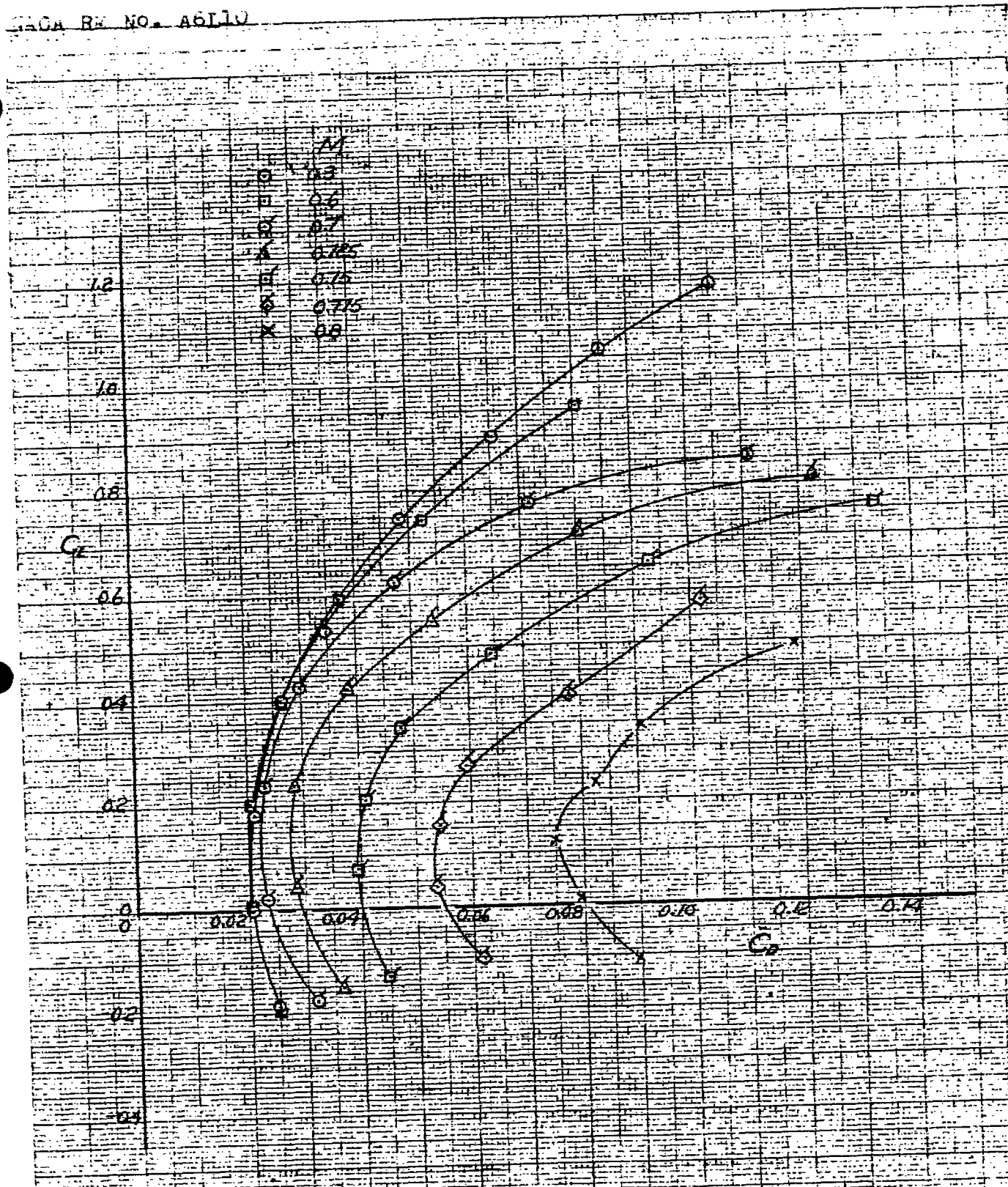

FIGURE 30 - VARIATION OF THE DRAG COEFFICIENT WITH THE LIFT COEFFICIENT FOR THE MODEL OF THE NORTH AMERICAN XP-82 AIRPLANE LONG-CHORD CENTER SECTION EXTENSION

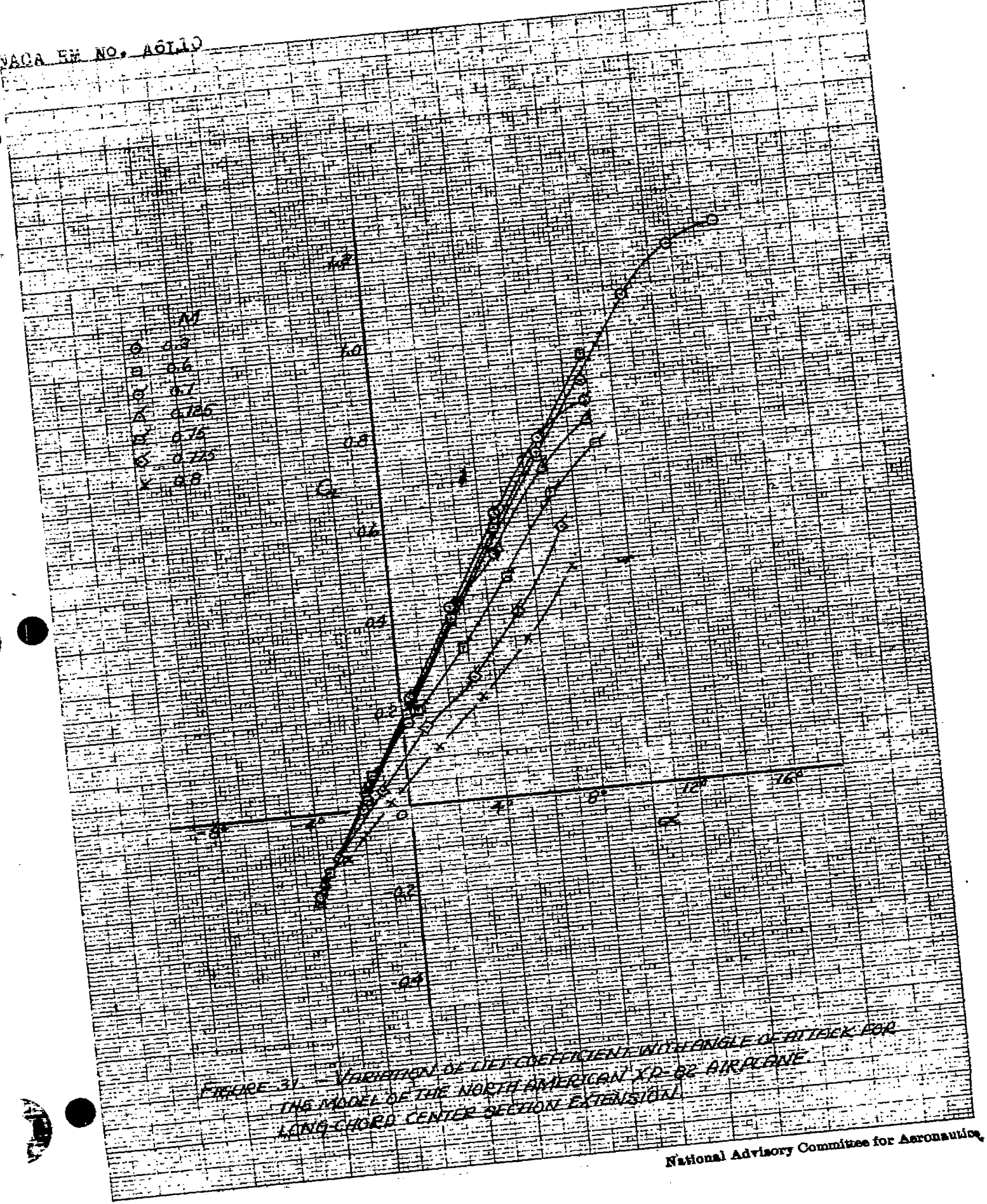

FIGURE 31. — VARIATION OF LIFT COEFFICIENT WITH ANGLE OF ATTACK FOR THE MODEL OF THE NORTH AMERICAN XP-82 AIRPLANE. LONG-CHORD CENTER SECTION EXTENSION.

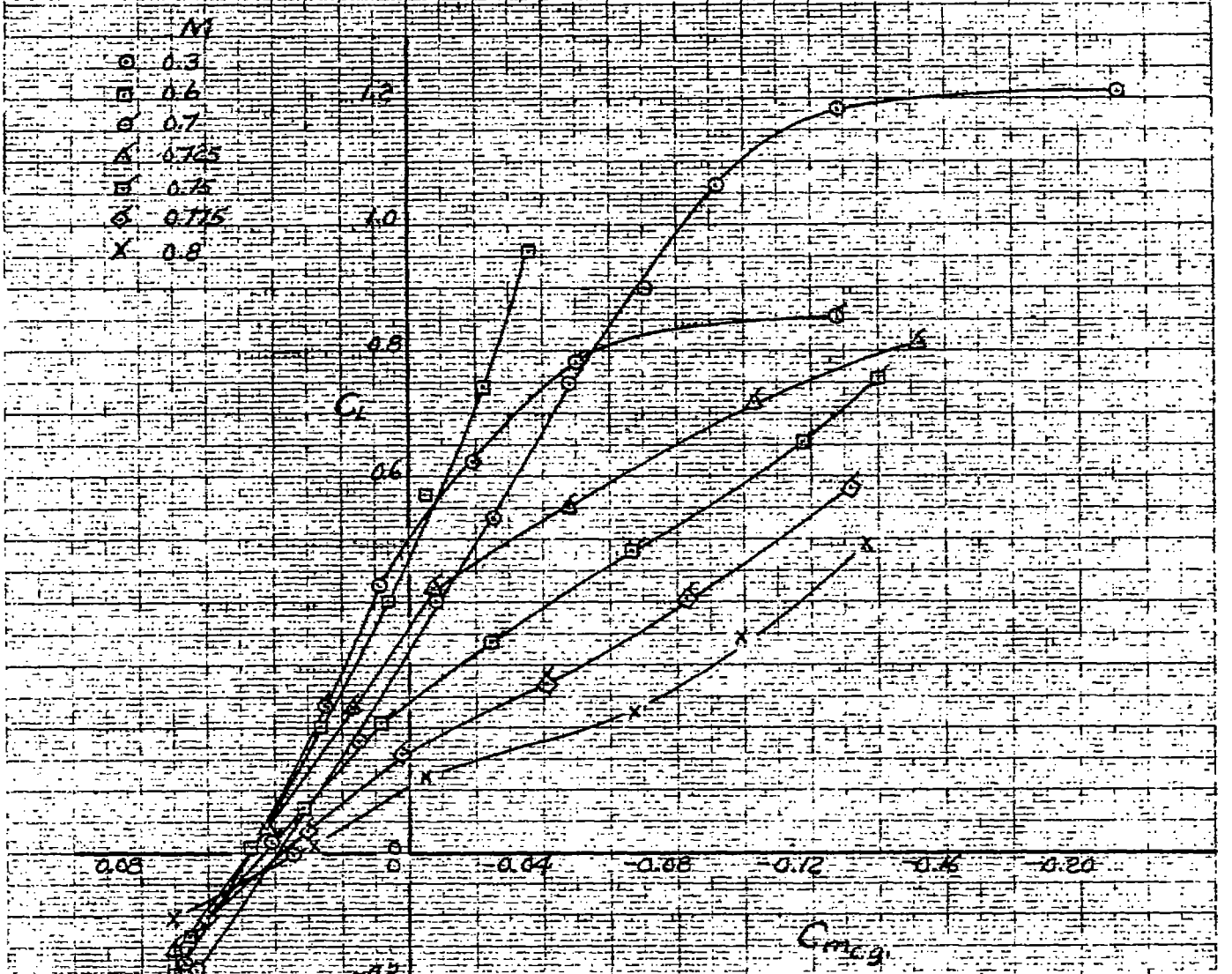

FIGURE 32 - VARIATION OF PITCHING-MOMENT COEFFICIENT WITH LIFT COEFFICIENT FOR THE MODEL OF THE NORTH AMERICAN XP-82 AIRPLANE.
LONG-CHORD CENTER SECTION EXTENSION.

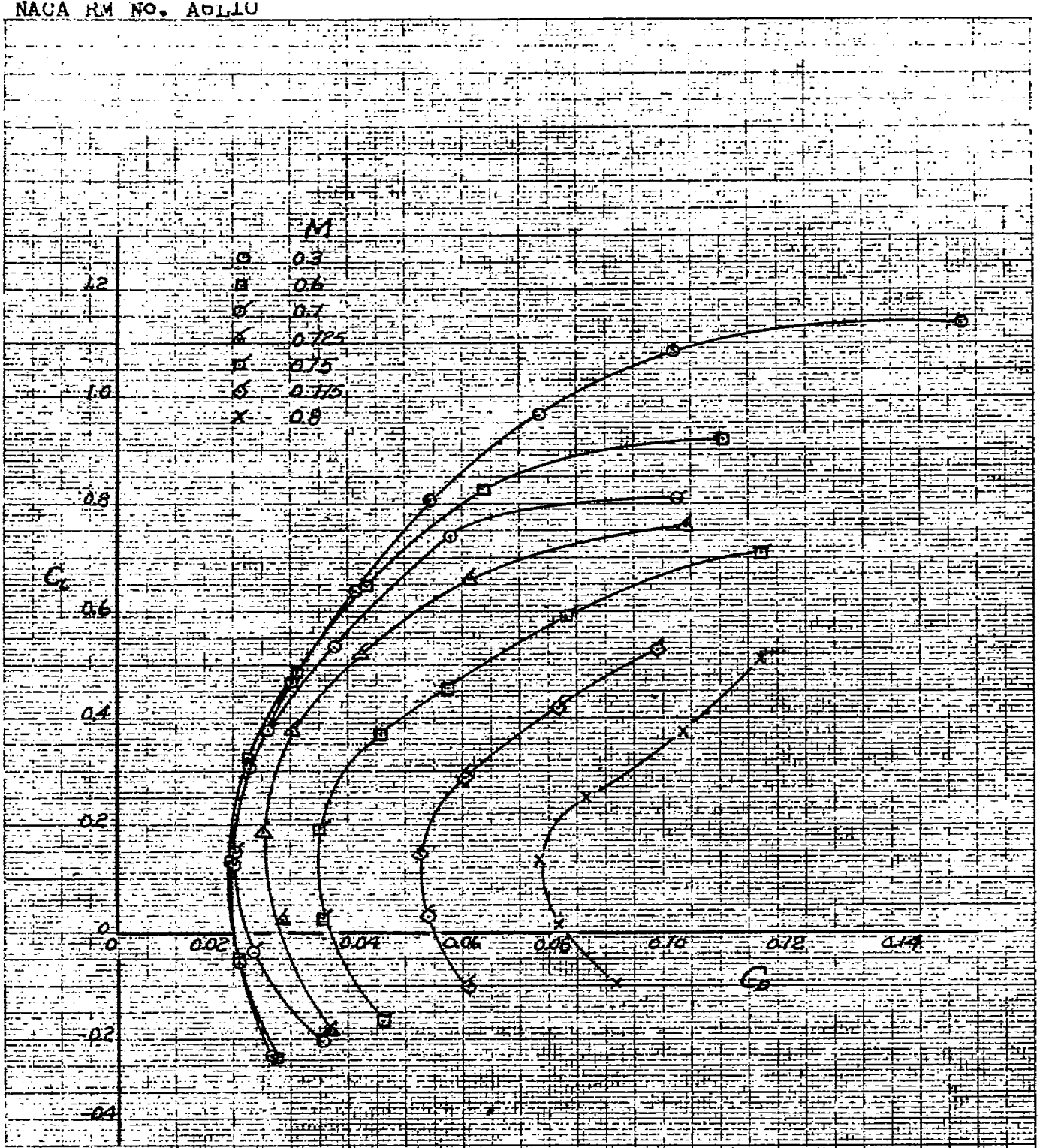

FIGURE 33.- VARIATION OF DRAG COEFFICIENT WITH LIFT COEFFICIENT FOR THE MODEL OF THE NORTH AMERICAN XP-82 AIRPLANE. REFLEXED TRAILING-EDGE CENTER SECTION.

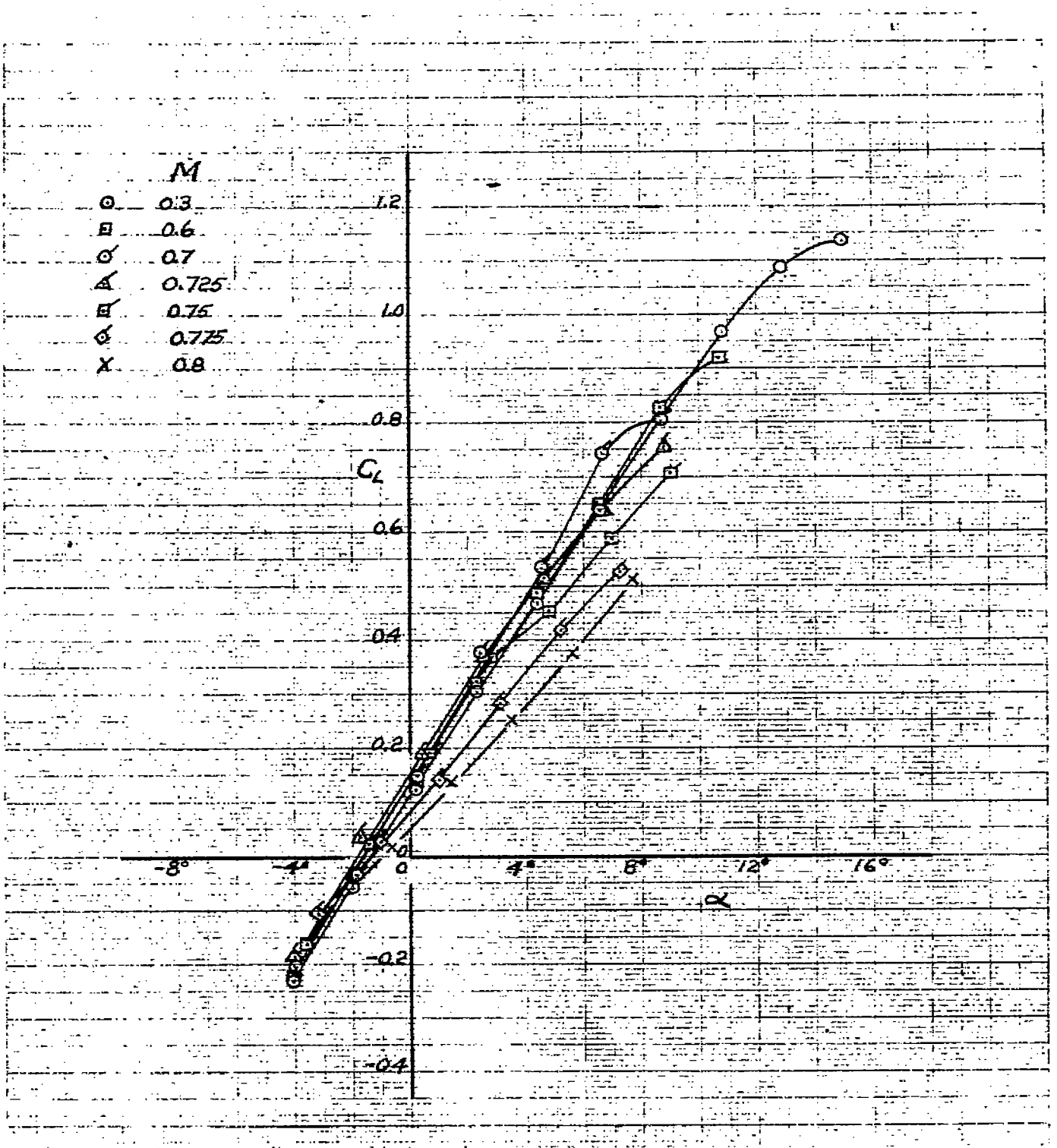

FIGURE 34.— VARIATION OF LIFT COEFFICIENT WITH ANGLE OF ATTACK FOR THE MODEL OF THE NORTH AMERICAN XP-82 AIRPLANE. REFLEXED TRAILING-EDGE CENTER SECTION.

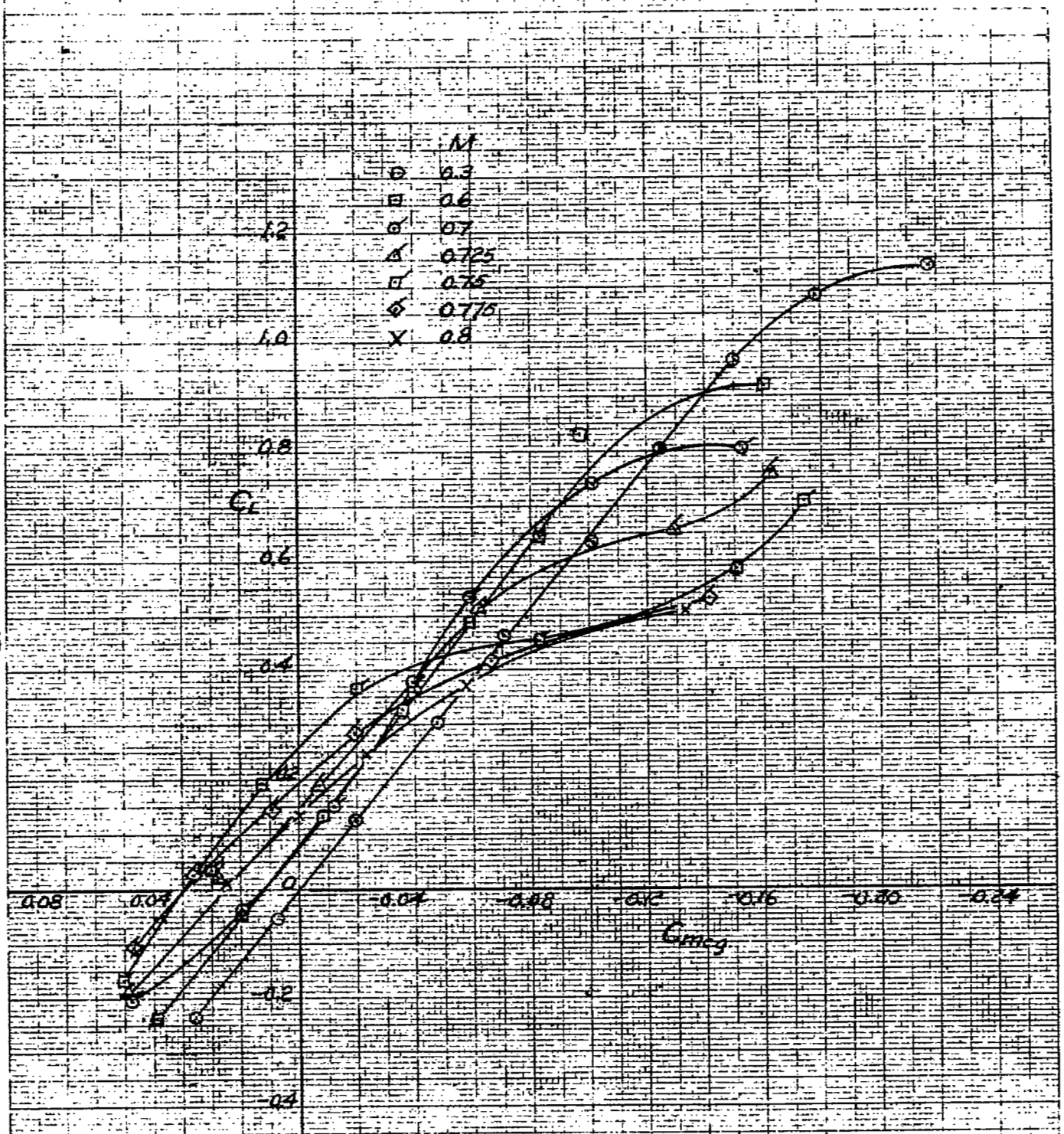

FIGURE 35 - VARIATION OF PITCHING-MOMENT COEFFICIENT WITH LIFT COEFFICIENT FOR THE MODEL OF THE NORTH AMERICAN XP-82 AIRPLANE. REFLEXED TRAILING-EDGE CENTER SECTION

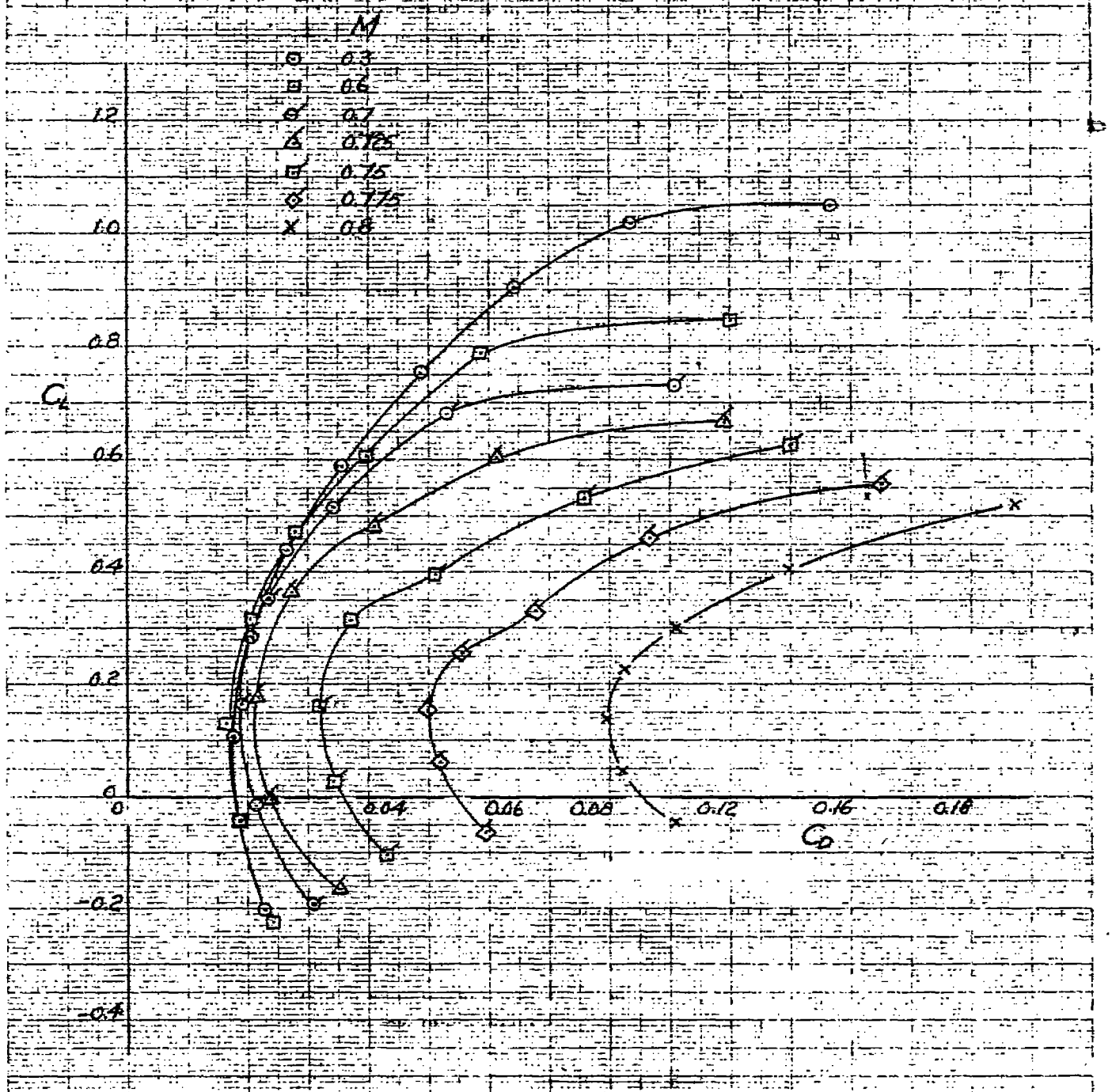

FIGURE 36.- VARIATION OF DRAG COEFFICIENT WITH LIFT COEFFICIENT FOR THE MODEL OF THE NORTH AMERICAN XP-82 AIRPLANE LESS THE EMPENNAGE. REFLEXED TRAILING-EDGE CENTER SECTION.

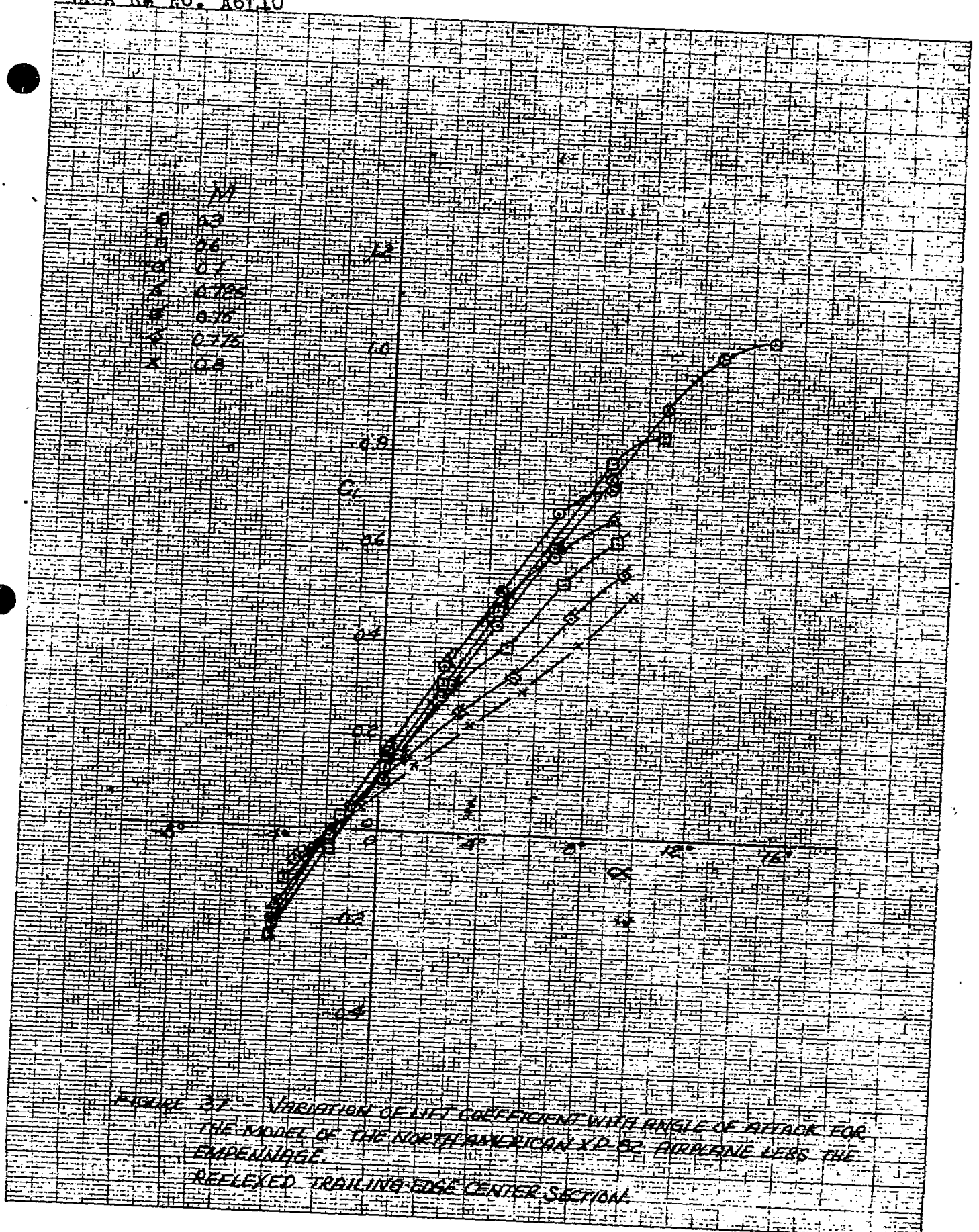

FIGURE 37 - VARIATION OF LIFT COEFFICIENT WITH ANGLE OF ATTACK FOR THE MODEL OF THE NORTH AMERICAN X-D-82 AIRPLANE WITH THE EMPENNAGE.
REFLEXED TRAILING EDGE CENTER SECTION.

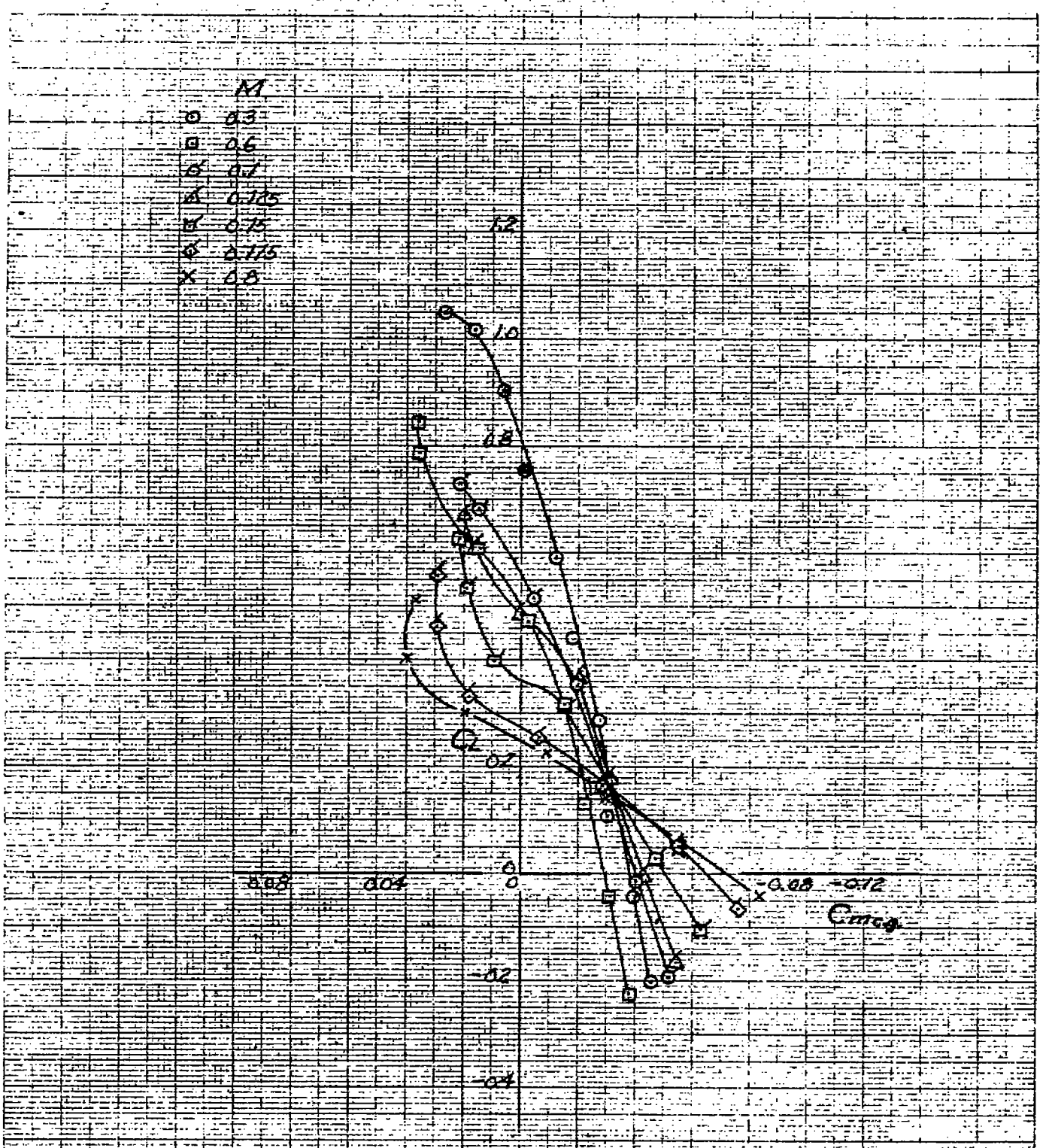

FIGURE 38.- VARIATION OF THE PITCHING-MOMENT COEFFICIENT WITH THE LIFT COEFFICIENT FOR THE MODEL OF THE NORTH AMERICAN XP-82 AIRPLANE LESS THE EMPENNAGE. REFLEXED TRAILING-EDGE CENTER SECTION.

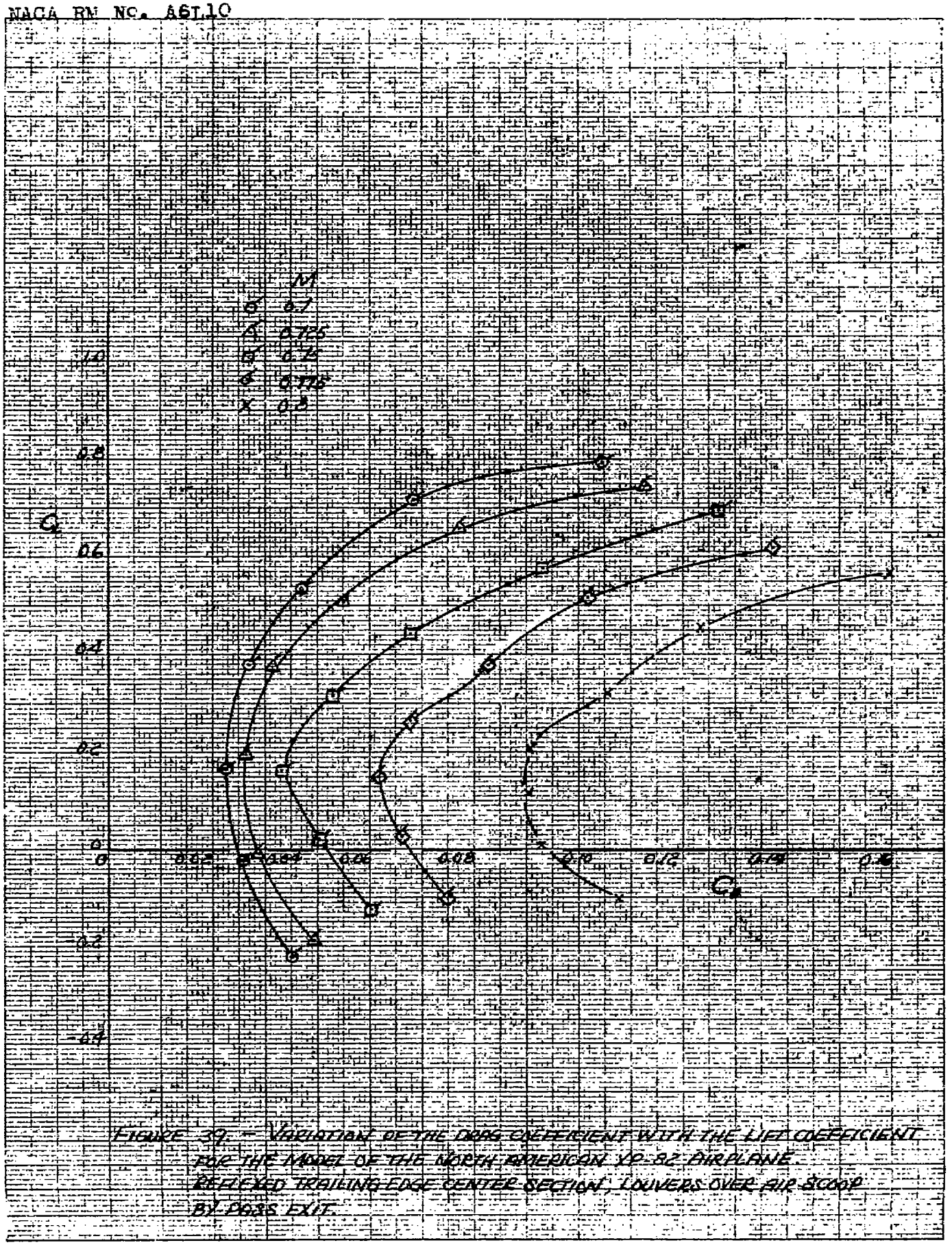

FIGURE 39. - VARIATION OF THE DRAG COEFFICIENT WITH THE LIFT COEFFICIENT FOR THE MODEL OF THE NORTH AMERICAN XP-82 AIRPLANE. REFLEXED TRAILING-EDGE CENTER SECTION, LOUVERS OVER AIR SCOOP BY DOORS EXIT.

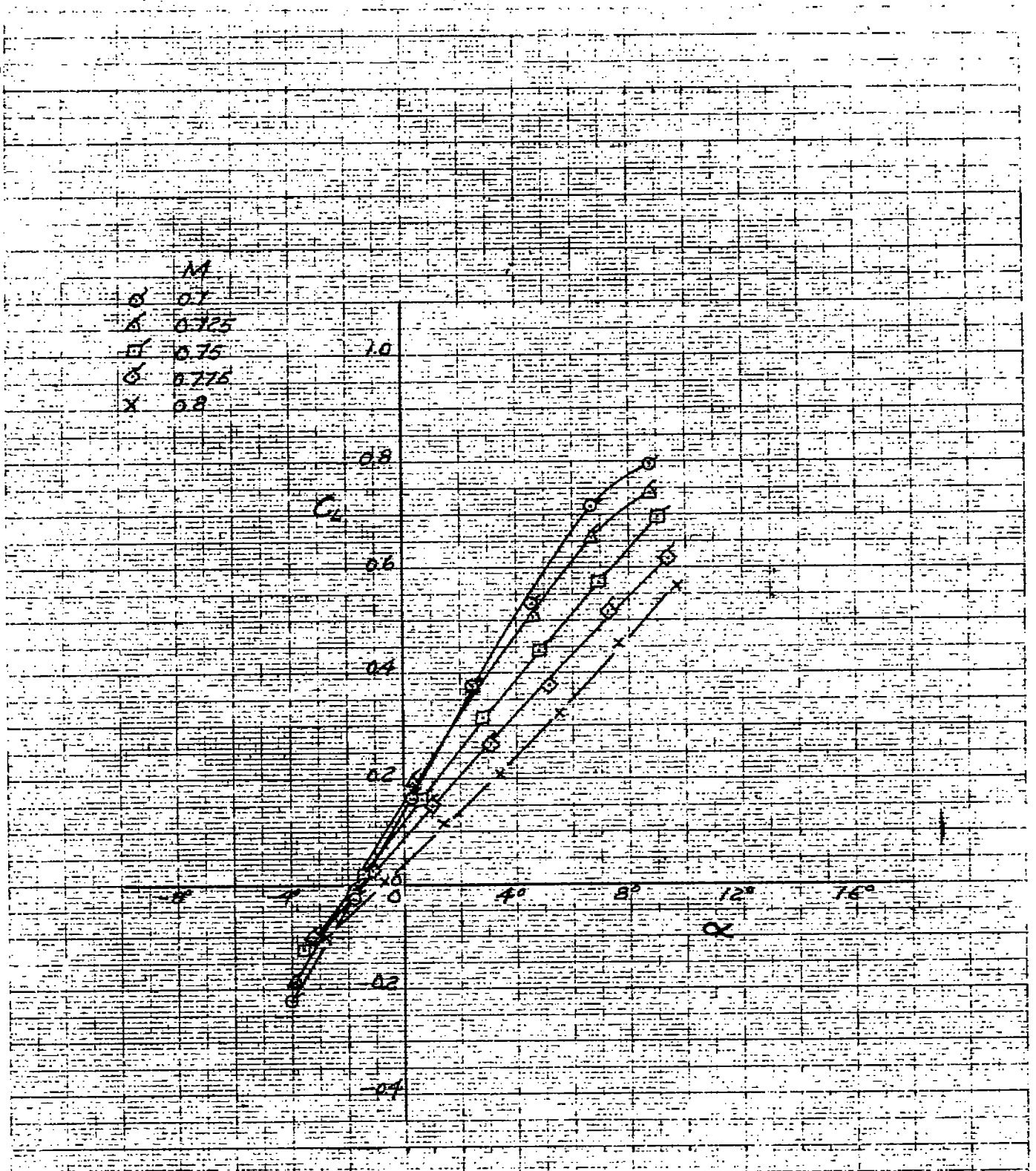

FIGURE 40 – VARIATION OF THE LIFT COEFFICIENT WITH ANGLE OF ATTACK FOR THE MODEL OF THE NORTH AMERICAN XP-82 AIRPLANE. REFLEXED TRAILING-EDGE CENTER SECTION; LOUVERS OVER AIR-SCOOP BY-PASS EXIT.

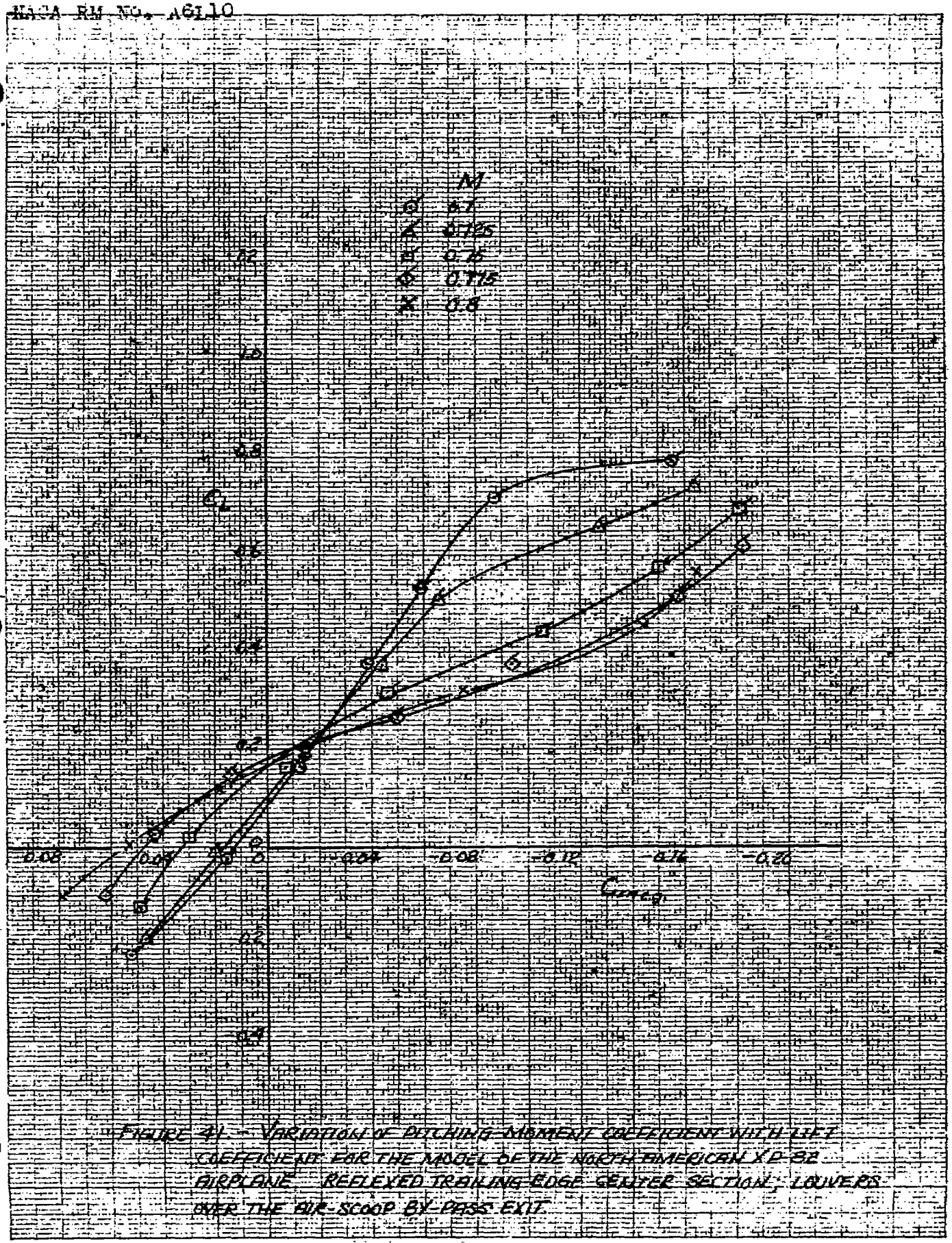

FIGURE 41.- VARIATION OF PITCHING-MOMENT COEFFICIENT WITH LIFT COEFFICIENT FOR THE MODEL OF THE NORTH AMERICAN XP-82 AIRPLANE. REFLEXED TRAILING EDGE CENTER SECTION; LOUVERS OVER THE AIR-SCOOP BY-PASS EXIT.

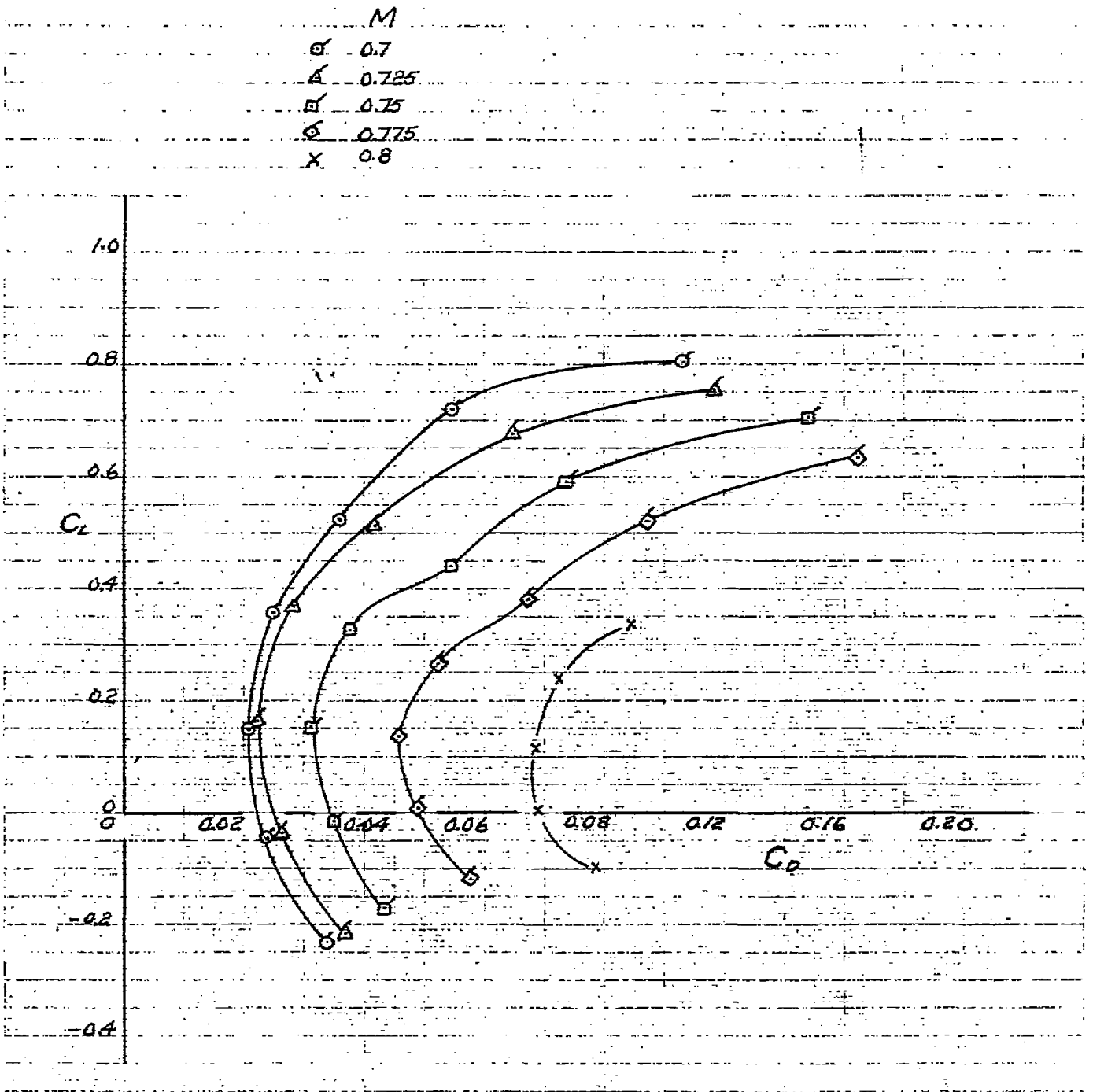

FIGURE 42. — VARIATION OF DRAG COEFFICIENT WITH LIFT COEFFICIENT FOR THE MODEL OF THE NORTH AMERICAN XP-82 AIRPLANE. REFLEXED TRAILING-EDGE CENTER SECTION; EXPANDING WING - AIR SCOOP FILLET.

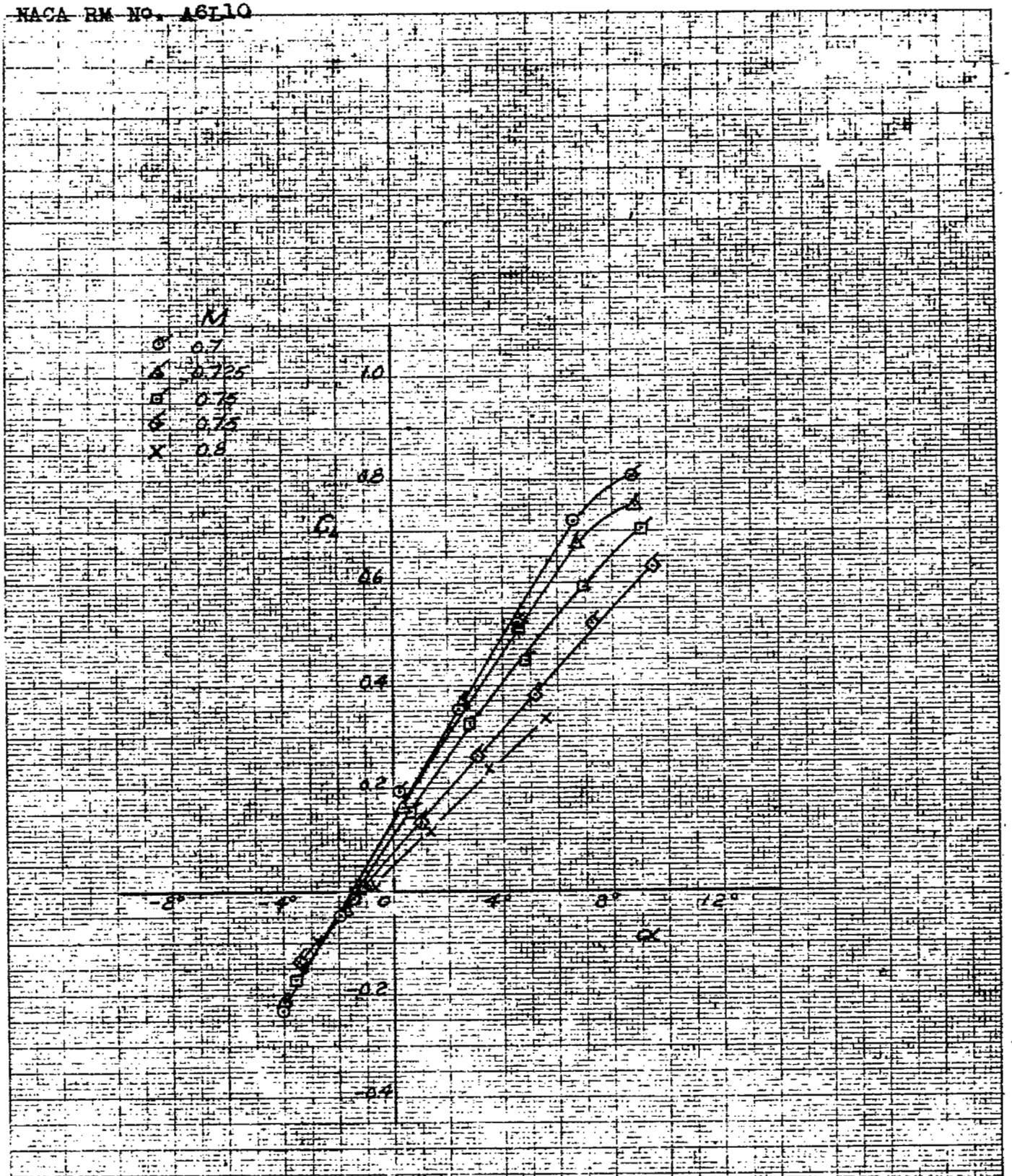

FIGURE 43. – VARIATION OF LIFT COEFFICIENT WITH ANGLE OF ATTACK FOR THE MODEL OF THE NORTH AMERICAN XB-70 AIRPLANE. REFLEXED TRAILING-EDGE CENTER SECTION; EXPANDING WING - AIR SCOOP FILLET.

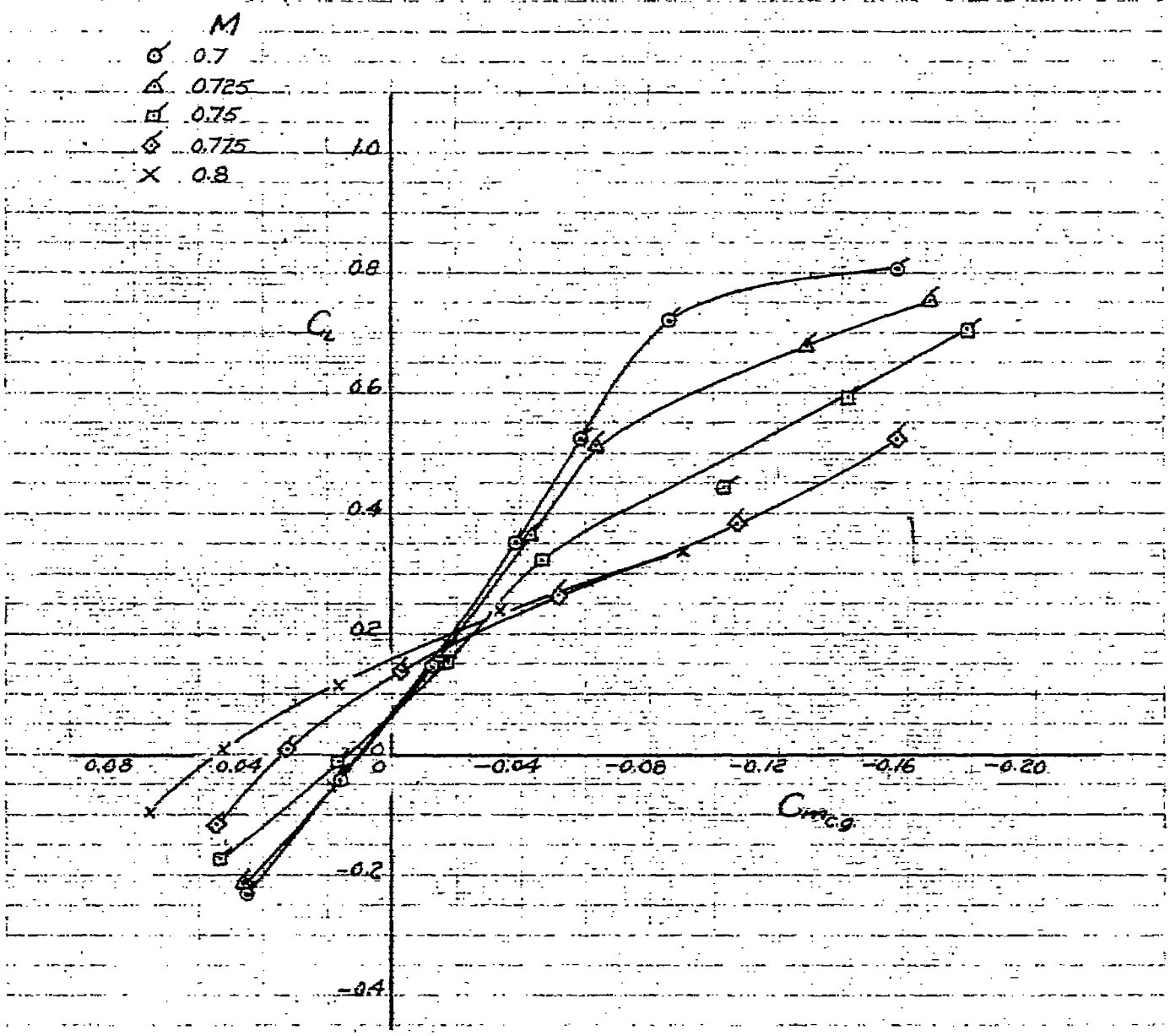

FIGURE 44. – VARIATION OF PITCHING-MOMENT COEFFICIENT WITH LIFT COEFFICIENT FOR THE MODEL OF THE NORTH AMERICAN XB-82 AIRPLANE. REFLEXED TRAILING-EDGE CENTER SECTION; EXPANDING WING – AIR SCOOP FILLET.

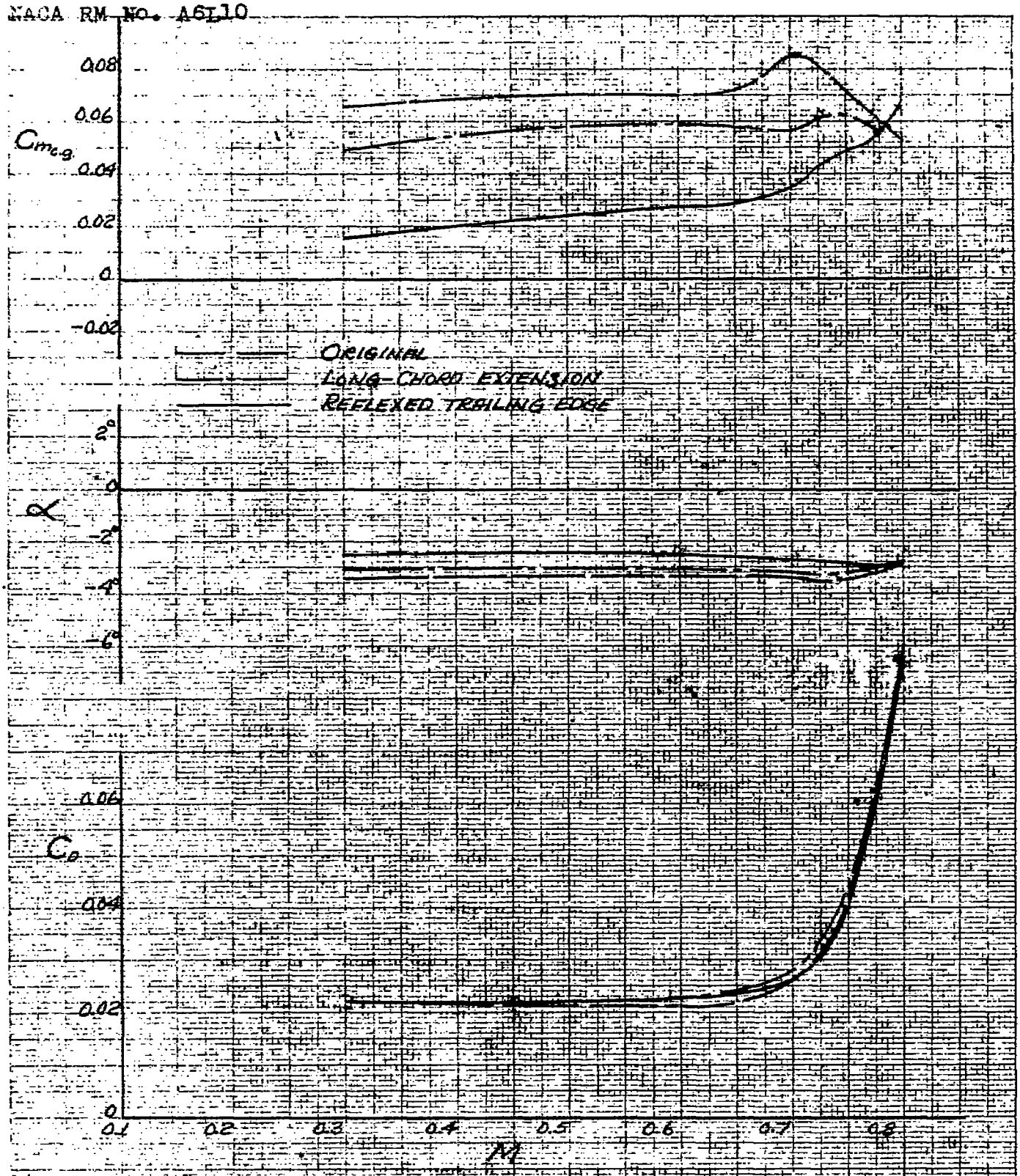

FIGURE 45.- VARIATION OF THE PITCHING-MOMENT COEFFICIENT, DRAG COEFFICIENT, AND ANGLE OF ATTACK WITH MACH NUMBER FOR SEVERAL CENTER SECTION TRAILING EDGES ON THE MODEL OF THE NORTH AMERICAN XP-82 AIRPLANE. C_L = 0.1

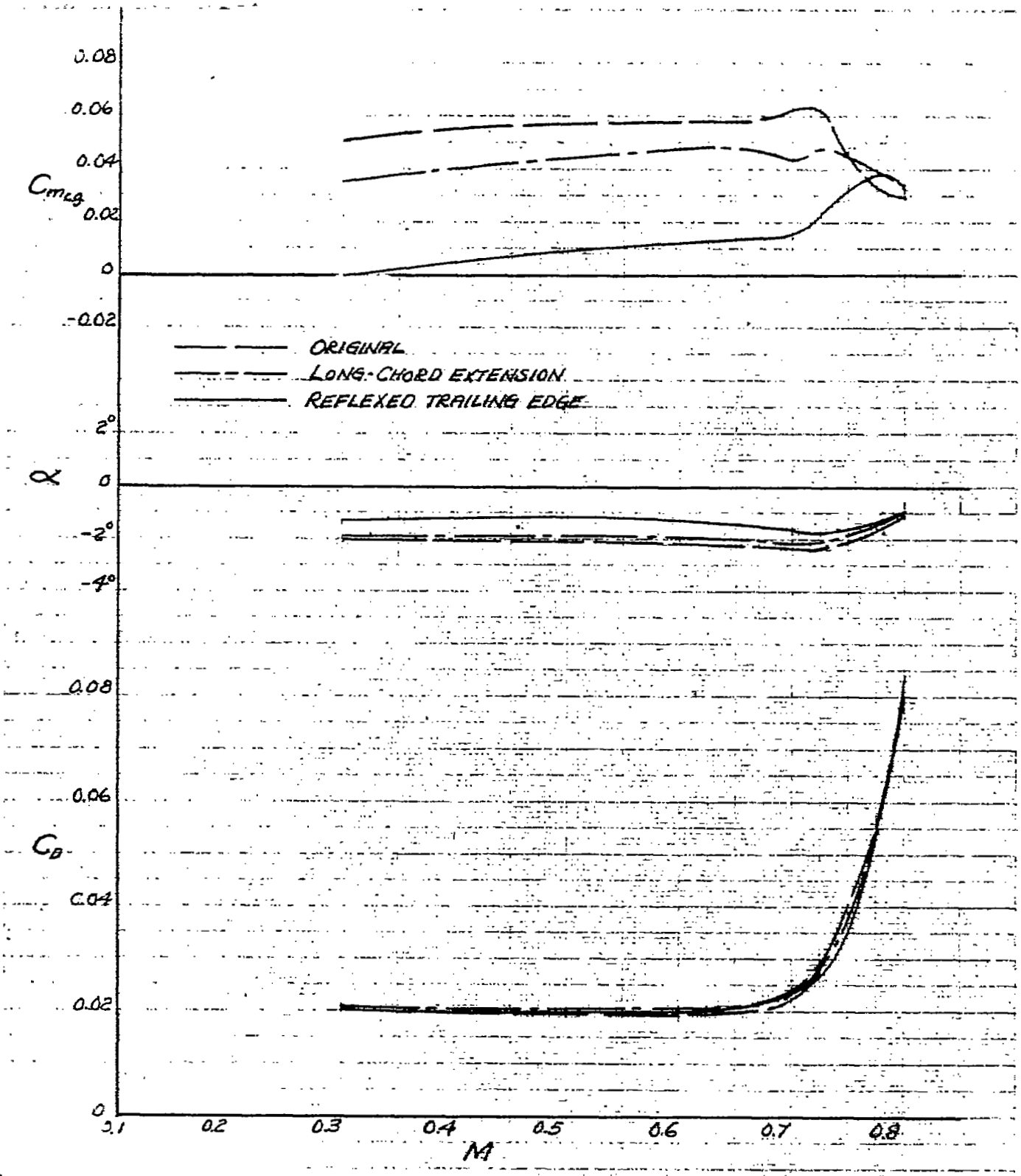

FIGURE 46. — VARIATION OF PITCHING-MOMENT COEFFICIENT, DRAG COEFFICIENT, AND ANGLE OF ATTACK WITH MACH NUMBER FOR SEVERAL CENTER-SECTION TRAILING EDGES ON THE MODEL OF THE NORTH AMERICAN XP-82 AIRPLANE. C_L, 0.0.

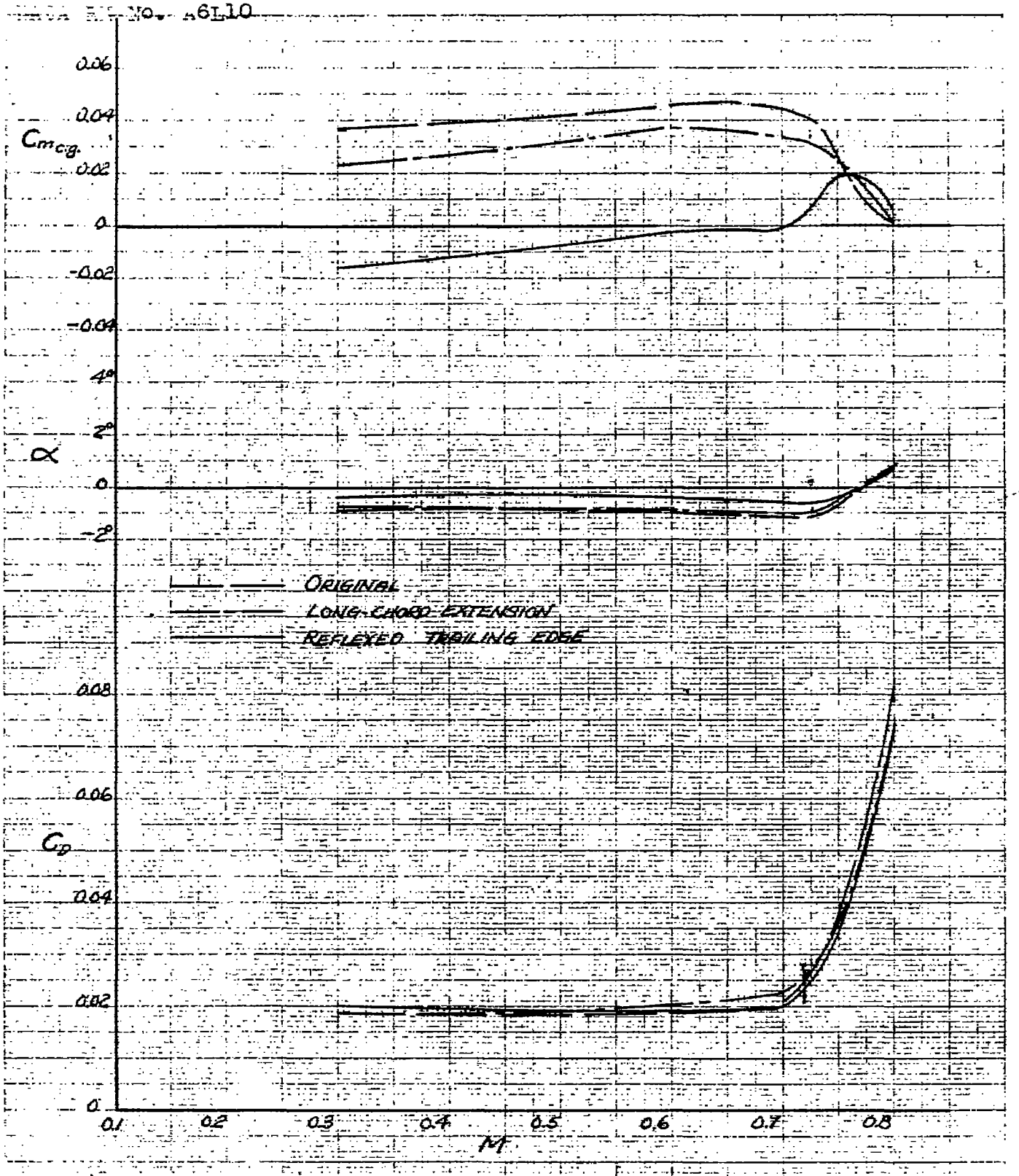

FIGURE 47. – VARIATION OF PITCHING-MOMENT COEFFICIENT, DRAG COEFFICIENT, AND ANGLE OF ATTACK WITH MACH NUMBER FOR SEVERAL CENTER SECTION TRAILING EDGES ON THE MODEL OF THE NORTH AMERICAN XP-82 AIRPLANE. C_L 0.1

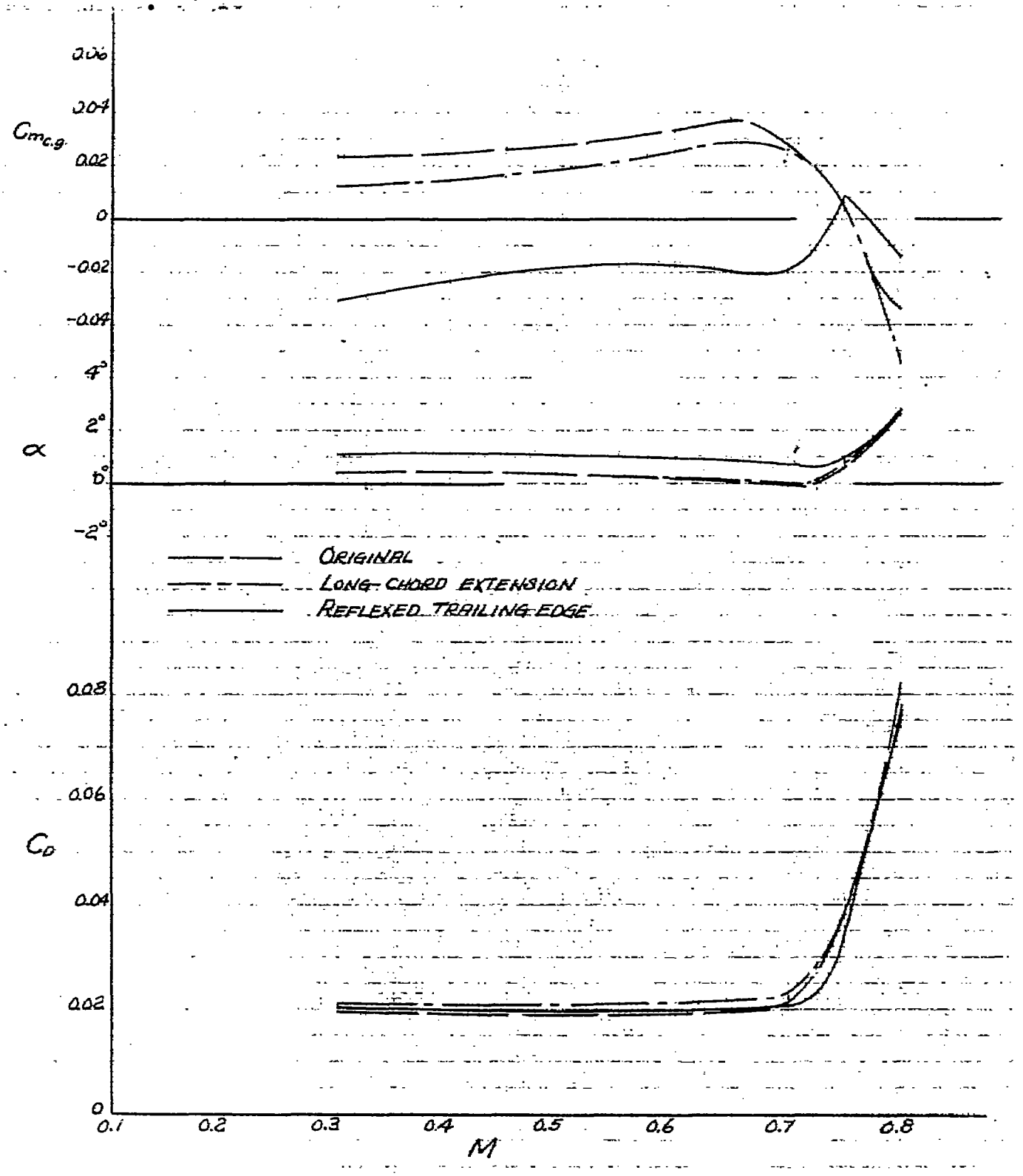

FIGURE 48. — VARIATION OF PITCHING-MOMENT COEFFICIENT, DRAG COEFFICIENT, AND ANGLE OF ATTACK WITH MACH NUMBER FOR SEVERAL CENTER SECTION TRAILING EDGES ON THE MODEL OF THE NORTH AMERICAN XP-82 AIRPLANE. C_L . 0.2 .

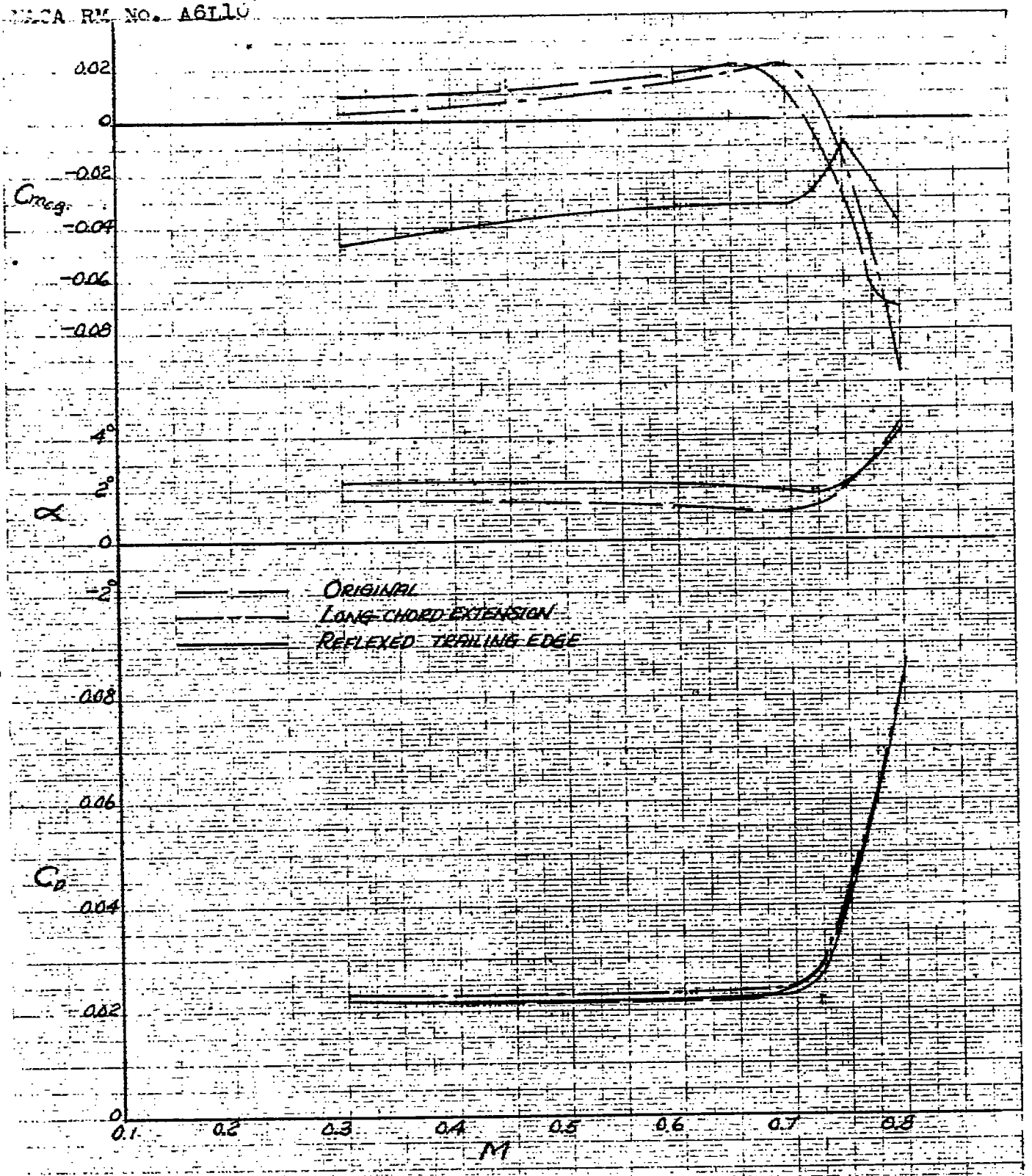

FIGURE 49. — VARIATION OF PITCHING-MOMENT COEFFICIENT, DRAG COEFFICIENT, AND ANGLE OF ATTACK WITH MACH NUMBER FOR SEVERAL CENTER-SECTION TRAILING EDGES ON THE MODEL OF THE NORTH AMERICAN XP-82 AIRPLANE. C_L, 0.3.

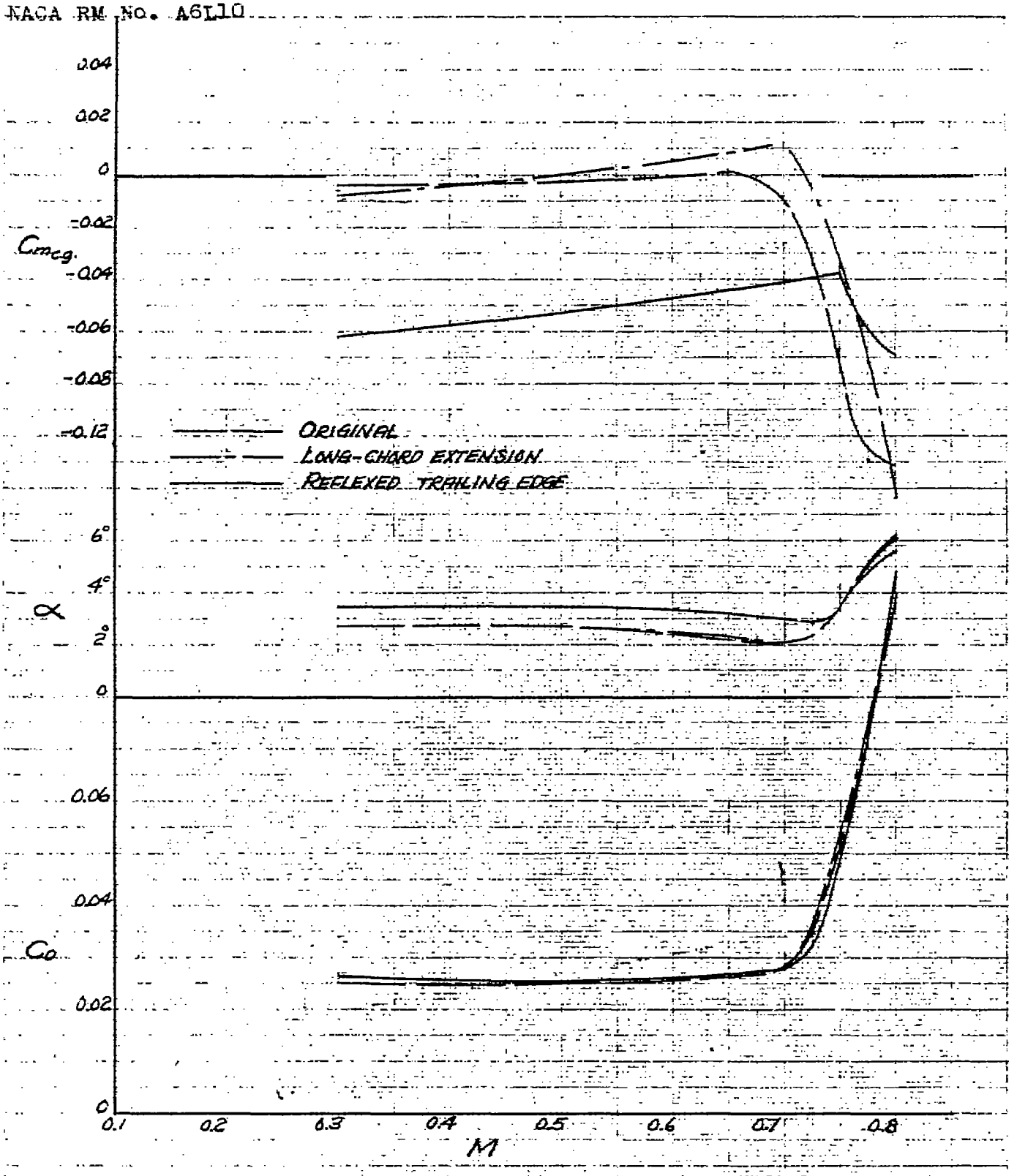

FIGURE 50. — VARIATION OF PITCHING-MOMENT COEFFICIENT, DRAG COEFFICIENT, AND ANGLE OF ATTACK WITH MACH NUMBER FOR SEVERAL CENTER-SECTION TRAILING EDGES ON THE MODEL OF THE NORTH AMERICAN XP-82 AIRPLANE. C_L, 0.4.

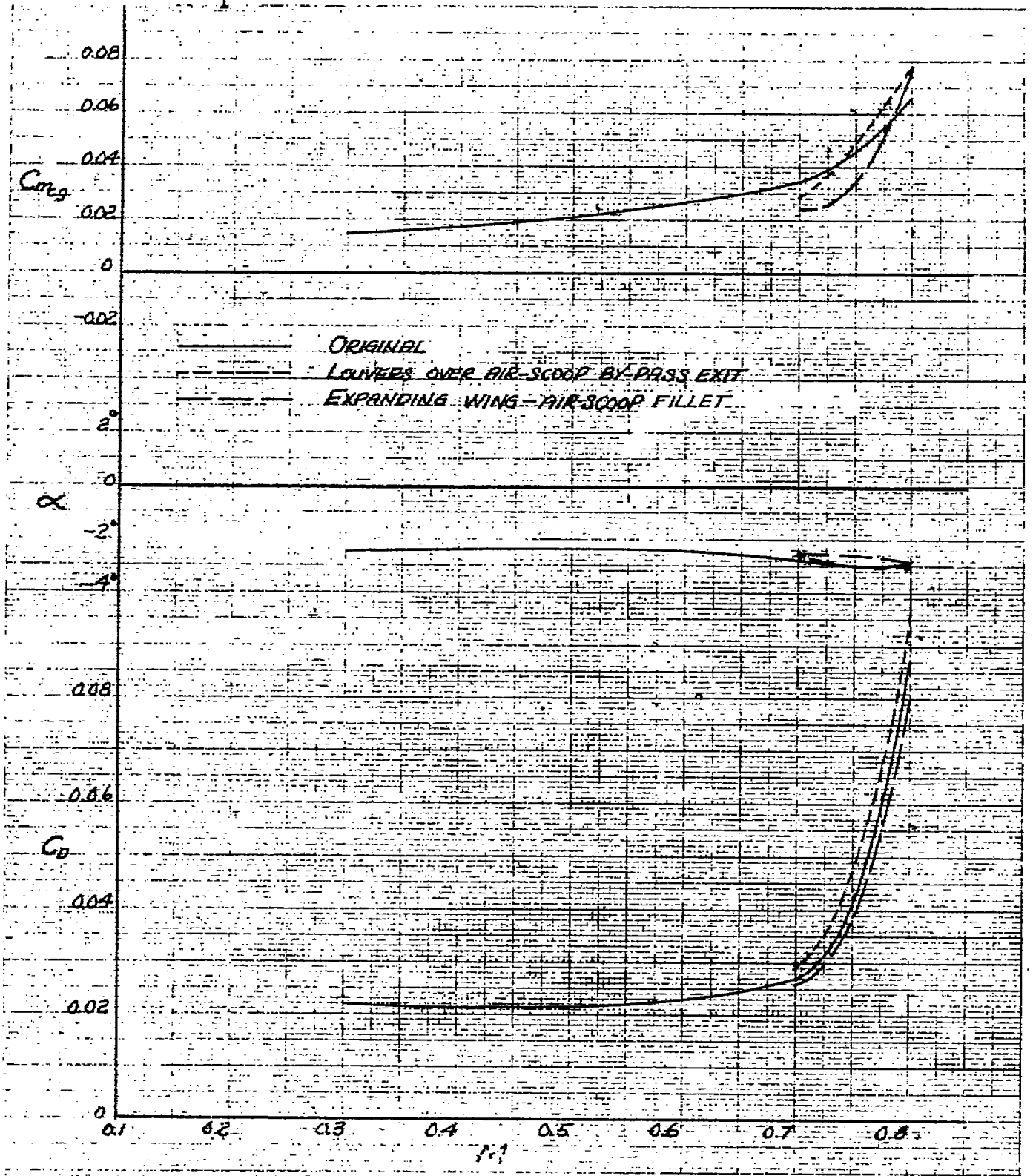

FIGURE 51.— VARIATION OF PITCHING-MOMENT COEFFICIENT, DRAG COEFFICIENT, AND ANGLE OF ATTACK WITH MACH NUMBER FOR SEVERAL AIR-SCOOP CONFIGURATIONS ON THE MODEL OF THE NORTH AMERICAN XP-82 AIRPLANE WITH THE REFLEXED TRAILING EDGE CENTER SECTION. C_L -0.1

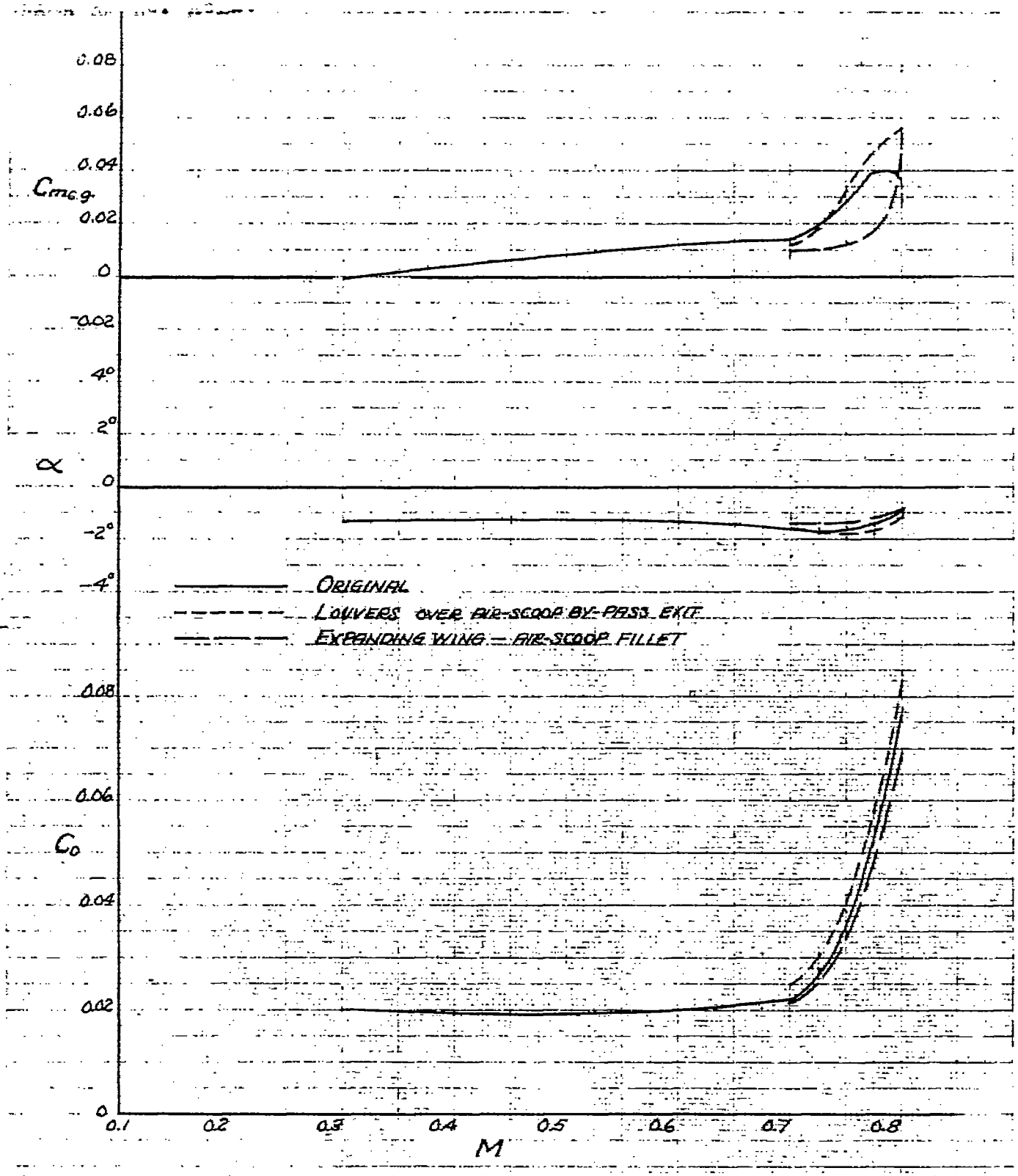

FIGURE 52. — VARIATION OF PITCHING-MOMENT COEFFICIENT, DRAG COEFFICIENT, AND ANGLE OF ATTACK WITH MACH NUMBER FOR SEVERAL AIR-SCOOP CONFIGURATIONS ON THE MODEL OF THE NORTH AMERICAN XP-82 AIRPLANE WITH THE REFLEXED TRAILING EDGE CENTER SECTION. C_L, 0.0 .

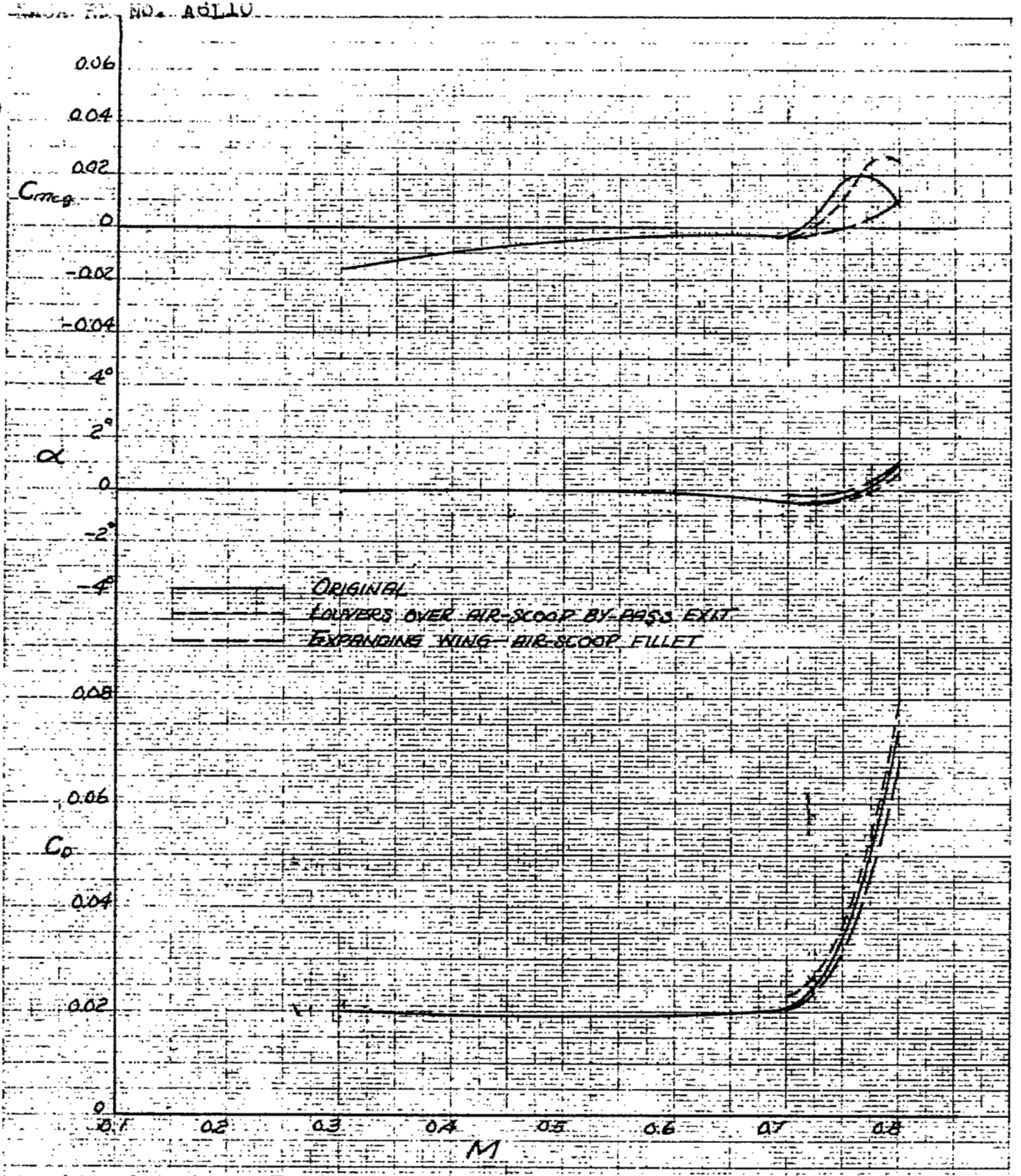

FIGURE 53. — VARIATION OF PITCHING-MOMENT COEFFICIENT, DRAG COEFFICIENT, AND ANGLE OF ATTACK WITH MACH NUMBER FOR SEVERAL AIR-SCOOP CONFIGURATIONS ON THE MODEL OF THE NORTH AMERICAN XP-82 AIRPLANE WITH THE REFLEXED TRAILING EDGE CENTER SECTION. C_L, 0.1

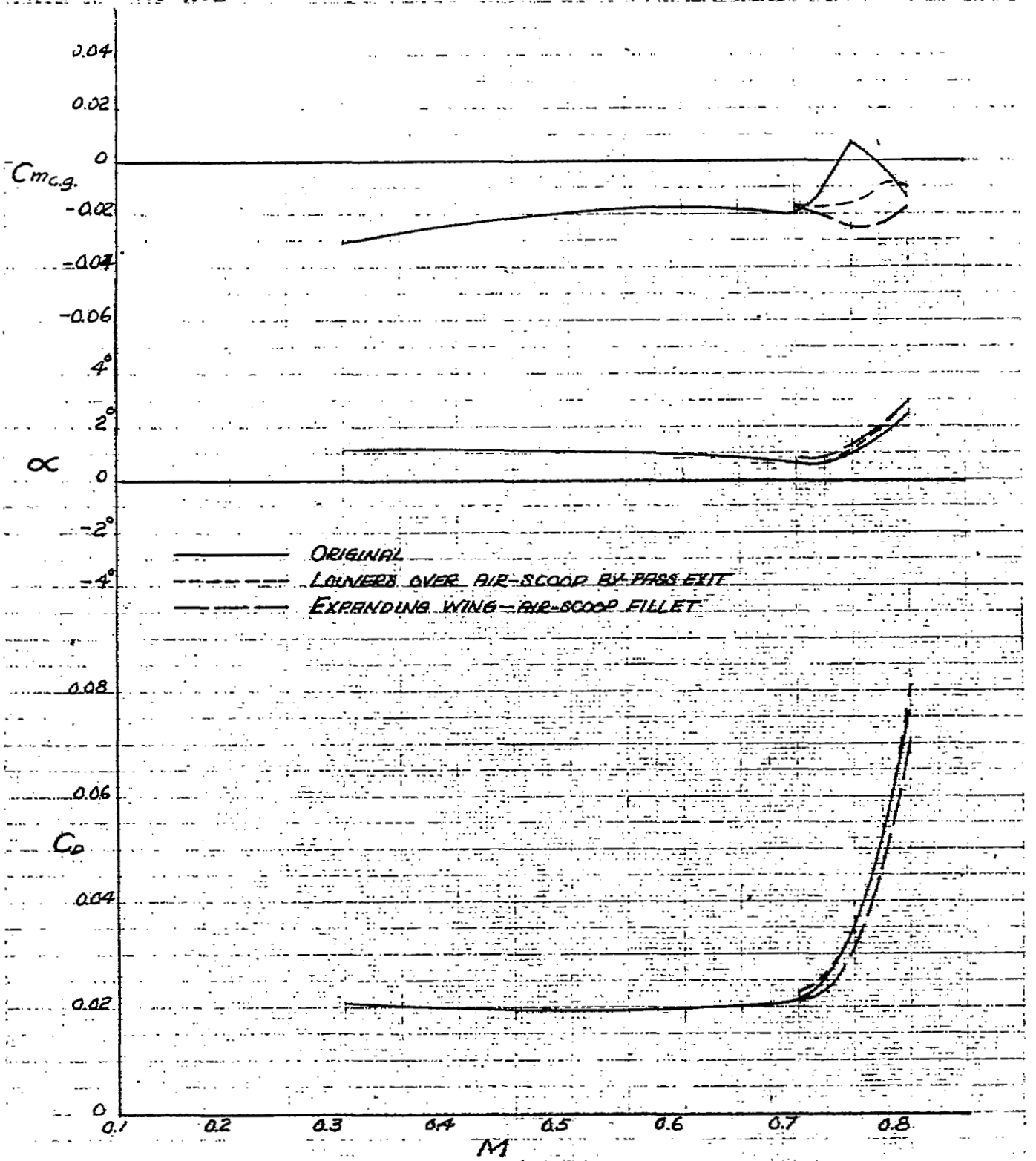

FIGURE 54. — VARIATION OF PITCHING-MOMENT COEFFICIENT, DRAG COEFFICIENT, AND ANGLE OF ATTACK WITH MACH NUMBER FOR SEVERAL AIR-SCOOP CONFIGURATIONS ON THE MODEL OF THE NORTH AMERICAN XP-82 AIRPLANE WITH THE REFLEXED TRAILING EDGE CENTER SECTION. C_L, 0.2

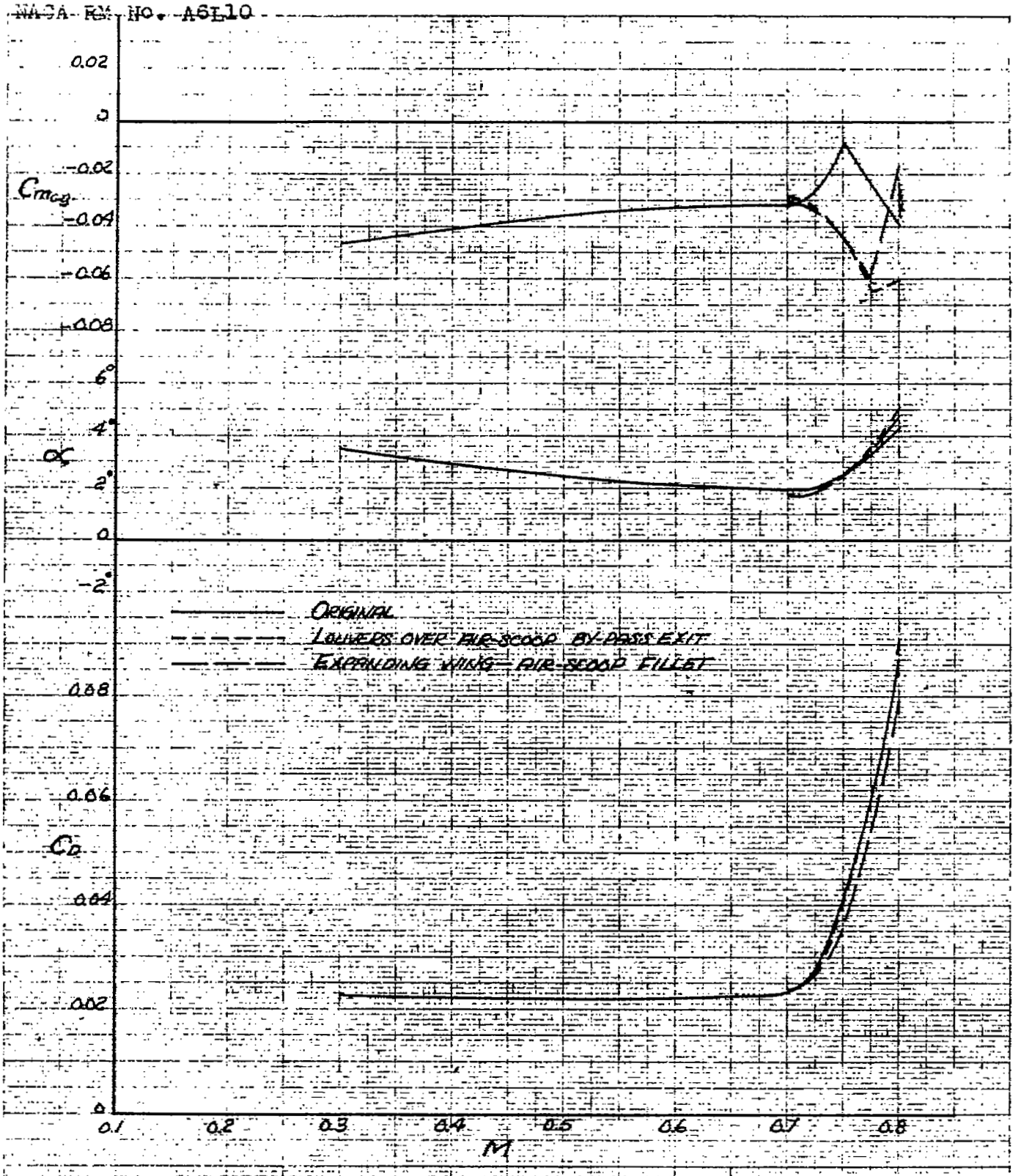

FIGURE 55.—VARIATIONS IN PITCHING-MOMENT COEFFICIENT, DRAG COEFFICIENT, AND ANGLE OF ATTACK WITH MACH NUMBER FOR SEVERAL AIR-SCOOP CONFIGURATIONS ON THE MODEL OF THE NORTH AMERICAN XP-82 AIRPLANE WITH THE REFLEXED TRAILING EDGE CENTER SECTION. C_L, 0.3.

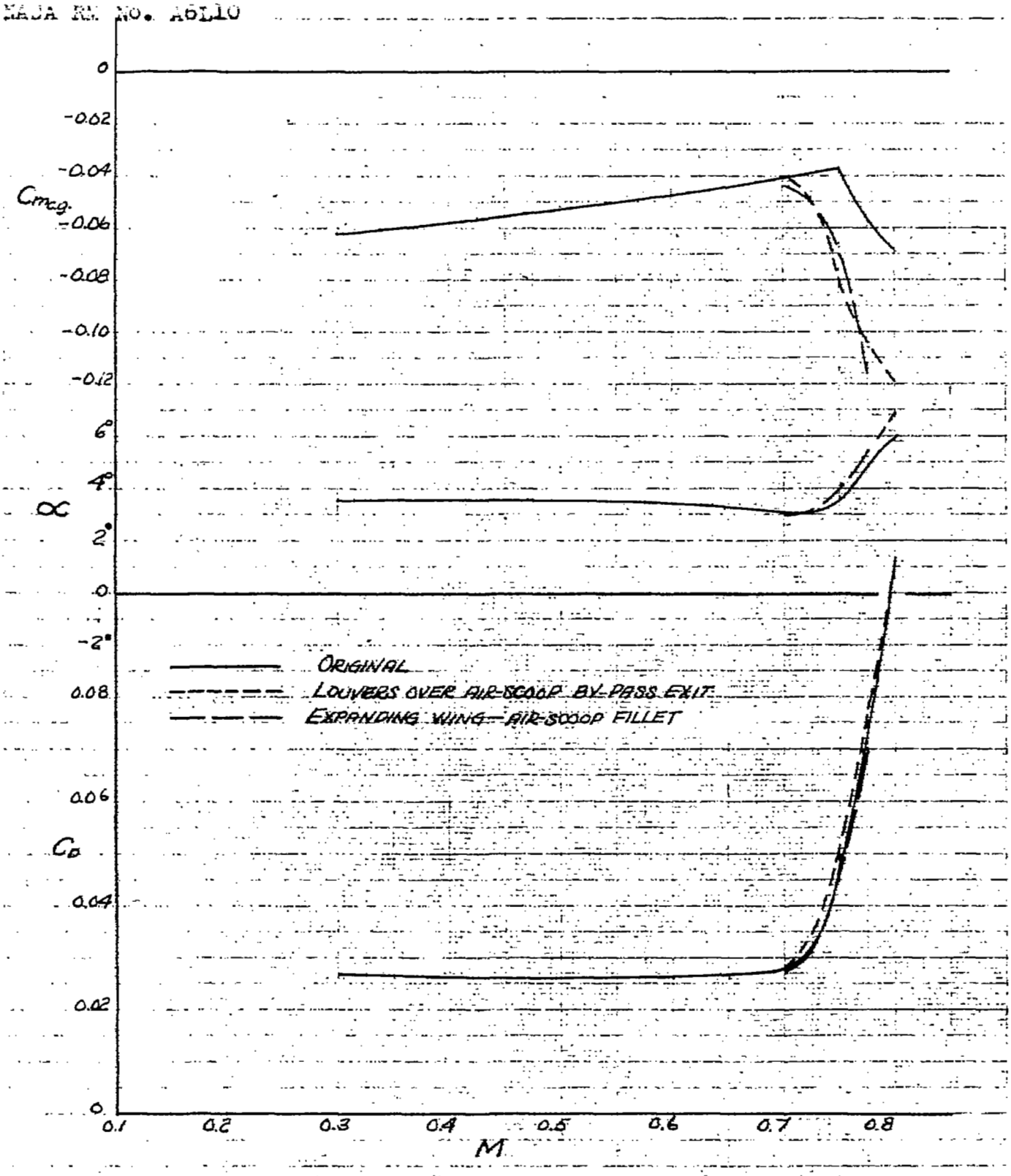

FIGURE 56.—VARIATION OF PITCHING-MOMENT COEFFICIENT, DRAG COEFFICIENT, AND ANGLE OF ATTACK WITH MACH NUMBER FOR SEVERAL AIR-SCOOP CONFIGURATIONS ON THE MODEL OF THE NORTH AMERICAN XP-82 AIRPLANE WITH THE REFLEXED TRAILING EDGE CENTER SECTION. C_L, 0.4.

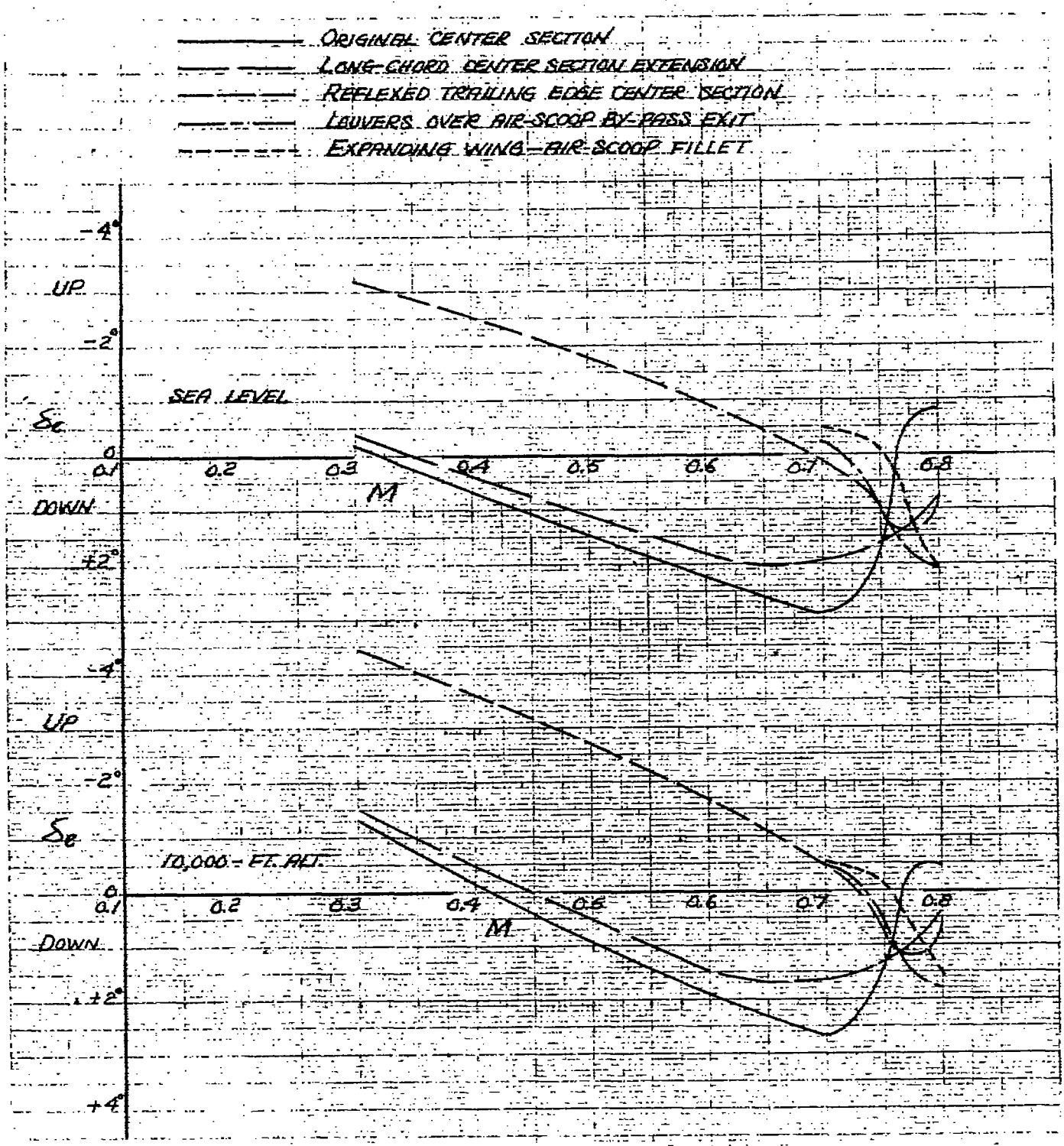

FIGURE 57.— PREDICTED ELEVATOR ANGLE TO BALANCE THE NORTH AMERICAN XP-82 AIRPLANE IN LEVEL FLIGHT AT SEA LEVEL AND AT 10,000 FEET ALTITUDE. WING LOADING 46.8 POUNDS PER SQUARE FOOT; ELEVATOR TAB 0°.

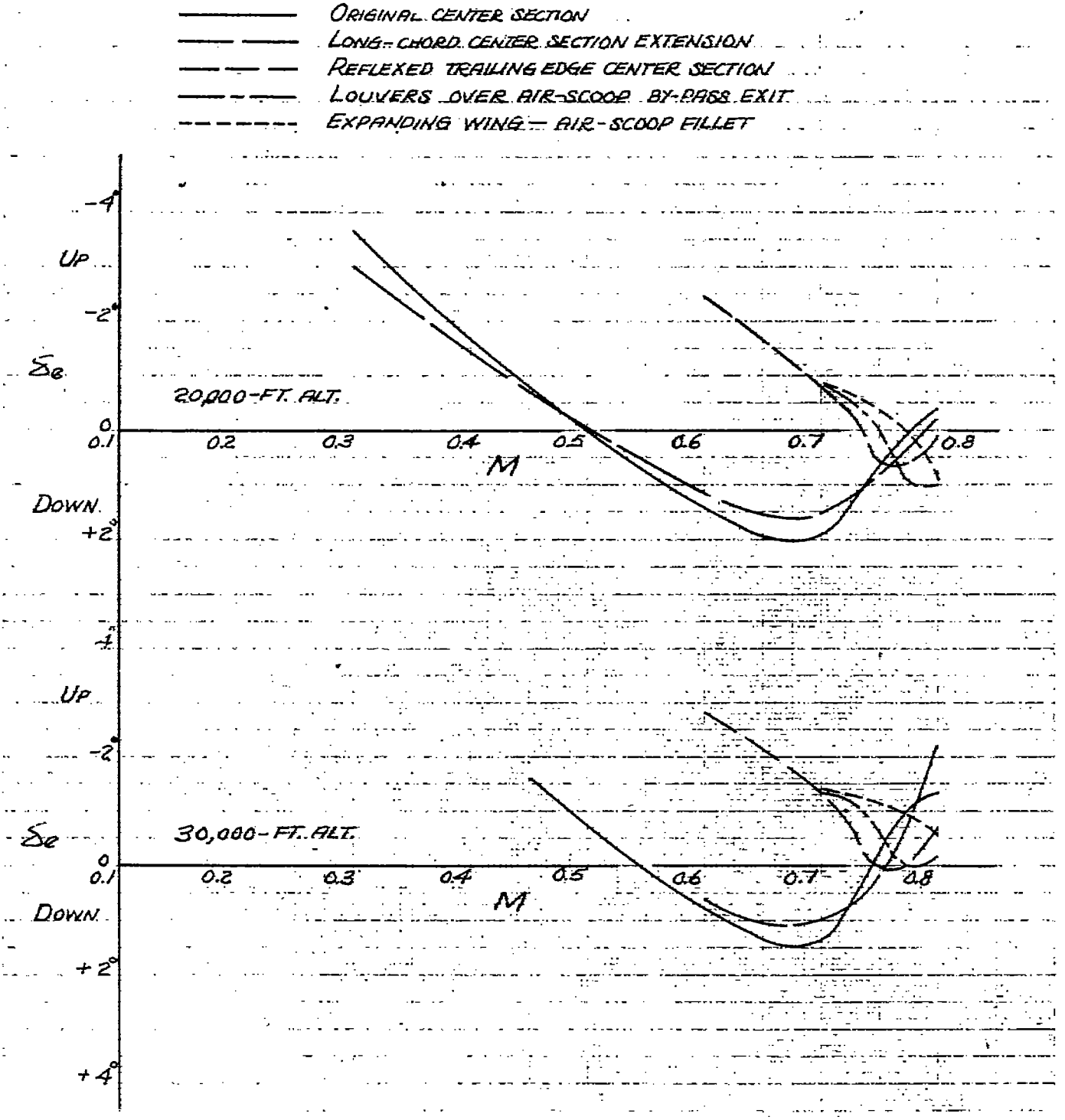

FIGURE 58. — PREDICTED ELEVATOR ANGLE TO BALANCE THE NORTH AMERICAN XP-82 AIRPLANE IN LEVEL FLIGHT AT 20,000 AND 30,000 FEET ALTITUDE. WING LOADING 46.8 POUNDS PER SQUARE FOOT; ELEVATOR TAB, 0°.